University of Glasgow

DEPARTMENT OF

AEROSPACE ENGINEERING

Wind tunnel investigations into the air flow around the existing and proposed bridges at Kingston.

by

M. Vezza, F.N. Coton and R.A.M. Galbraith.

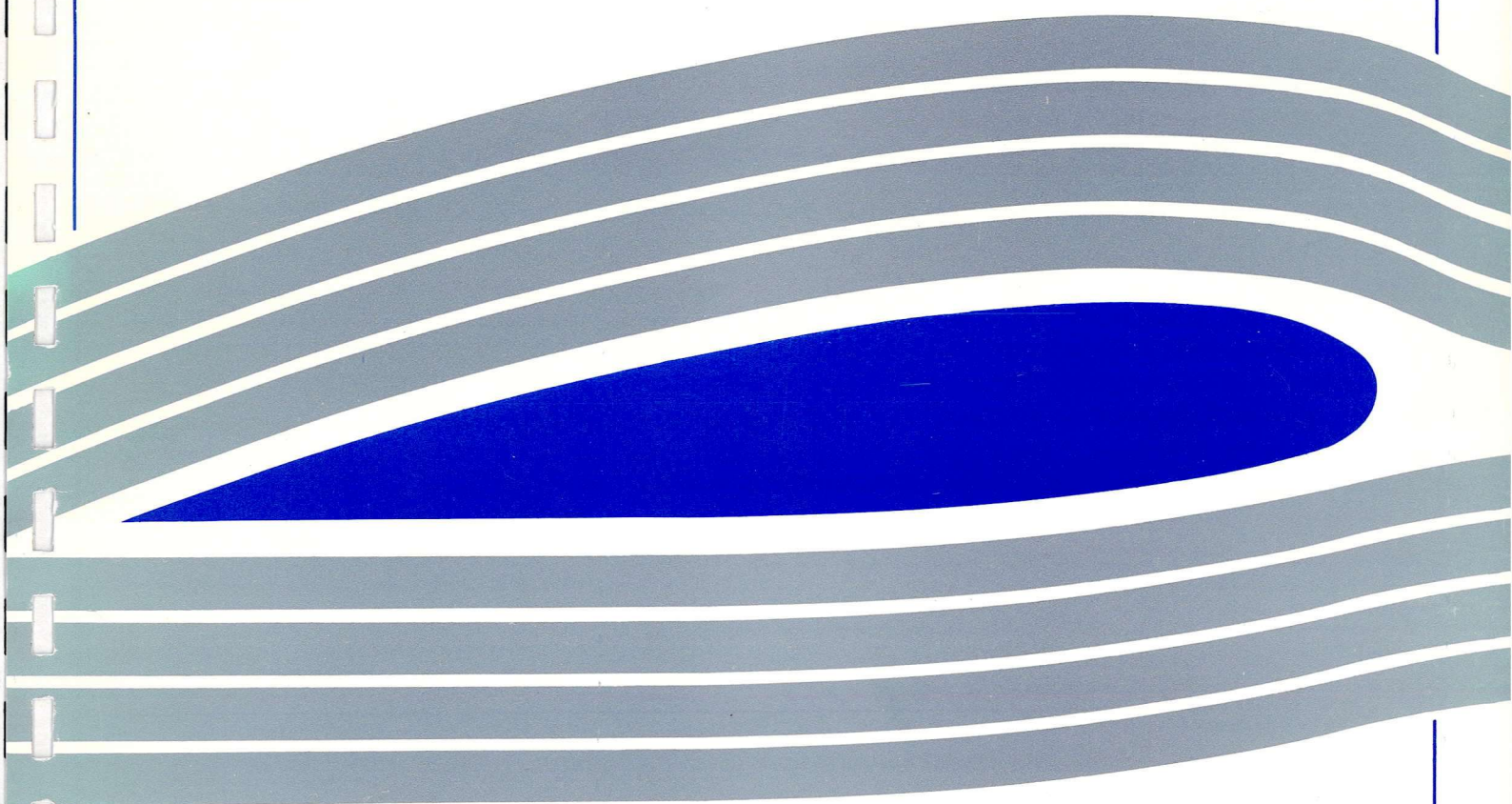

Contract report for Strathclyde Regional Council,
Department of Roads.

Wind tunnel investigations into the air flow around the existing and proposed bridges at Kingston.

by

M. Vezza, F.N. Coton and R.A.M. Galbraith.

Department of Aerospace Engineering
University of Glasgow
Glasgow G12 8QQ.

G.U. Aero Report No. 9316
August 1993.

SUMMARY.

This report presents the results obtained from a series of flow visualisation and flow measurement wind tunnel tests, carried out at Glasgow University, on models of the existing and proposed Kingston bridges. The background to the tests, commissioned by Strathclyde Regional Council after discussions with staff from the Department of Aerospace Engineering, is provided in the Introduction. Details of the facilities employed and bridge representation are included also. The important experimental consideration of Similarity is addressed in some detail, with particular reference to the use of appropriate scaling parameters for flow frequencies and velocities in the vicinity of the bridges.

Test results are presented firstly in the form of still photographs of the illuminated smoke traces, with the main features illustrated by the provision of flow diagrams for each test. Secondly, the more quantitative measurements are presented as graphs of velocity versus time at a variety of measuring stations. In addition, selected video records have been made and are available on an accompanying, indexed VHS cassette.

A detailed discussion of the results is presented, and five main conclusions are made concerning the structure of the flow around the existing and proposed bridges.

CONTENTS.

INTRODUCTION.

Presented in this report are the results of a series of flow tests carried out on models of the Kingston bridge and two proposed low level bridges spanning the River Clyde. The tests were commissioned by Strathclyde Regional Council, Department of Roads, after consultation with staff from the Department of Aerospace Engineering, University of Glasgow. Observations are made on the results obtained and a number of conclusions are drawn on the structure of the flow, including the influence of several modifying factors.

Background.

Concerns over the flow regime around the bridge at Kingston led Strathclyde Regional Council to approach the Department of Aerospace Engineering at the University of Glasgow with a view to commissioning a series of investigative wind tunnel tests. The concerns centred on the output from anemometers positioned above and below the centre of the bridge at midspan, which appeared to indicate that two distinct flow regimes were operating as the wind speed increased from a very low value. At low wind speeds the air velocity under the bridge was lower than that above, but at high wind speeds the reverse was the case, with instantaneous values up to seven or eight times those above the bridge. The Council wished to assertain whether the indicated phenomenon was reproducible in a wind tunnel environment and whether the anemometer under the bridge was providing a true indication of the flow under the bridge in general. After consultation the Council decided to commission a more comprehensive series of tests to investigate, in addition, the flow around prototype models of the low level bridges.

Wind Tunnel Facilities.

All of the tests were carried out in the 3' by 3' flow visualisation tunnel within the Department of Aerospace Engineering. This facility is illustrated in Fig. 1. The smoke emitted from the dispersal pipe can be visualised through the front wall of the tunnel which is constructed from perspex. Access to the tunnel, through the rear wooden wall, was required in between tests to alter the model arrangement and position the hot wire probes.

Model Construction.

Scale models (1:161) representative of the existing and proposed bridge segments spanning the river were constructed for the series of tests carried out. The restricted spanwise extent of the models corresponds to the region of the existing bridge exposed to the highest mean wind speeds. Beyond this region the surface terrain of tall buildings would effectively reduce the mean wind speed impinging on the bridges and is, therefore, of lesser concern. The requirements for the flow visualisation tests dictated the choice of perspex sheeting as the model material. In addition, fixing plates with a facility for height adjustment and a wooden ground board were constructed to enable the effect of tide conditions to be modelled. The initial tests were carried out on the bridge models without parapets attached. Subsequently, parapets were constructed and mounted on the models. Tapered blocks of wood were made for the tests modelling the effects of reducing the river width, and lorry traffic was modelled using a perspex block of rectangular section. A photograph of the models in the wind tunnel is given in Fig. 2. Details of the river narrowing are given in Fig. 3. All construction work was carried out by technician staff within the Department of Aerospace Engineering.

Similarity.

When flow tests are carried out on scale models, it is important to ensure that the aerodynamic forces and flow structures pertaining to the full scale are reproduced accurately. Normally, apart from geometric similarity, the two most important dimensionless parameters in low speed wind tunnel testing are the Reynolds number (Re) and the Strouhal number (S). These parameters indicate the magnitude of the inertial to viscous forces in the fluid, in the case of Re, and the rate at which shed vortices travel a typical characteristic structural dimension, in the case of S. They are defined as follows:

$$Re = VD/\nu \qquad ; \qquad S=nD/V$$

where ν is the fluid kinematic viscosity, V is the wind speed, D is a characteristic dimension (normally cross-wind for bluff bodies) and n is the vortex shedding frequency.

If it is impossible to match the model and full-scale Reynolds numbers, the flow patterns around the two may be different. Fortunately, bridges are bluff bodies with sharp edges, giving the same flow patterns for the model and full-scale, and no Reynolds number corrections are necessary. This was shown in correlating the model tests of the first Tacoma Narrows bridge with the prototype, and in later tests of the Golden Gate and new Tacoma Narrows bridges. The present series of tests rely on this behaviour since the difference in size between the model and the full-scale prevents Reynolds number matching.

The Strouhal number provides the mechanism by which the frequency of turbulence measured in the tests can be related to those experience on the actual bridge. Geometric similarity of the model and full-scale should result in both having the same Strouhal number. Thus

$$(nD/V)_m = (nD/V)_f$$

where f and m relate to the full-scale and model respectively. The Strouhal number for vortex shedding was measured in the tests to be approximately 0.11. The Strouhal number can, however, be used to scale the frequency of turbulence in a more general manner. If we rearrange the above equation we obtain

$$n_m/n_f = (V/D)_m \,.\, (D/V)_f$$

which, if the velocity scale is known may be used to calculate the frequency of turbulence on the bridge from measured test values.

In bridge model testing, the Froude number, which is the ratio of inertial force to gravitation force, is used for scaling wind speeds, as the Reynolds number correlation is generally ignored for bluff bodies. The Froude number is given by

$$Fr = V^2/Dg$$

where g is the acceleration due to gravity. Thus, if we assume Froude number similarity, the velocity of the model is related to the full scale by the square root of the length scale, i.e. in this case

$$V_f = 12.69\, V_m$$

When this is applied within the frequency relation given above, it is possible to relate the frequency of turbulence measured in a test to that of the full-scale by

$$n_m = 12.69\, n_f$$

In this way it is possible to scale both the frequency and velocity of the gross flow field. However, the dependency of detailed measurements on the viscous scale (Re) means that, when considering phenomena such as that experienced immediately below the bridge in the vicinity of the gap, the scaled tunnel velocities at which changes in flow state occur will not exactly match that of the full scale. Nonetheless, outside this region, velocities can be expected to scale well. Thus, for example, tests conducted at 0.97m/s will reflect the general characteristics of a full scale wind speed of 27.5mph.

TEST PROGRAMME AND RESULTS.

The series of flow tests carried out were divided into two stages. Stage 1 involved flow visualisation tests only in the investigation of introducing the proposed bridges and the effect of tide. The programme is illustrated in Fig. 4. These results were assessed before proceeding with stage 2, which involved selected hot wire testing and further visualisation tests. Fig. 5 illustrates the second stage programme. Also at this stage parapets were added to the models. The results of these tests are given below, with observations on any significant features. The visualisation and hot wire tests are divided into sections A and B respectively, with corresponding figure labels.

A. Smoke Flow Visualisation Tests.

Patterns of flow are identified by introducing a mist of Ondina 90 oil into the stream, and illuminating with a light sheet. Flow patterns for the first series of tests carried out were recorded using still photography only. In subsequent tests video records were made in addition to the photographs taken. Only the stills are presented with this report; the video records are available on an accompanying, indexed VHS cassette. In the test results given below, the freestream speeds referred to were obtained from the results of the hot wire tests. The lower and higher wind speeds mark the limiting conditions for effective use of the smoke generating apparatus.

Results and Observations.

The results of each flow visualisation test are presented in the form of a series of still photographs and an annotated diagram highlighting the main features of the flow.

The first set of tests were carried out with the single bridge configuration. Figs. A1 and A2 illustrate the resulting midspan flow patterns for low and high tide conditions at wind speeds of 0.57 m/s and 0.48 m/s respectively. Figs A1(a) to A1(c) indicate the zones of recirculating flow above and below the windward end of the bridge, and in the gap between the two bridge sections. In this latter region some of the air crossed over into the stream above the bridge, undoubtedly due to the pressure differential across the opening. Immediately below this gap the position of the streaklines appeared to fluctuate, indicating unsteadiness in the velocity: further below, the unsteadiness disappears. Above the opening the flow over the bridge appeared smooth and undisturbed. The flow pattern for the high tide condition, Figs. A2(a) to A2(c), is essentially the same as above, with some increase in the flow speed under the bridge indicated by the slightly closer spacing of the streaklines.

The next set of tests investigated the effect of introducing the two lower level bridges upstream and downstream of the main bridge. The midspan flow patterns for low and high tide conditions at speeds of 0.45 m/s and 0.48 m/s are illustrated in Figs. A3 and A4. Flow over the windward bridge is accelerated as indicated by the compression of the steaklines in Figs. A3(a) and A4(a). The wake from this bridge passes under the main bridge, Figs. A3(b) and A4(b), and impinges on the leeward bridge, which is immersed in turbulent flow, Figs. A3(c) and A4(c). There is little effect of tide, although the wake expansion is slightly greater in the low tide case. These features are illustrated in Figs. A3(d) and A4(d).

Tests were carried out at a spanwise location away from midspan towards the haunch of the main bridge at speeds of 0.45 m/s and 0.88 m/s. The effects of the larger projected area of the main bridge are illustrated in Figs. A5 and A6. The increased deviation of the flow over the main bridge is illustrated in Figs. A5(a) and A6(a), the effect accentuated with increasing speed. The flow directly behind the windward bridge is accelerated downwards through the constricted area, Figs. A5(b) and A6(b), energising the upper region of the

shed wake. The leeward bridge is again immersed in a turbulent flow, Figs A5(c) and A6(c), although the flow pattern is affected by the windward acceleration. Flow diagrams are provided in Figs. A5(d) and A6(d). Throughout all haunch tests significant three dimensional effects were observed, in the form of a smoke sheet distorted out of the plane of the bridge section. These are due to the greater rate of variation in the projected area of the main bridge at the haunch, and to some extent the proximity of the wind tunnel wall.

The effects of reducing the river width by extending the existing quay walls was investigated by visualising the flow at midspan and haunch positions, at a wind speed of 0.56 m/s. The results are illustrated in Figs. A7 and A8. Above the main bridge at midspan, Fig. A7(a), the effect of the reduced width is to increase the upward deflection of the flow and hence increase the extent of the shear layer emmanating from the leading edge of the bridge. The pattern of flow over the low level bridges indicate no obvious differences from previous cases. Little effect of reduced width is indicated by the flow pattern at the haunch, apart from a small increase in the vertical extent of the main bridge upper surface shear layer, Fig. A8(a). This is again due to the increased upward deflection of the flow over the main bridge.

Tests were carried out on the effect of traffic, representative of a line of articulated lorries, on the windward bridge. The wind speed was 0.58 m/s and the results obtained at midspan and haunch are illustrated in Figs. A9 and A10. The blockage effect of the traffic results in a steeper angle of flow onto the leading edge of the main bridge. At midspan this produces a significant increase in the extent of the vortical flow over the bridge, Fig. A9(a). Flow underneath the main bridge is strongly influenced by the regular, well defined vortex shedding from the edge of the traffic block, Figs. A9(b) and A9(c). The leeward bridge is directly in the path of this vortex wake, FigA9(d). At the haunch the flow over the main bridge experiences a similar upward deflection, Fig. A10(a). However the tendency of the traffic block to generate a strong vortical wake is ammeliorated by the downward acceleration of the flow due to the larger projected area, Fig. A10(b). The effect on the leeward bridge is therefore less marked, Fig. A10(c). Figs. A9(e) and A10(e) provide diagramatic representations.

A test was carried out to investigate the effect of increasing the separation between the main bridge and the lower bridges from 1 metre to 12 metres, at a

wind speed of 0.52 m/s. Fig. A11(a) shows that the effect on the windward bridge is negligable, and the structure of the wake directly behind this bridge is substantially the same, Fig. A11(b). However the increased separation leads to wake dissipation and the flow impinging on the leeward bridge is clear of much of the turbulence seen previously, Fig. A11(c). The rear of the bridge is immersed in the wake generated at the leading edge. The situation is illustrated in Fig. A11(d).

The initial series of tests were carried out on the bridges without parapets attached. It was considered that the addition of parapets would not significantly change the overall flow structure, although some local effect may be evident. Figs. A12(a) and A12(b) illustrate the results of repeating the first test with the single bridge arrangement. These confirm the prior expectations.

B. Hot Wire Tests.

A hot-wire anemometer consists of a thin wire probe which is heated well above ambient temperature. When an air stream passes over this probe the change in resistance of the probe can be used to infer the flow velocity. The system used in these tests consisted of a DANTEC 56C hot-wire system connected to an Apple MacII computer via a National Instruments MIO16 multi-function data acquisition board. All probe measurements were controlled using software developed in the Department of Aerospace Engineering, Glasgow University, using the National Instruments LabVIEW2 package. In all, tests were conducted at eight probe locations for a variety of onset flow speeds and geometric configurations. The probe locations used in the study are indicated in Fig. B. Each data series represents 200 measurements made over a four second period. The data are presented in graphical form for the purposes of this report but will be made available in tabulated form as required.

Results and Observations.

The first phase of the testing programme concentrated on the main bridge in isolation. In Fig. B1., the results of two tests carried out at very low wind speeds are presented for both low and high tide cases. At these wind speeds, the performance of the hot-wire is compromised by natural convection but, nonetheless, a qualitative assessment of flow behaviour can still be made.

Tests at these low wind speeds were made at probe locations 1 and 2 which correspond to current cup anemometer positions on the main bridge. Results of measurements on the full-scale bridge had indicated that, at very low wind speeds, the wind speed above the bridge was consistently higher than that measured below the bridge. This is confirmed by the results presented in Fig. B1 which, in addition to this behaviour, show that the flow is relatively steady below the bridge. The slight perturbations in the two graphs are a combination of system noise and small flow perturbations which are below the resolution of the data acquisition board.

Figures B2 and B4 show the results from the same measuring locations at three higher wind speeds for the high and low tide configurations respectively. For these cases the flow at probe location 1 behaves much as before but considerable turbulence is observed at location 2. This effect is little influenced by tidal conditions and is representative of a similar phenomenon experienced on the full-scale bridge. At the highest wind speeds there are several incursions in velocity above that measured at point 1. In Fig. B4, there is an apparent trend towards increased velocity overshoot below the bridge with increasing mean wind speed. This is related to the behaviour of the separated shear layer which is, to a large extent, governed by Reynolds number. It seems reasonable to postulate that increasing the Reynolds number towards those experienced on the full-scale bridge would produce velocity surges of sufficient duration and magnitude to result in very high readings from the cup-anemometers. This postulation could, however, only be confirmed by subsequent model tests in a wind tunnel of higher velocity.

The results shown in Figs. B3 and B5 show that in the absence of the lower bridges the flow at probe locations 3 to 6 is almost uniform and steady. The velocity values measured at location 4 are more representative of the true velocities in clear air below the bridge than those measured at location 2.

When the two lower bridges were added to the model set-up, the velocity variations shown in Figs. B6 and B8 were measured at probe locations 1 and 2. These velocity variations show little change from those previously observed with no lower bridges present although there is a slight increase in the unsteadiness of the flow at probe location 1. The increased blockage presented to the air by the lower bridges is the likely cause of this effect. As

before, the general nature of the flow in these two locations seems unaffected by tidal variations.

Comparisons of the velocities experienced by the lower bridges are presented in Figs B7 and B9 for the high and low tide configurations respectively. Of particular relevance in these figures is the velocity at location 4 which represents the flow of 'clean' air underneath the bridge and can be used as a reference velocity in this case. The most significant difference between the two sets of graphs is the behaviour of the velocity at probe position 3 just above the front lower bridge. Although the flow at this position is steady when the tide is low, there is considerable turbulence in the flow when the tide is high. This occurs as a result of the effect of the increase in blockage which is created when the air passage between the ground plane and the front bridge is constricted. Under these conditions the front bridge acts more like a bluff body with separation from the upper leading edge. The flow over the rear bridge is very turbulent in both cases and appears unaffected by tidal variations. Additionally, the mean velocity at location 6 is consistently lower than that at location five. The widest velocity variations are experienced at location six.

Figure B10 illustrates the wind velocities measured at two wind speeds in the haunch of the bridge. In this case, the velocity at location 4 can again be used as a reference velocity. As was observed in the previous tests, the mean velocity at location 6 was consistently below that at location 5. Unlike the previous test series, however, the velocity at location 5 is higher than the reference and closer to the freestream wind speed. This is apparently due to acceleration of the flow through the haunch due to the proximity effect of the upper bridge and the interaction with the faster moving flow near the mid span. The magnitude of velocity experienced at the two measurement locations on the rear bridge, behind the haunch of the main bridge, are very similar to the equivalent measurements at the mid-span.

The effect of reducing the river width by extending the existing quay walls is shown in Fig. B11. It should be noted that by effectively reducing the total air channel below the bridge, the shear layer trajectory from the leading edge of the upper bridge has been steepened to the extent that measurement position 1 now falls within the influence of the shear layer. Consequently, the probe in this position has registered the characteristic vortex shedding frequency for the bridge. The only other significant feature of the flow at the

mid-span is the slight increase in the mean value of velocity at location 6. The measurements taken in the haunch of the main bridge show a similar effect. Additionally, the velocity at location 4 is quite unsteady and of greater comparative magnitude than the previous haunch tests.

In Fig. B12., the effect on the rear bridge of stationary traffic on the front bridge is presented for both the mid-span and the haunch. In both cases, the effect of the traffic is to marginally reduce the magnitude of the mean velocities registered on the rear bridge.

As indicated above, tests were also carried out at locations 7 and 8 which were indicative of the conditions experienced by traffic on the main bridge. Figure B13 shows the wind loadings measured at these points for a clean three bridge configuration. Although the windward location experiences little turbulence, location 8 experiences turbulence which is comparable to that experienced on the rear lower bridge.

Finally, the effect of separating the lower bridges from the main bridge by a distance of 12m was examined. In this case, as may be observed in Fig. B14., the level of turbulence on the rear bridge is considerably reduced at location 5 but virtually unchanged at location six. Above the bridge, the velocity at location 7 is increased and the intensity of the turbulence at 8 is reduced.

CONCLUSIONS.

From the results obtained, the following conclusions can be drawn:

1. The velocities obtained below the main bridge at midspan appear to indicate the presence of similar flow regimes to those obtained from the anemometer on the actual bridge. The levels of turbulence and velocity peaks observed at higher wind speeds appear to be local phenomena, not in evidence outwith this particular zone.

2. Under certain conditions, in particular for reduced river width and traffic on the windward bridge, the position above the main bridge at midspan corresponding to the anemometer location is not in clear air.

3. The leeward bridge is generally immersed in a turbulent flow produced by the wake of the windward bridge, although the level appears to be

no worse than that measured on the rear upper surface of the main bridge.

4. The effects of traffic, tide conditions and reduced river width appear to be marginal on the leeward bridge.

5. The effect of increased separation is to reduce the general level of turbulence on the leeward bridge.

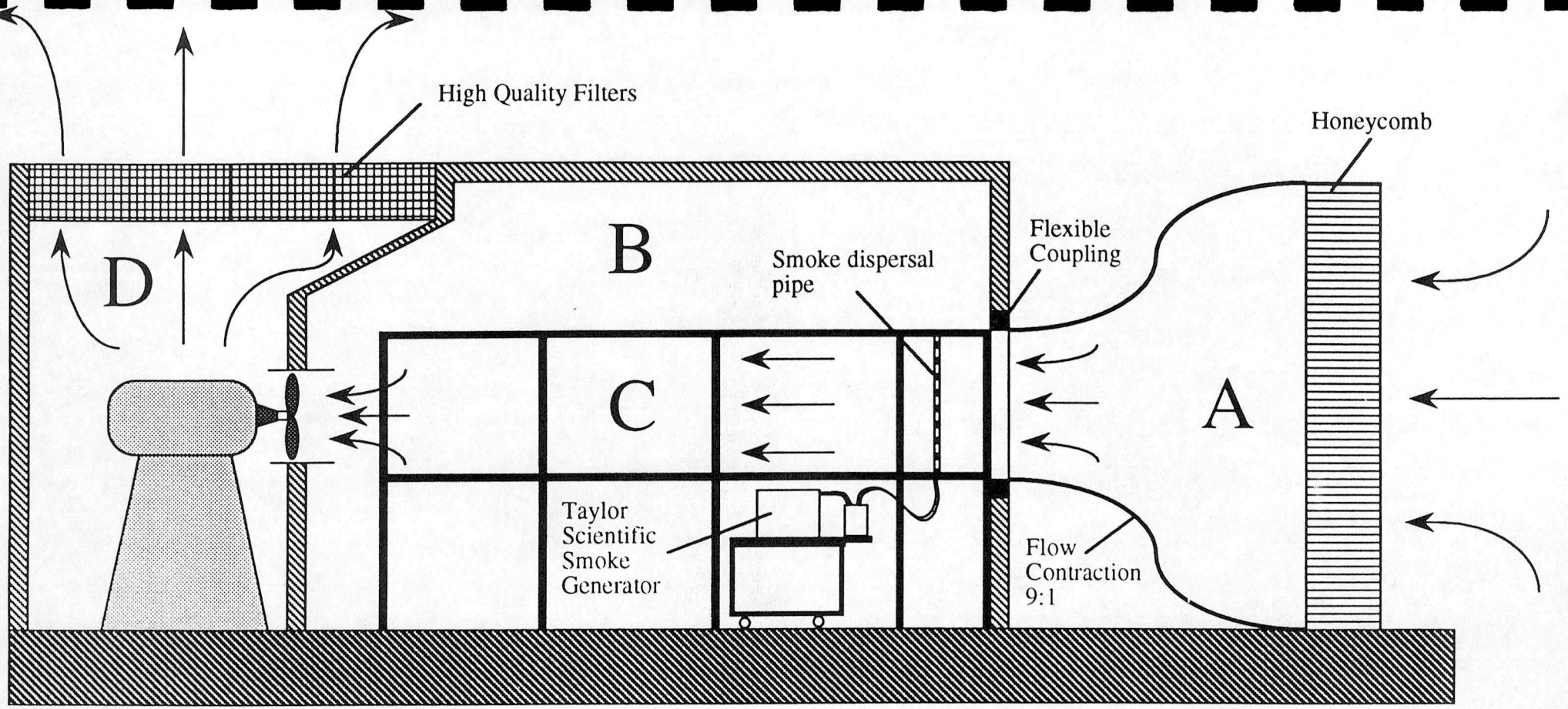

A Flow conditioning section. Air from lab enters tunnel and passes through a screen and honeycomb and is then accelerated and straightened in a 9:1 contraction.

B Test Room. During operation, the action of the fan is to lower the pressure in this room. The room is sealed from the lab and so the only way in which the pressure differential can be relieved is by air entering through the contraction and into the test section.

C Test Section. The well-conditioned low-turbulence flow enters the test section through section A. Smoke is supplied from a smoke generator through a small bore pipe in which is drilled a series of holes. A series of smoke lines are visible in the test section. This allows the flow patterns around various body shapes to be examined.

D High Pressure Chamber. The flow enters this room through the fan which is vibration isolated from the test section. During operation, the pressure in the room is higher than the surroundings. The walls of the room are sealed and so, to relieve the pressure differential, the air travels through high quality filters before being discharged into the lab.

Fig. 1. Flow visualisation wind tunnel facility.

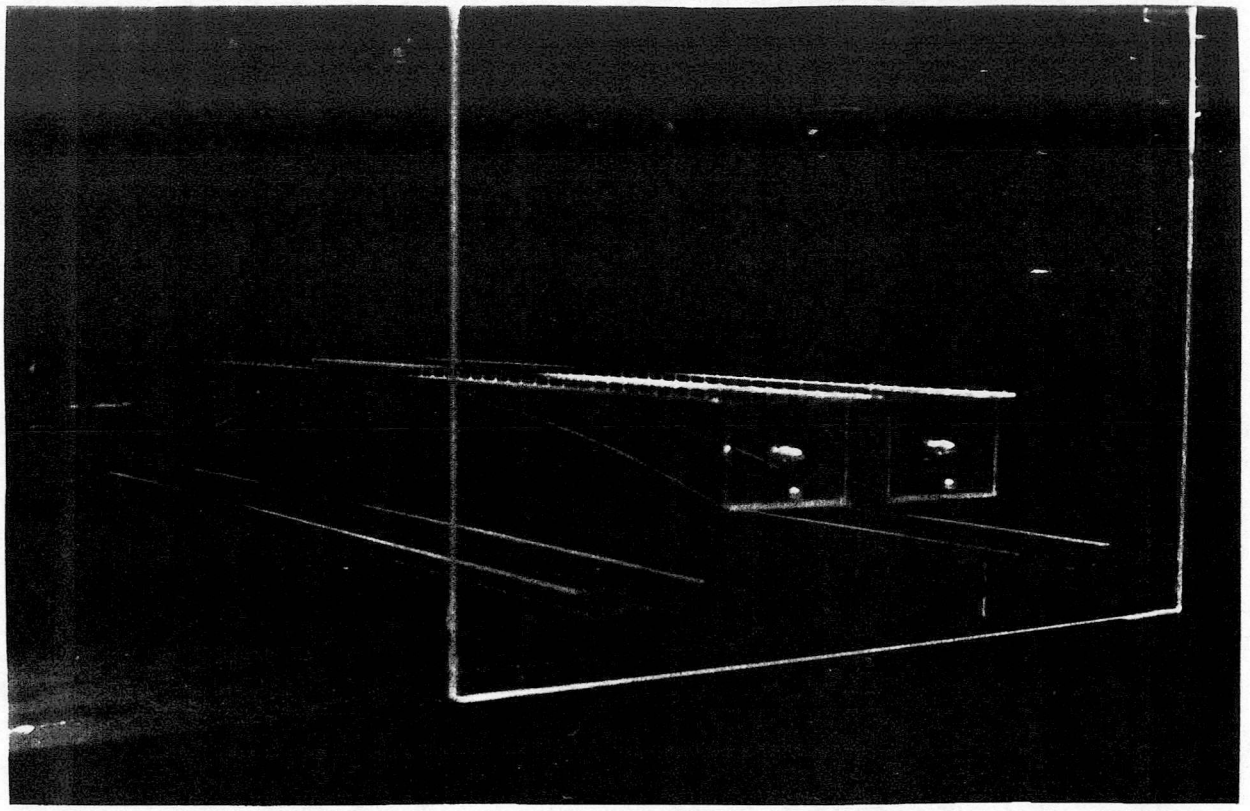

Fig. 2. Three bridge models located in wind tunnel.

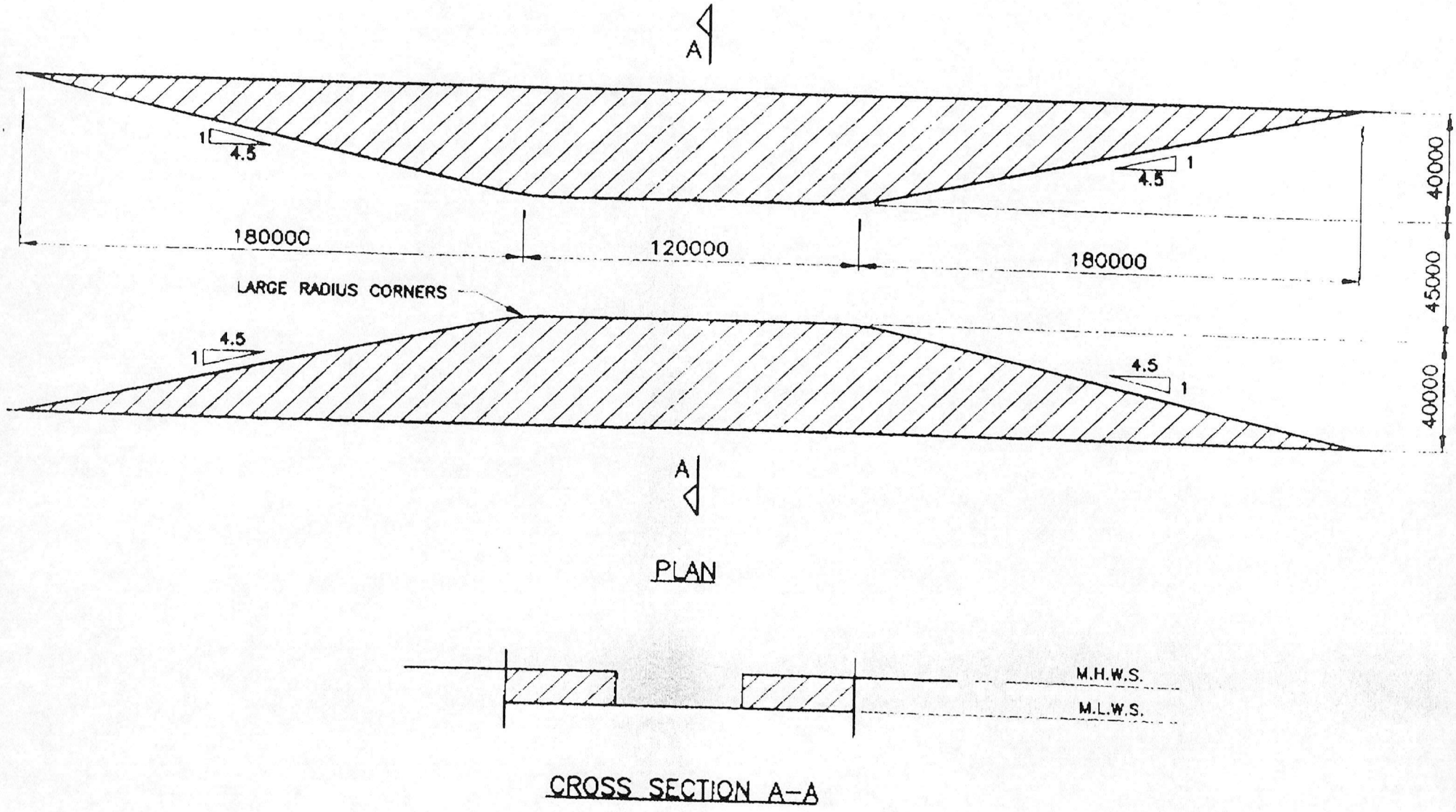

(All dimensions mm).

Fig. 3. Outline dimensions of proposed river narrowing option (supplied by SRC).

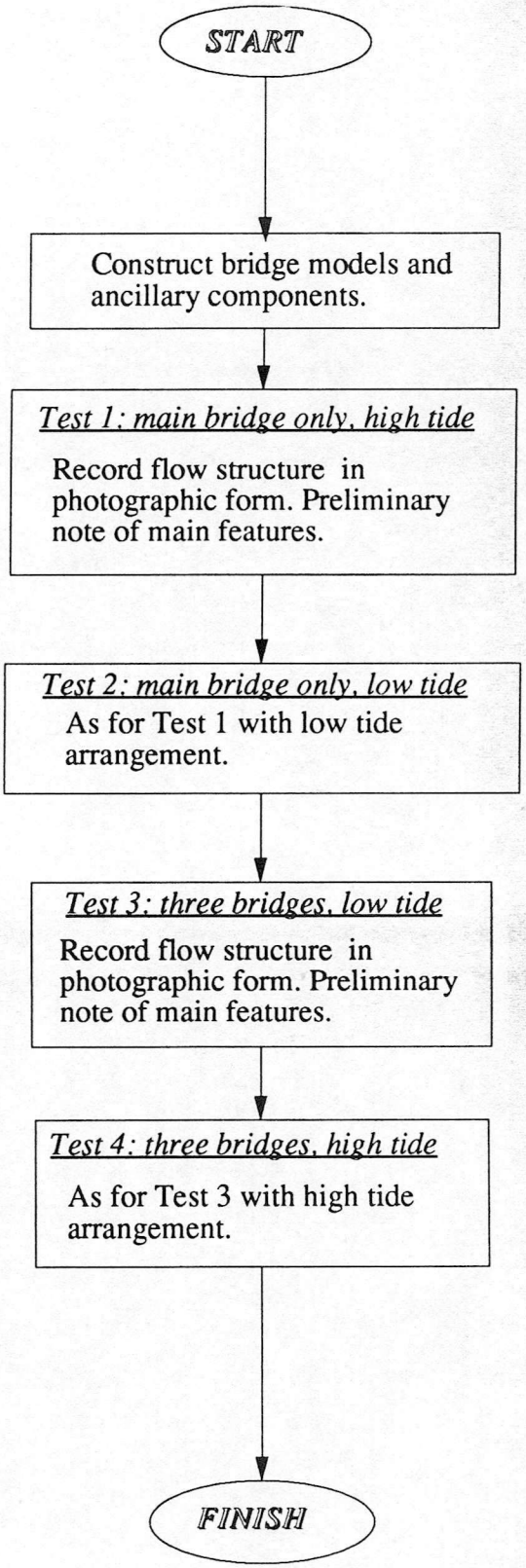

Fig. 4. Stage 1 test programme.

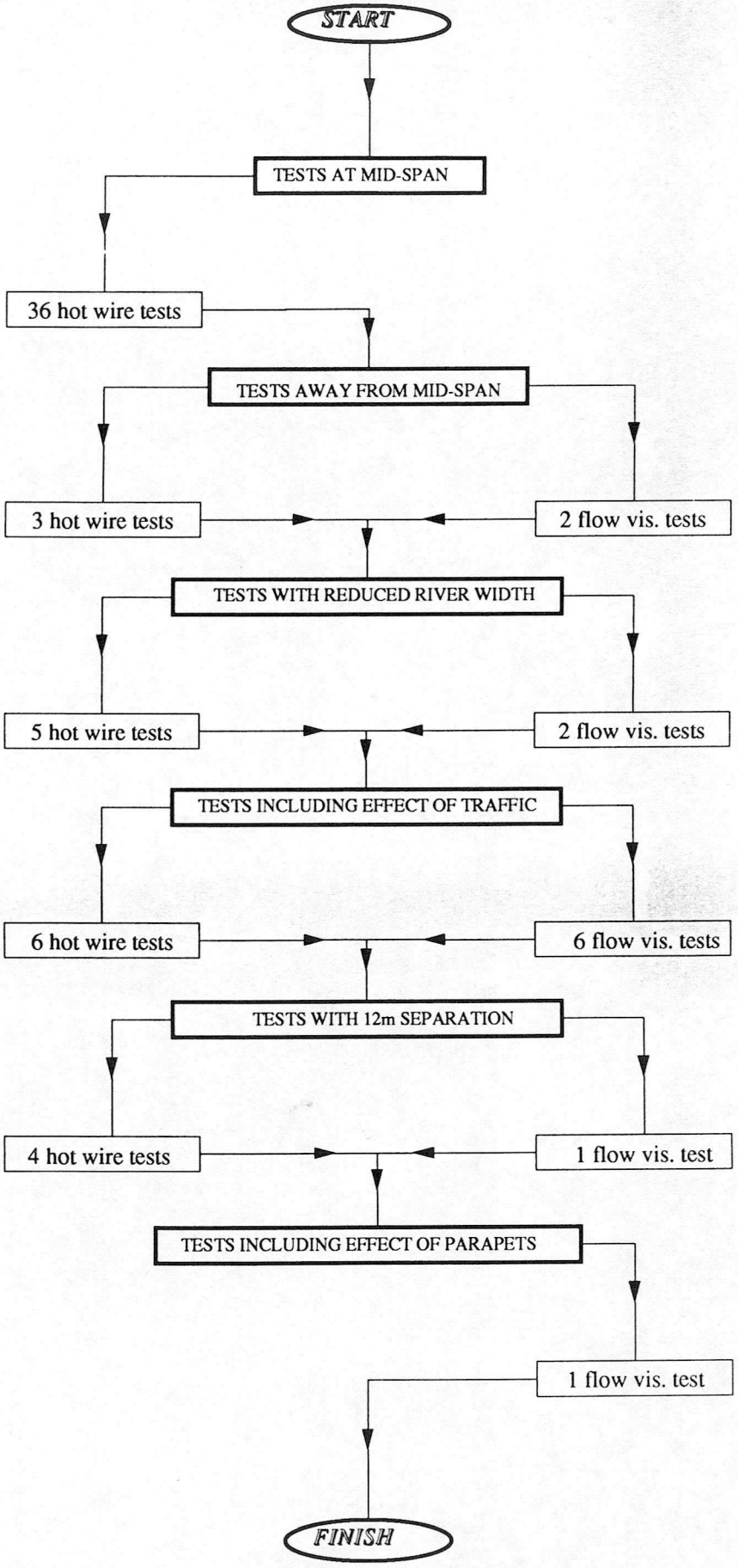

Fig. 5. Stage 2 test programme.

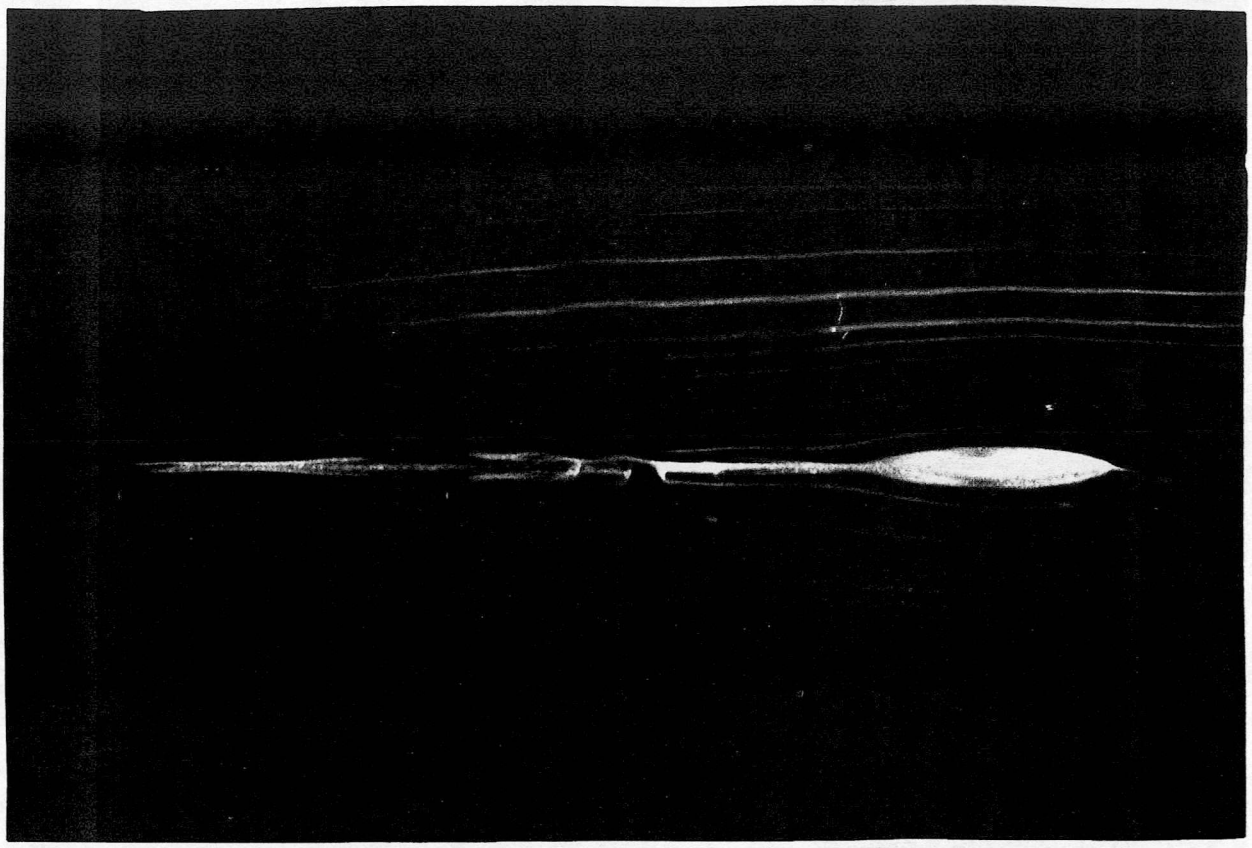

Fig. A1(a). Single bridge, low tide, midspan, V= 0.57 m/s : flow over bridge.

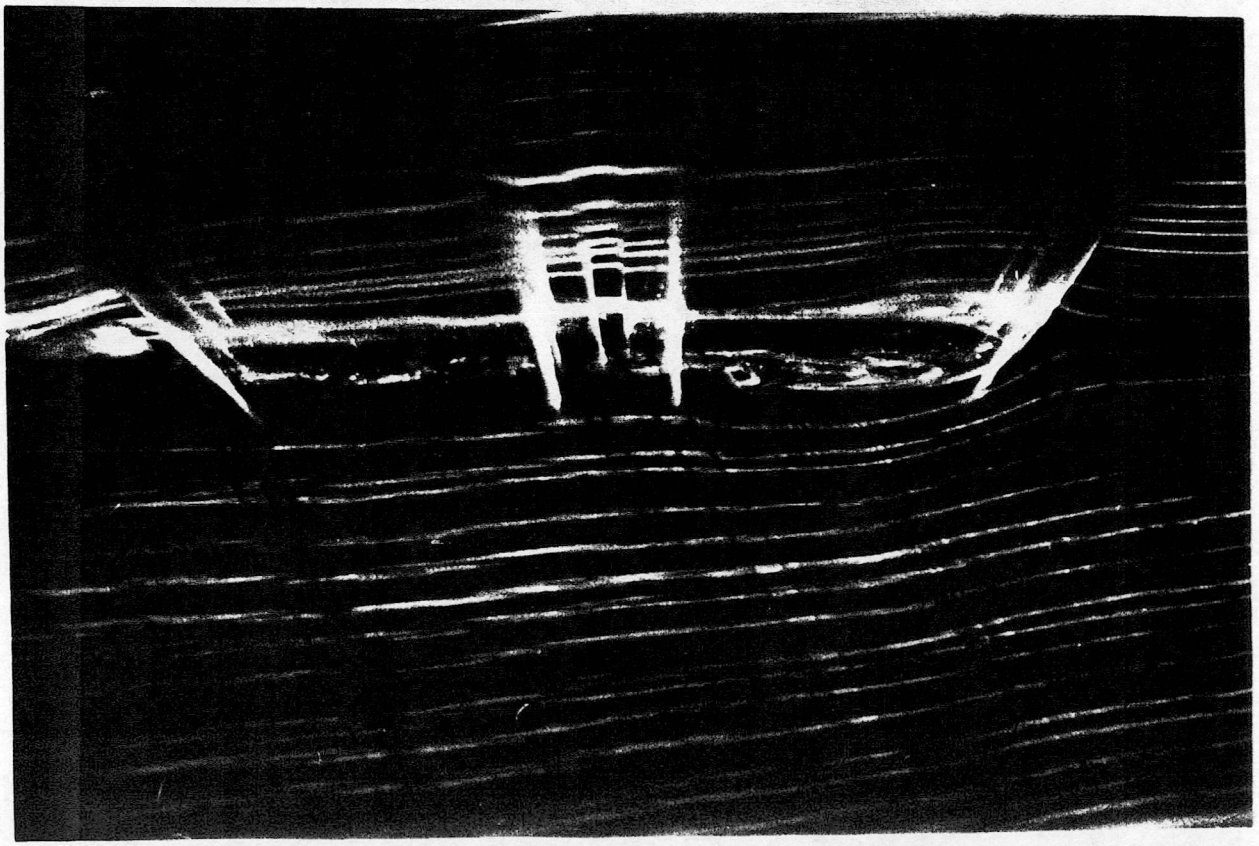

Fig. A1(b). Single bridge, low tide, midspan, V= 0.57 m/s : flow under bridge.

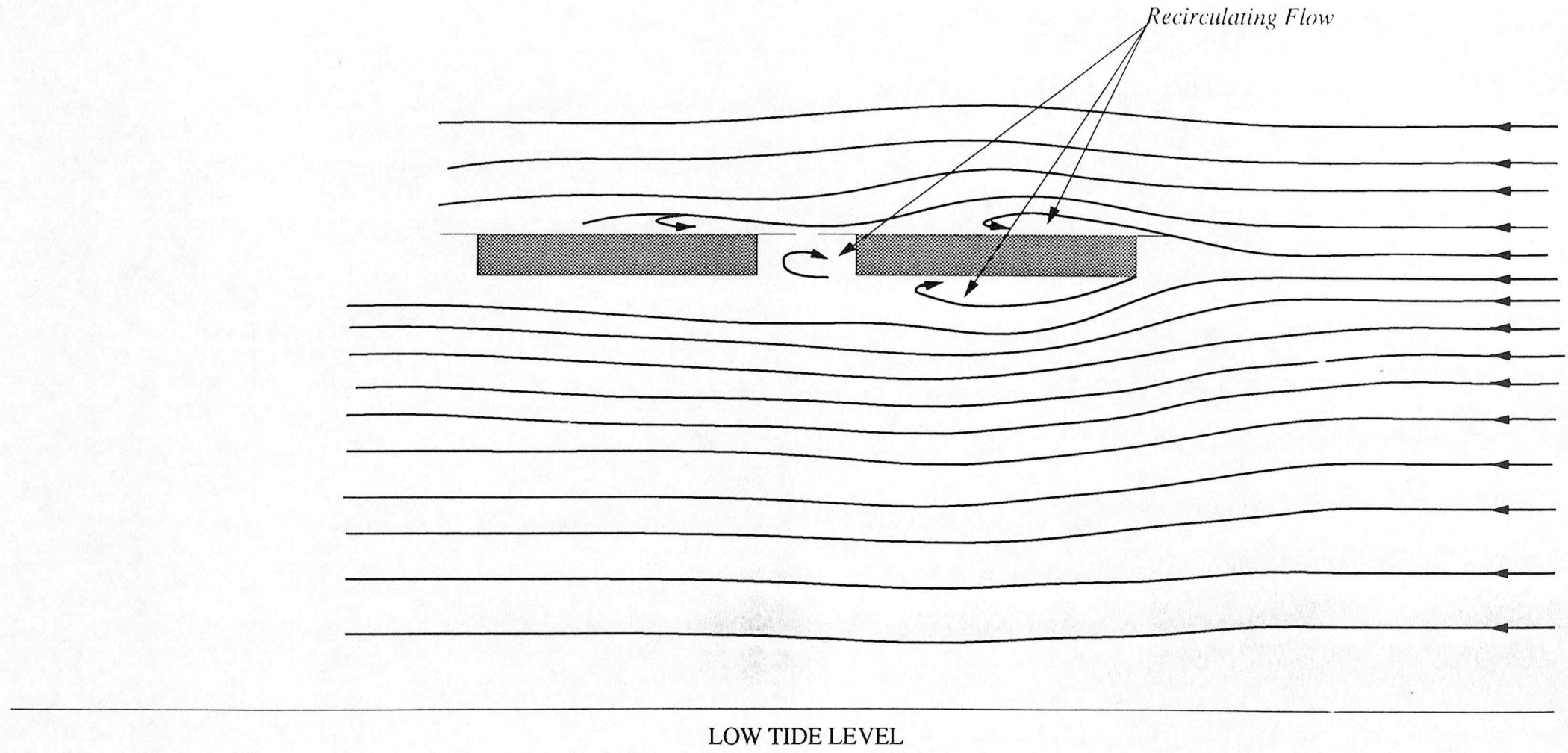

FIG. A1(c) : Flow pattern - single bridge, low tide, midspan, V = 0.57 m/s

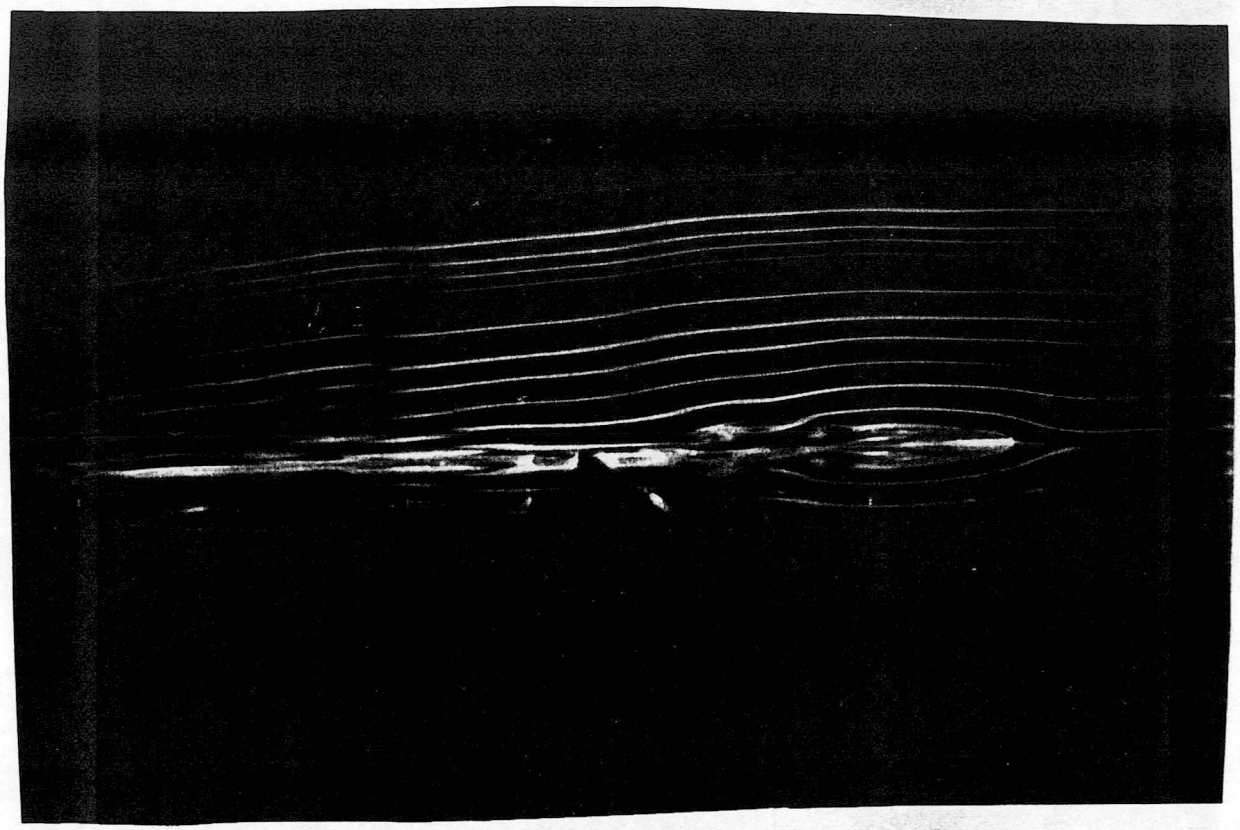

Fig. A2(a). Single bridge, high tide, midspan, V= 0.48 m/s : flow over bridge.

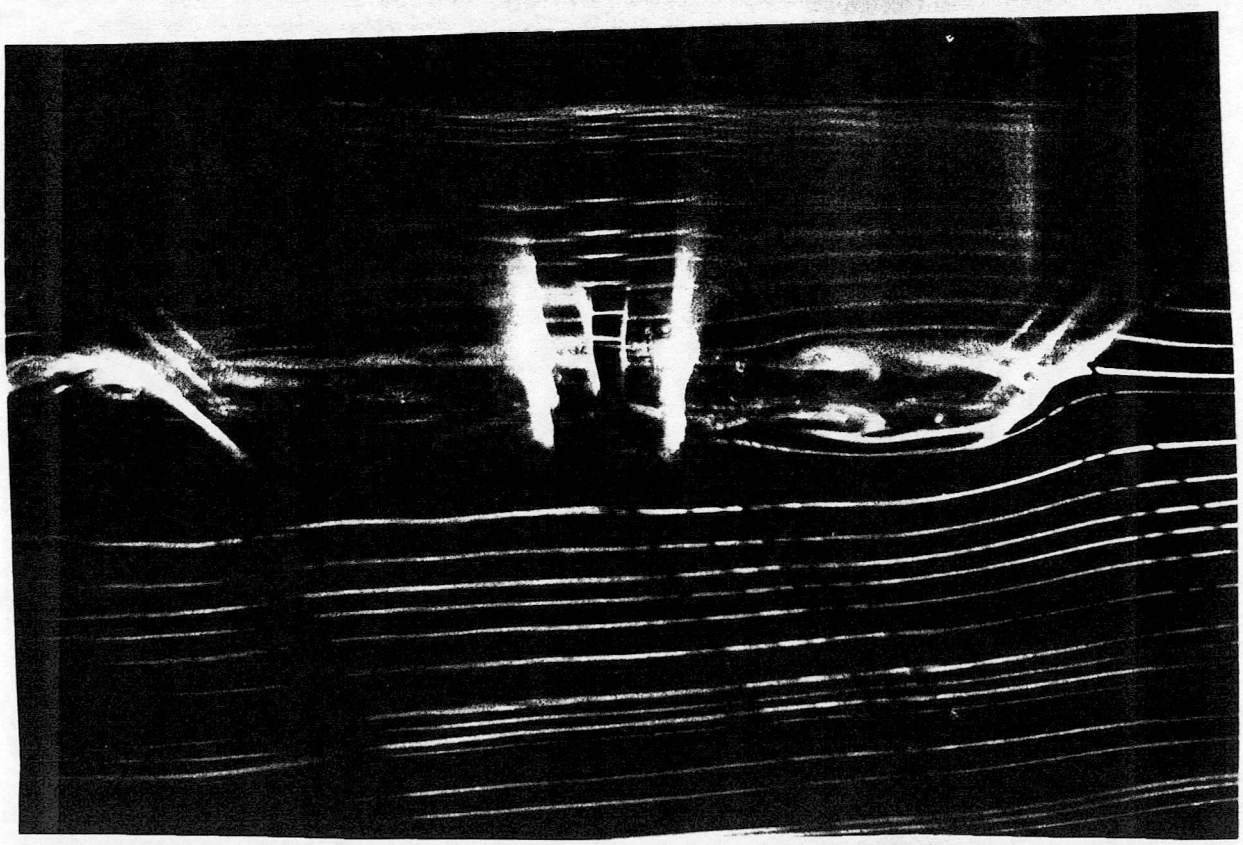

Fig. A2(b). Single bridge, high tide, midspan, V= 0.48 m/s : flow under bridge.

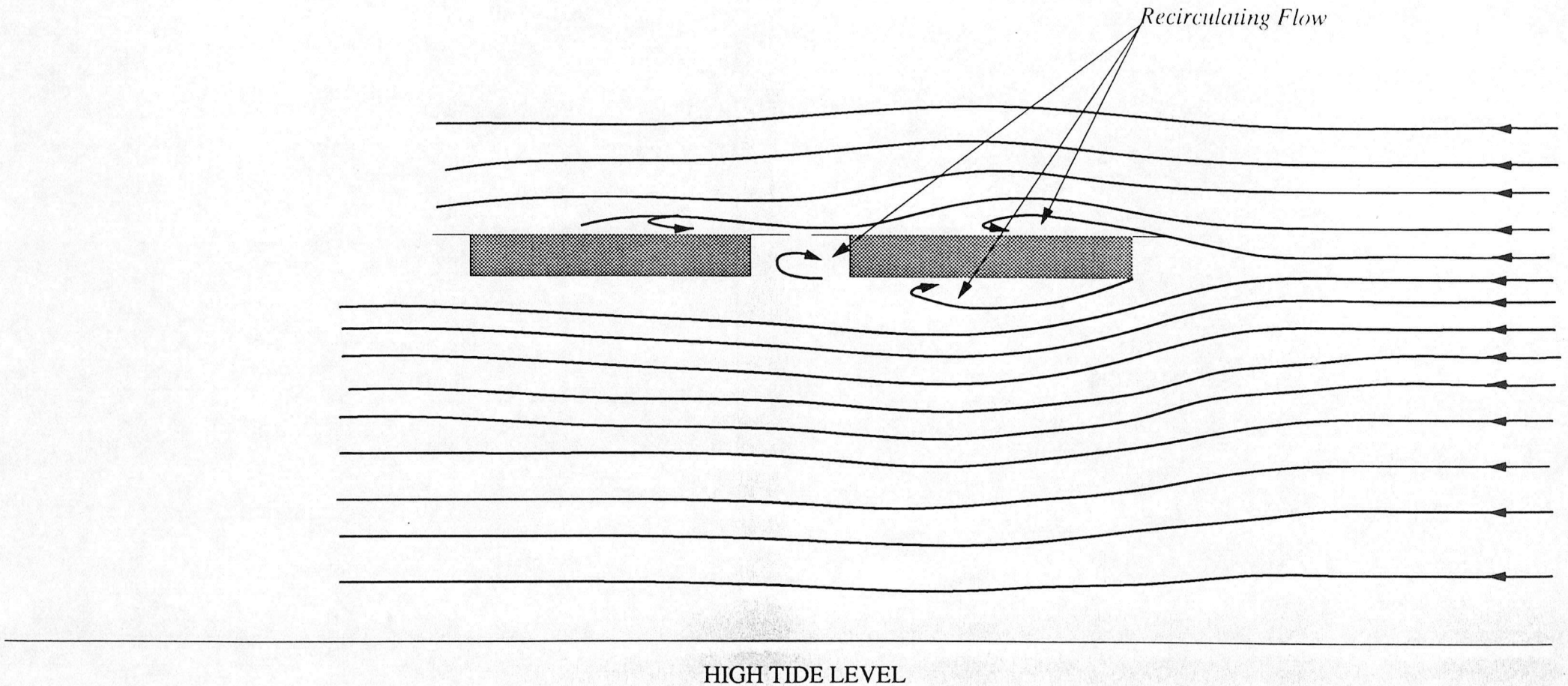

FIG. A2(c) : Flow pattern - single bridge, high tide, midspan, V = 0.48 m/s

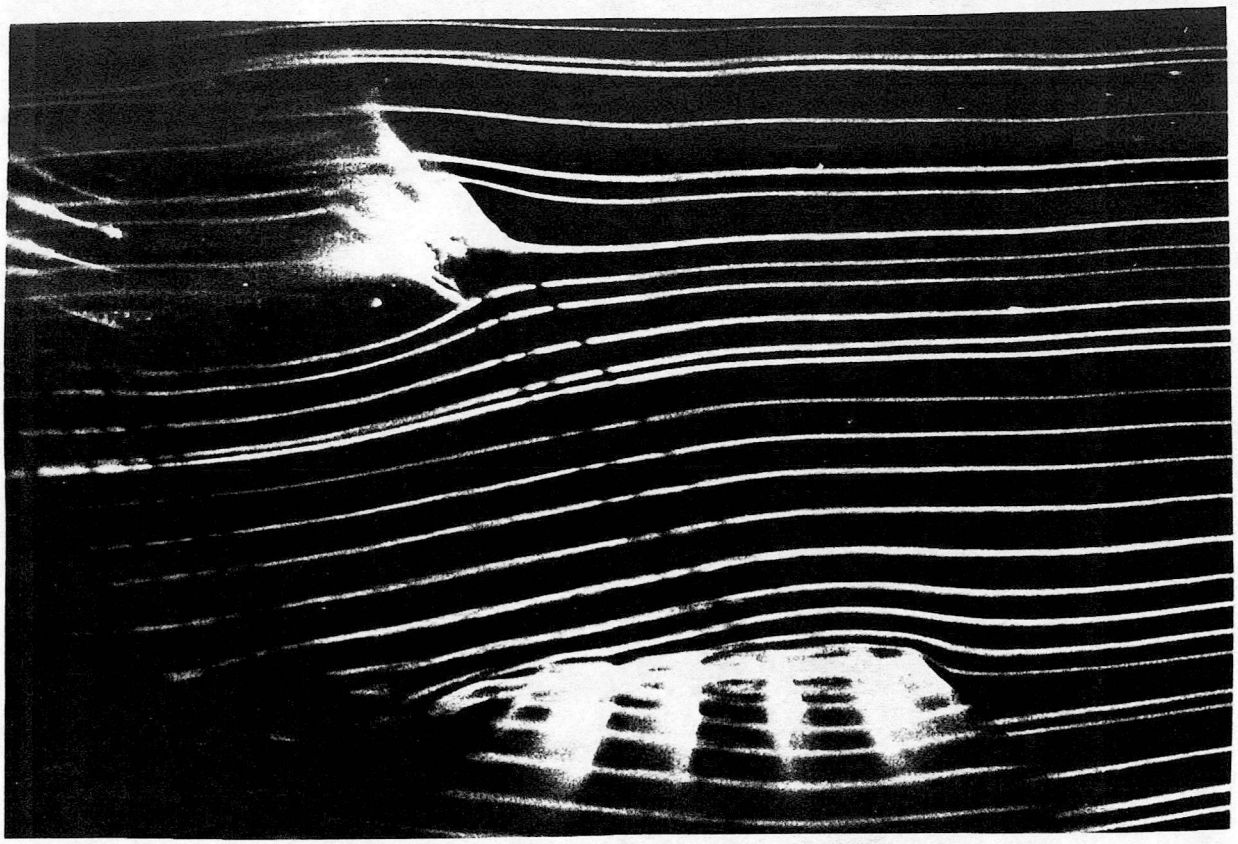

Fig. A3(a). Three bridges, low tide, midspan, V= 0.45 m/s : flow over windward bridge.

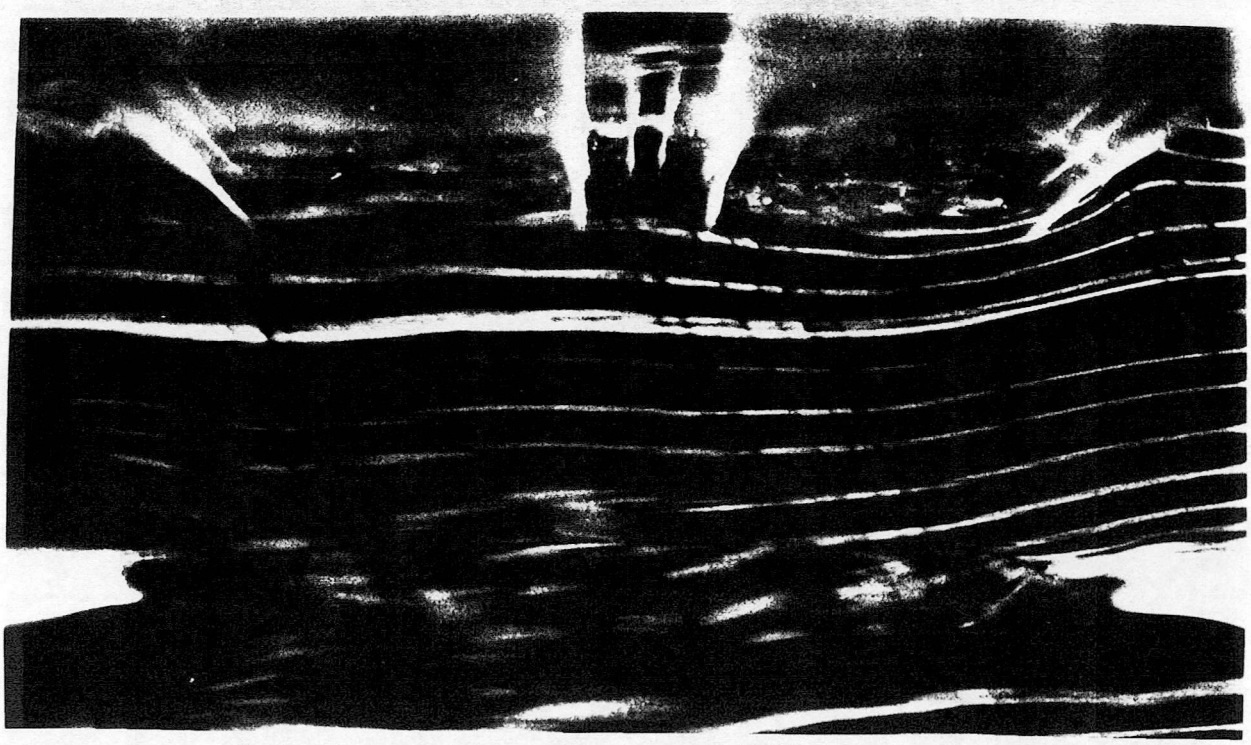

Fig. A3(b). Three bridges, low tide, midspan, V= 0.45 m/s : flow between bridges.

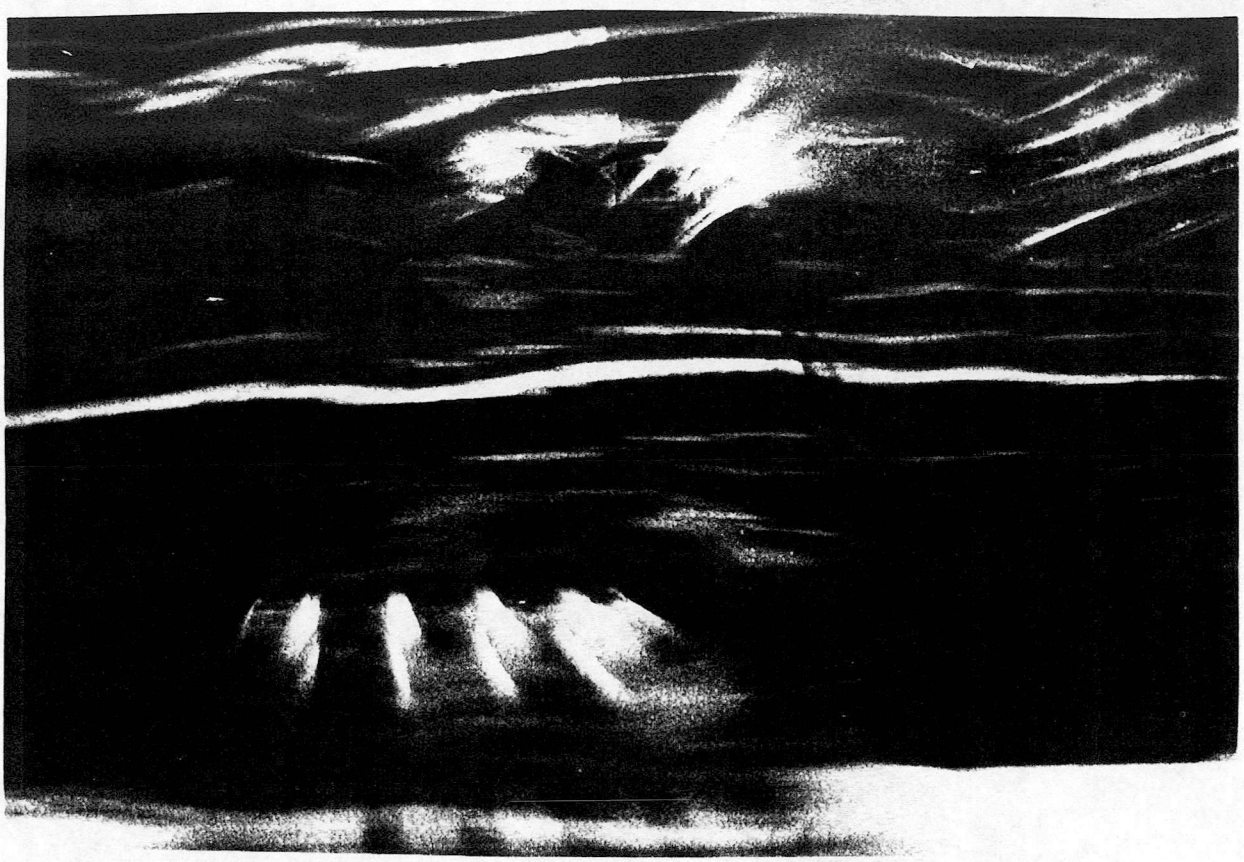

Fig. A3(c). Three bridges, low tide, midspan, V= 0.45 m/s : flow over leeward bridge.

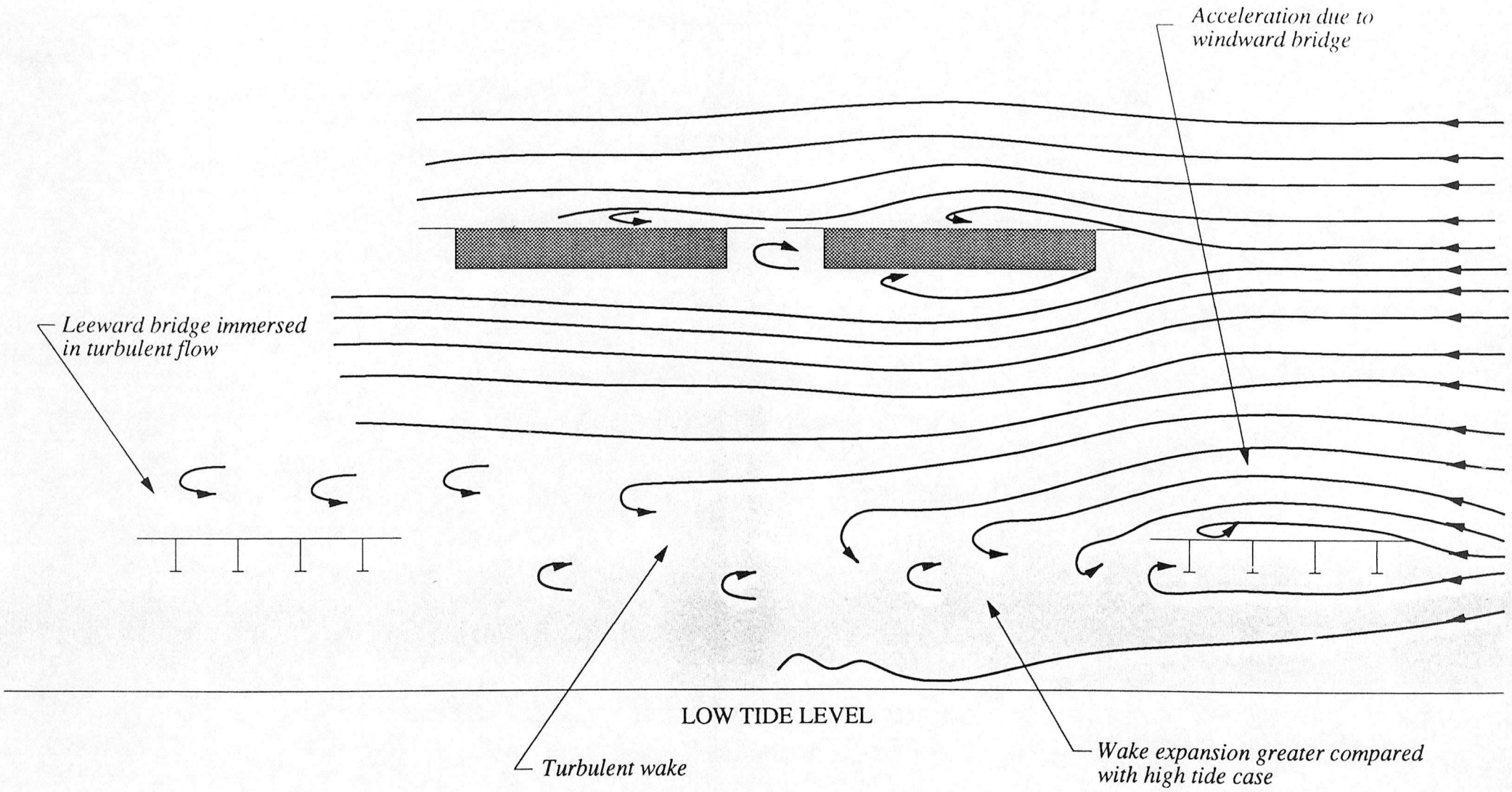

FIG. A3(d) : Flow pattern - three bridges, low tide, midspan, V = 0.45 m/s

Fig. A4(a). Three bridges, high tide, midspan, V= 0.48 m/s : flow over windward bridge.

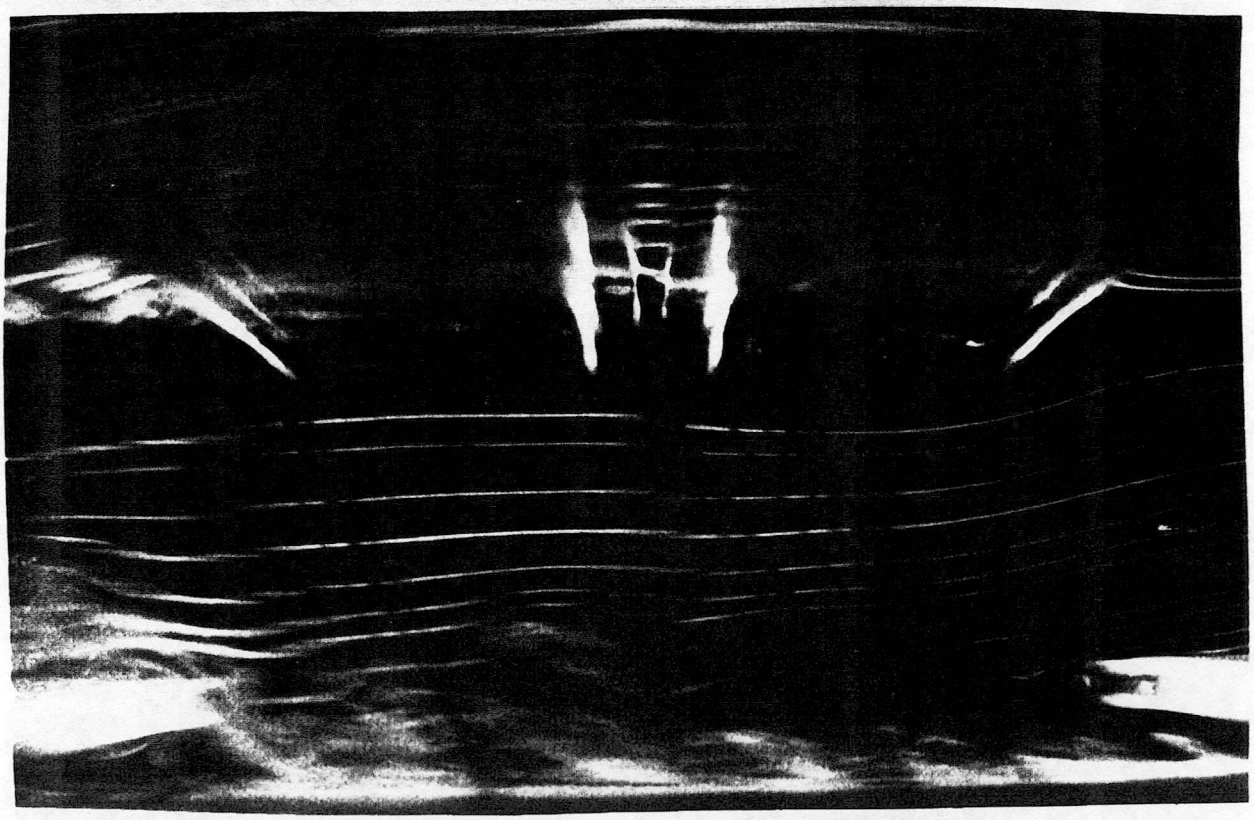

Fig. A4(b). Three bridges, high tide, midspan, V= 0.48 m/s : flow between bridges.

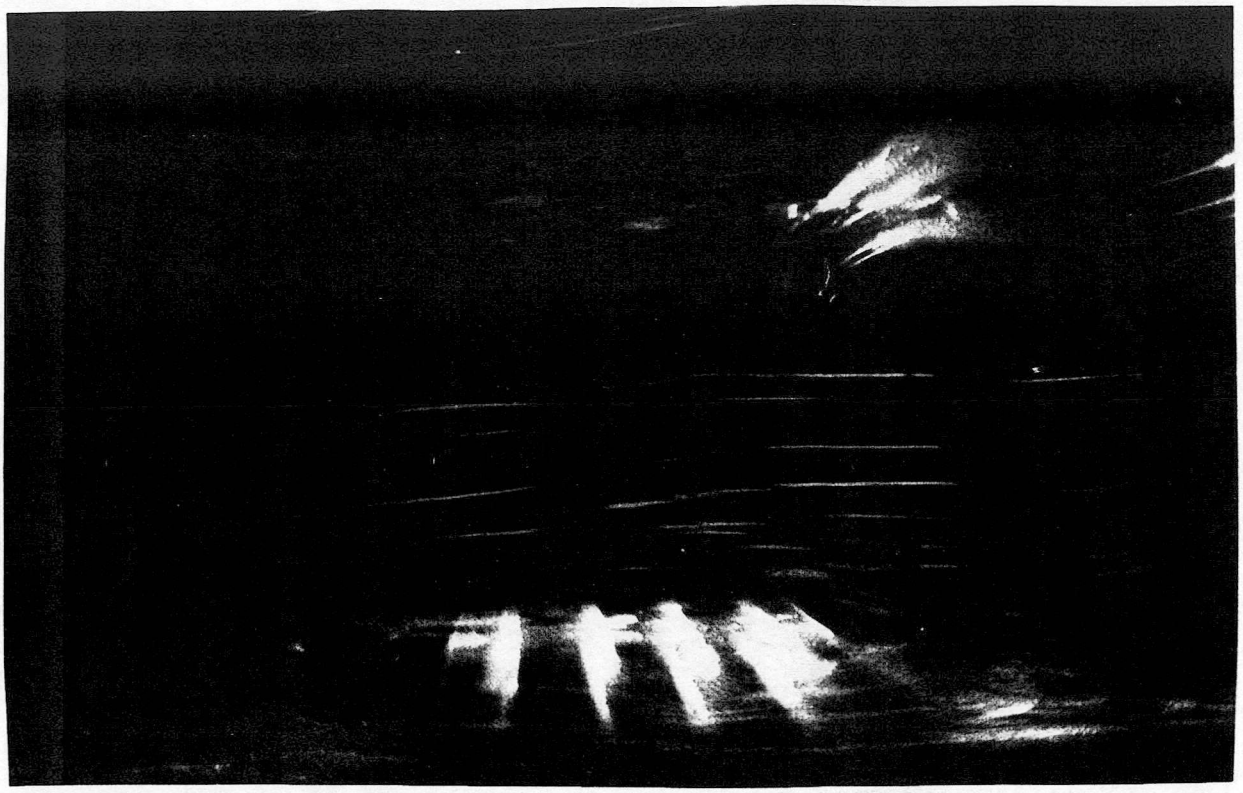

Fig. A4(c). Three bridges, high tide, midspan, V= 0.48 m/s : flow over leeward bridge.

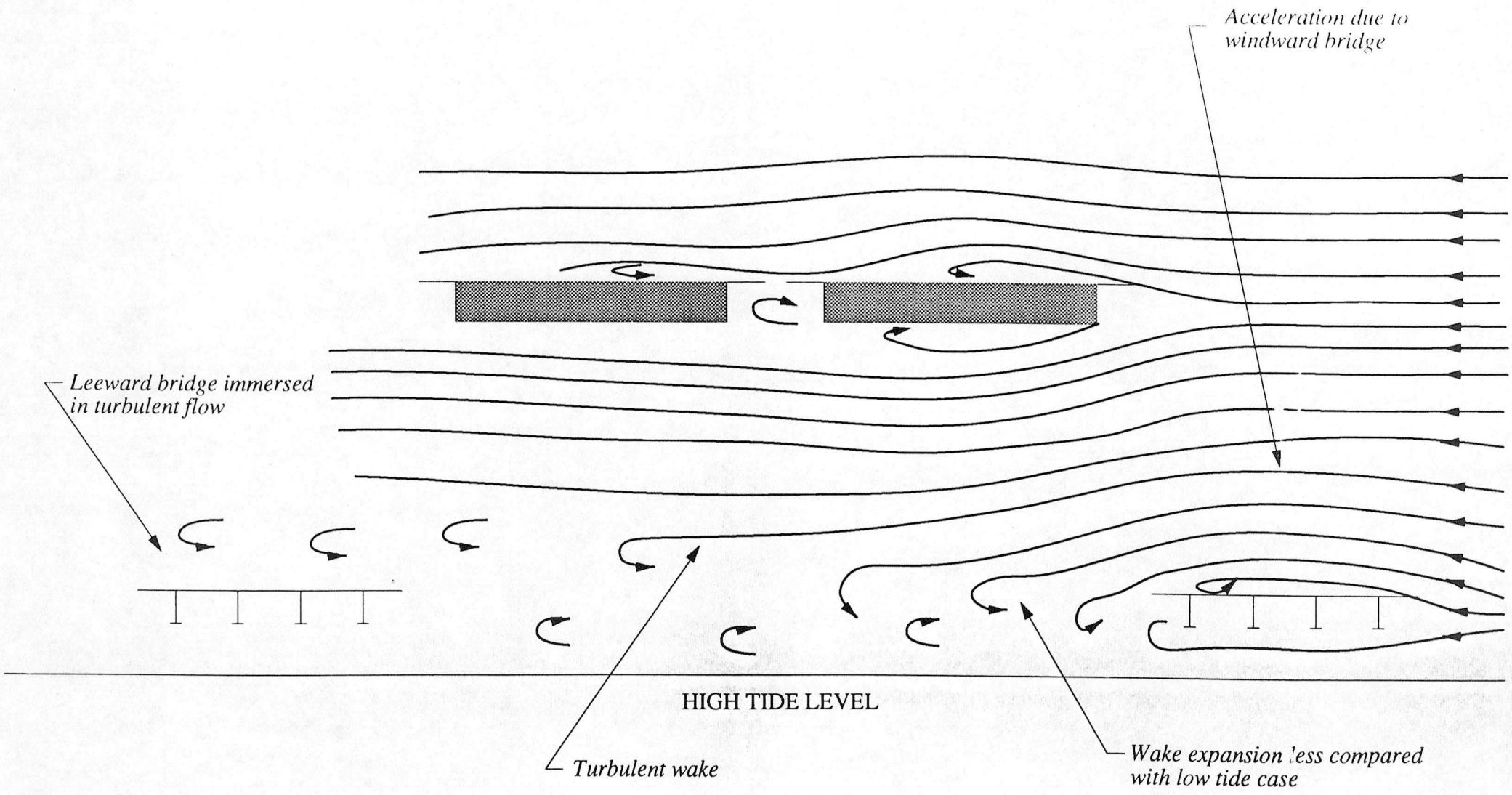

FIG. A4(d) : Flow pattern - three bridges, high tide, midspan, V = 0.48 m/s

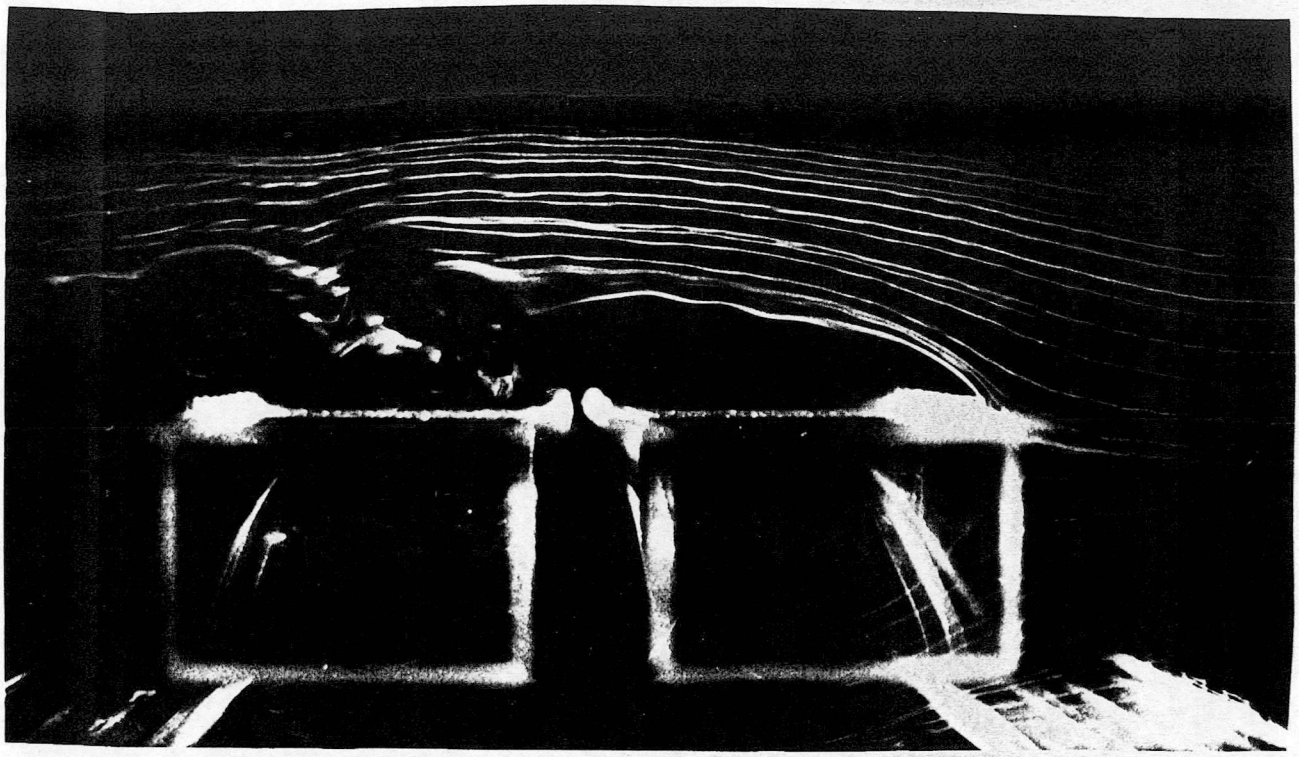

Fig. A5(a). Three bridges, low tide, haunch, V= 0.45 m/s : flow over high level bridge.

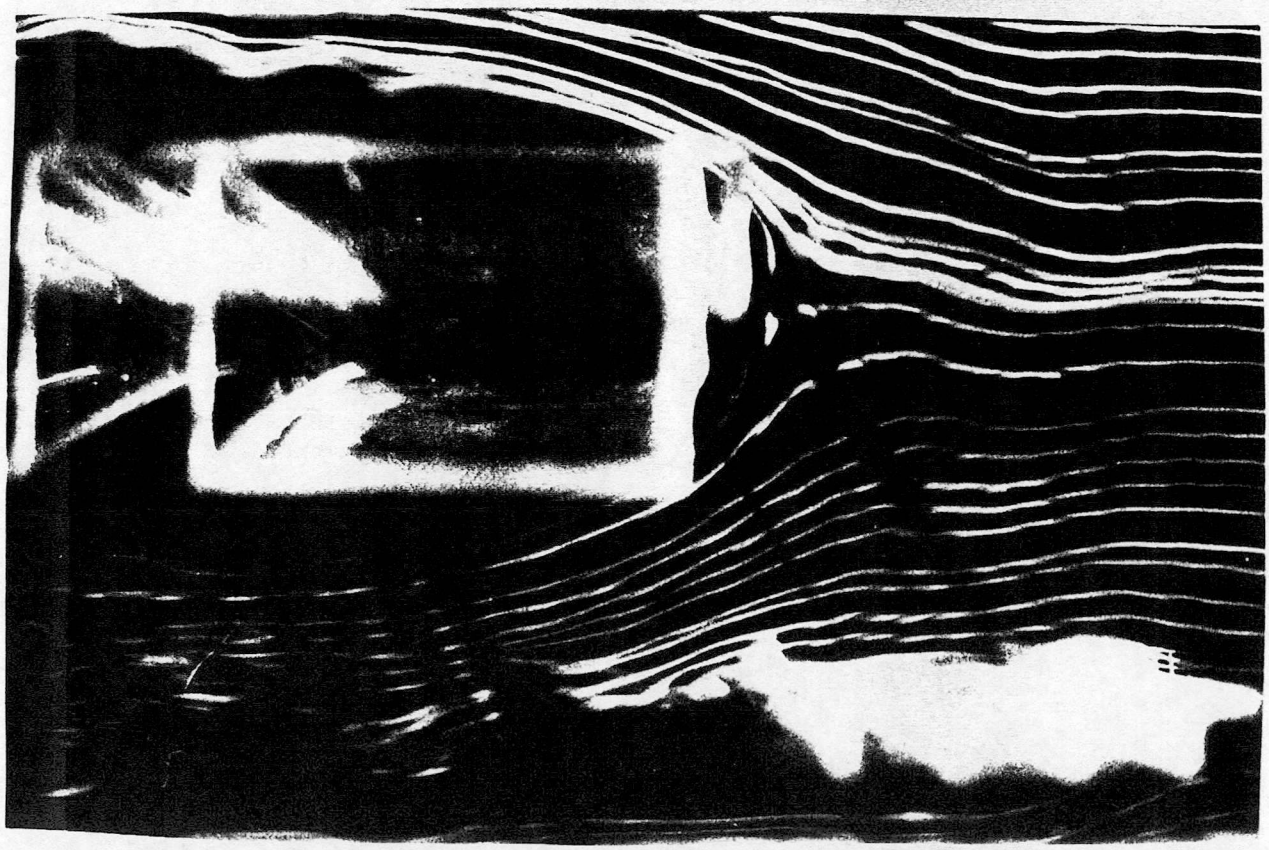

Fig. A5(b). Three bridges, low tide, haunch, V= 0.45 m/s : flow over windward bridge.

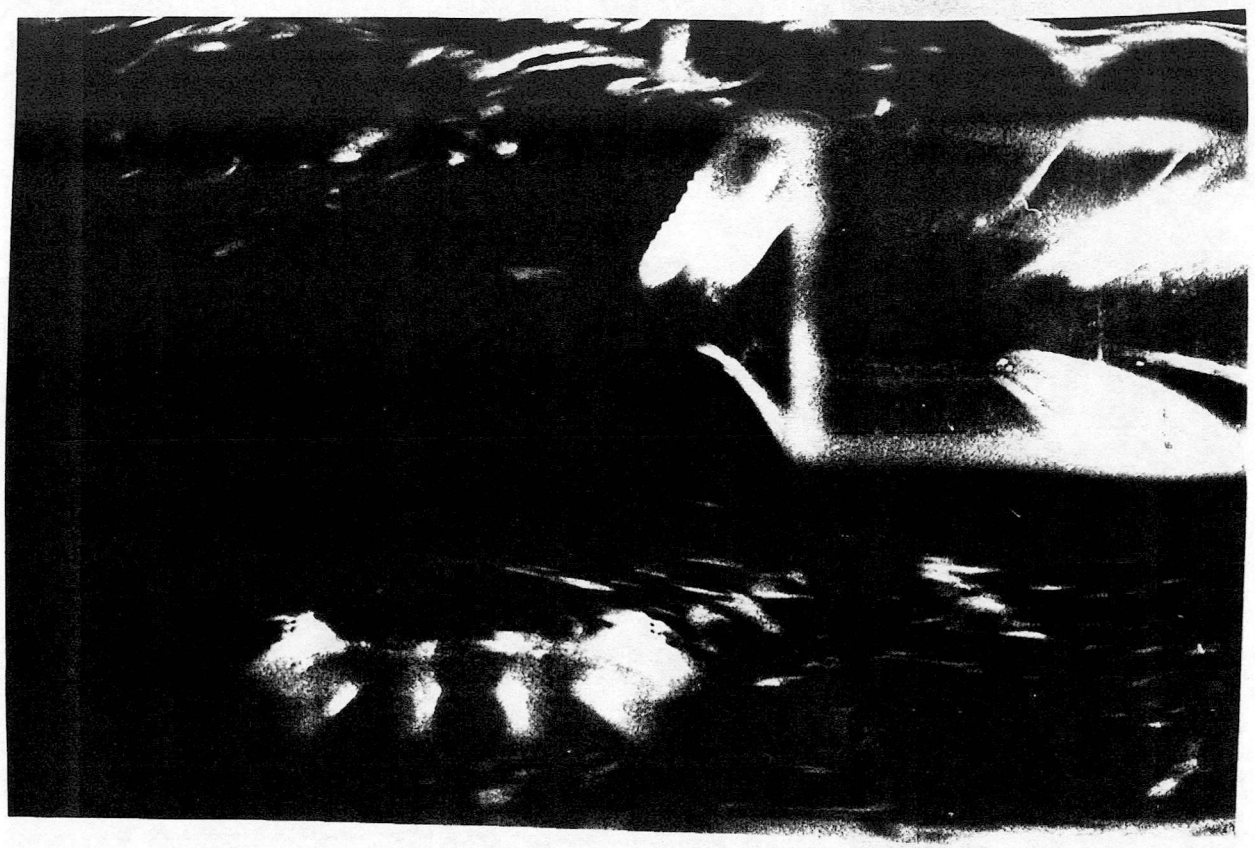

Fig. A5(c). Three bridges, low tide, haunch, V= 0.45 m/s : flow over leeward bridge.

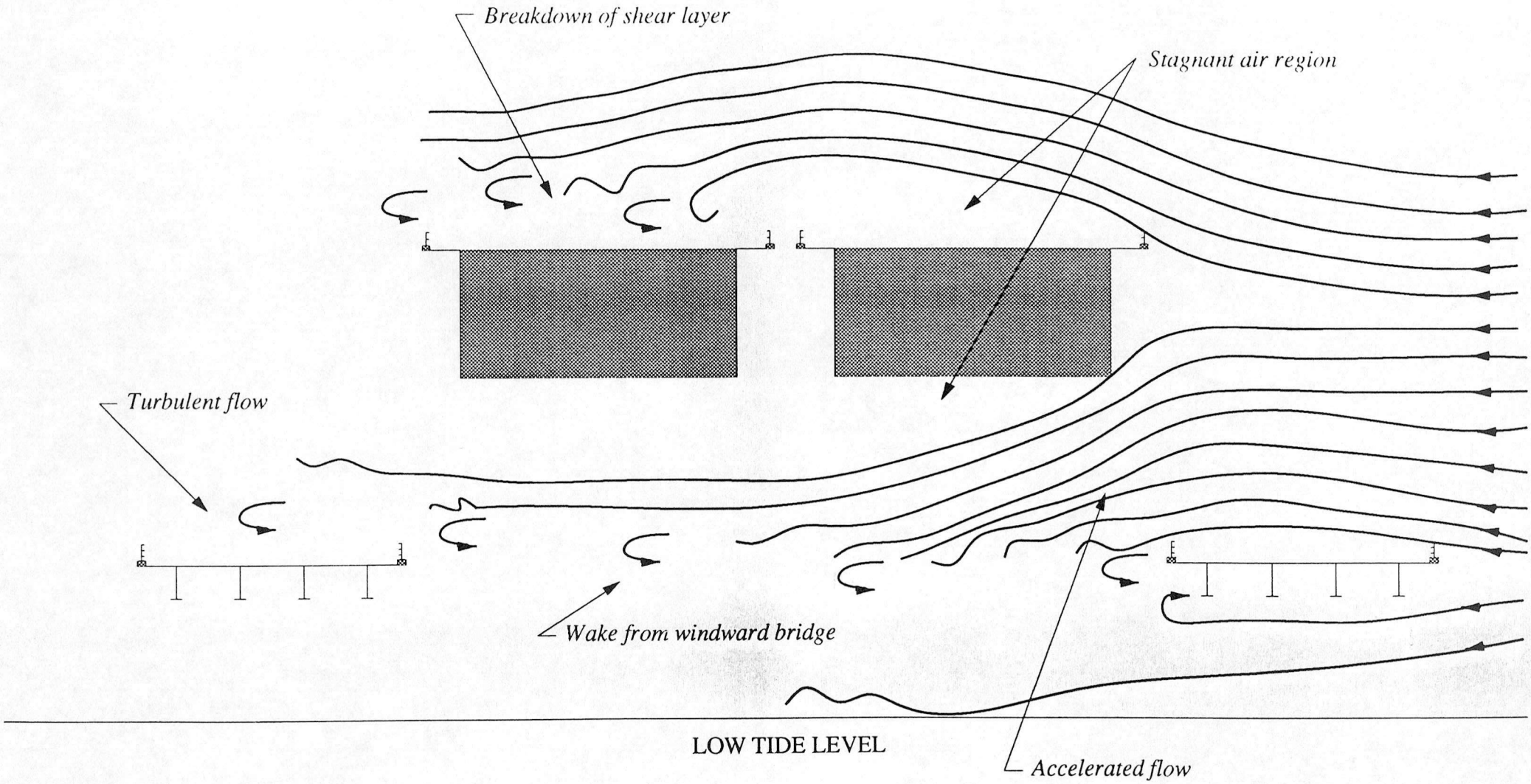

FIG. A5(d) : Flow pattern - three bridges, low tide, haunch, V = 0.45 m/s

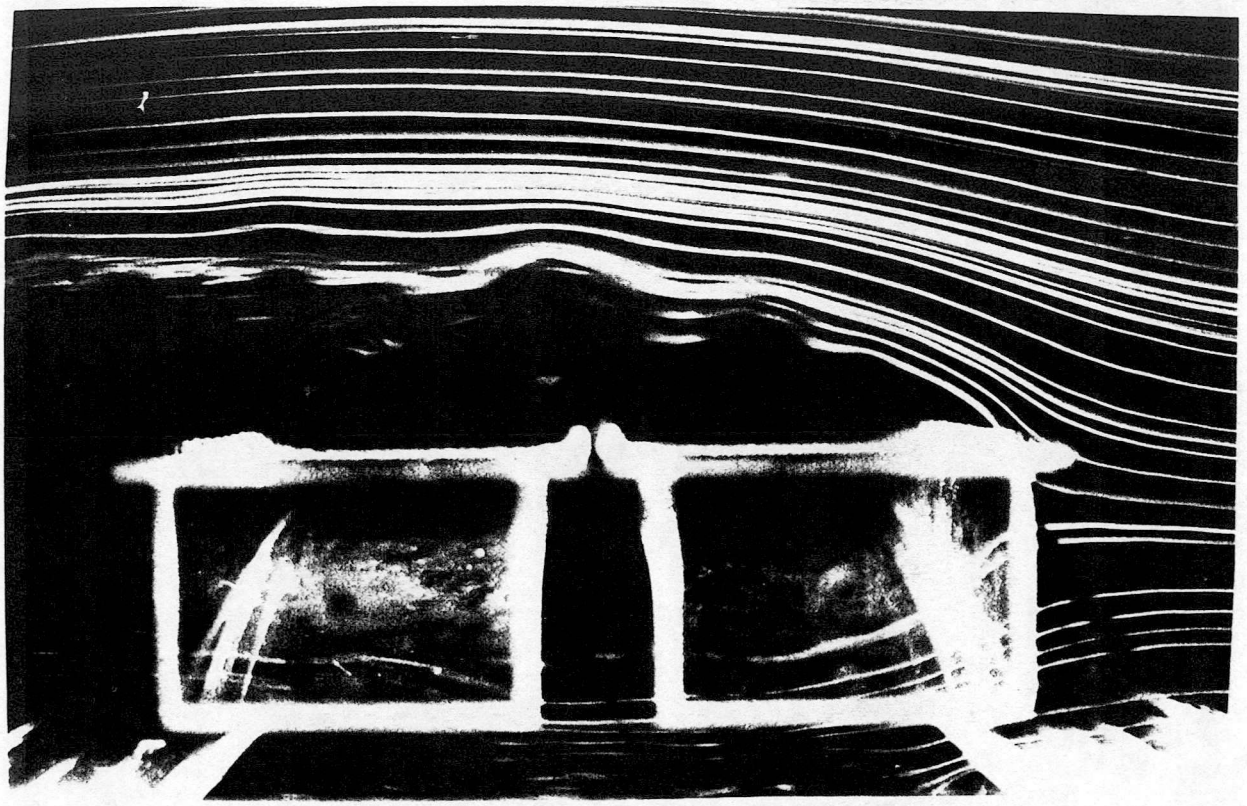

Fig. A6(a). Three bridges, low tide, haunch, V= 0.88 m/s : flow over high level bridge.

Fig. A6(b). Three bridges, low tide, haunch, V= 0.88 m/s : flow over windward bridge.

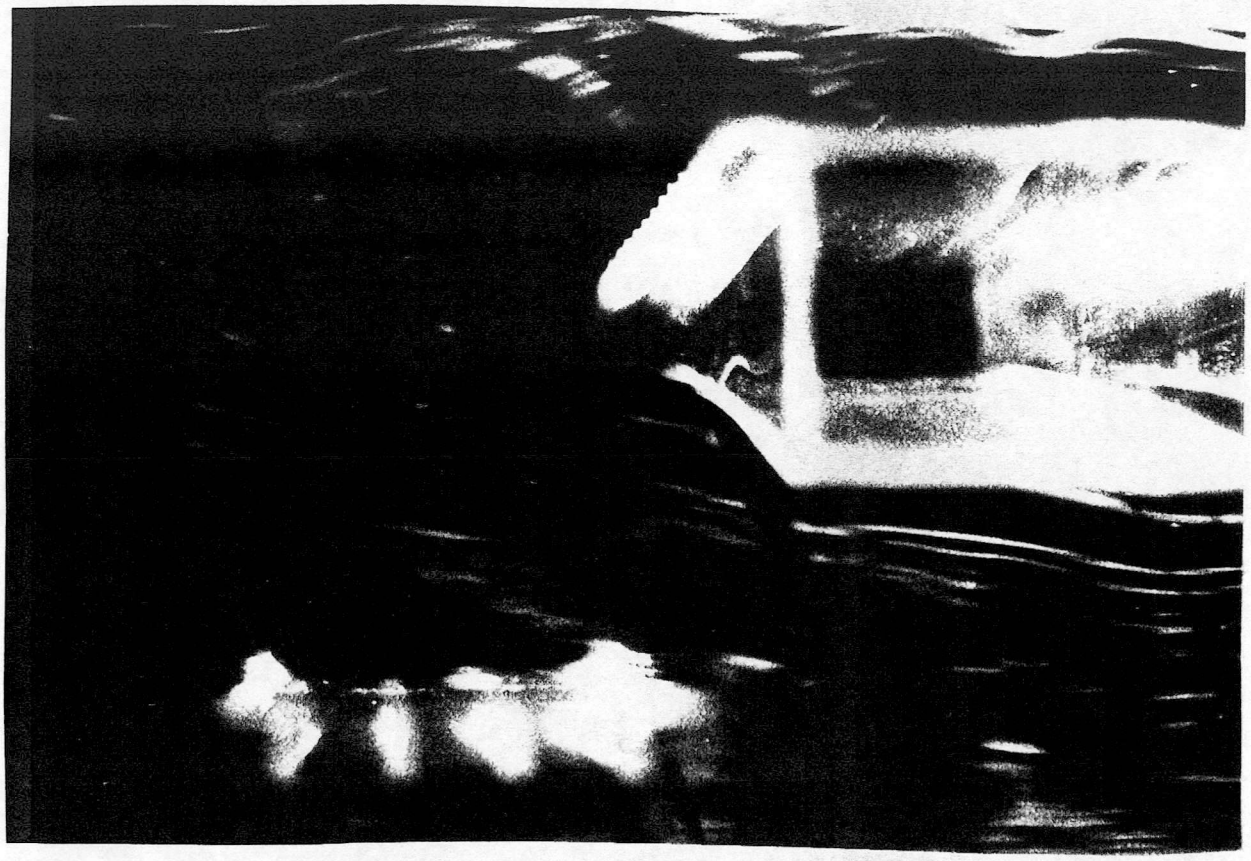

Fig. A6(c). Three bridges, low tide, haunch, V= 0.88 m/s : flow over leeward bridge.

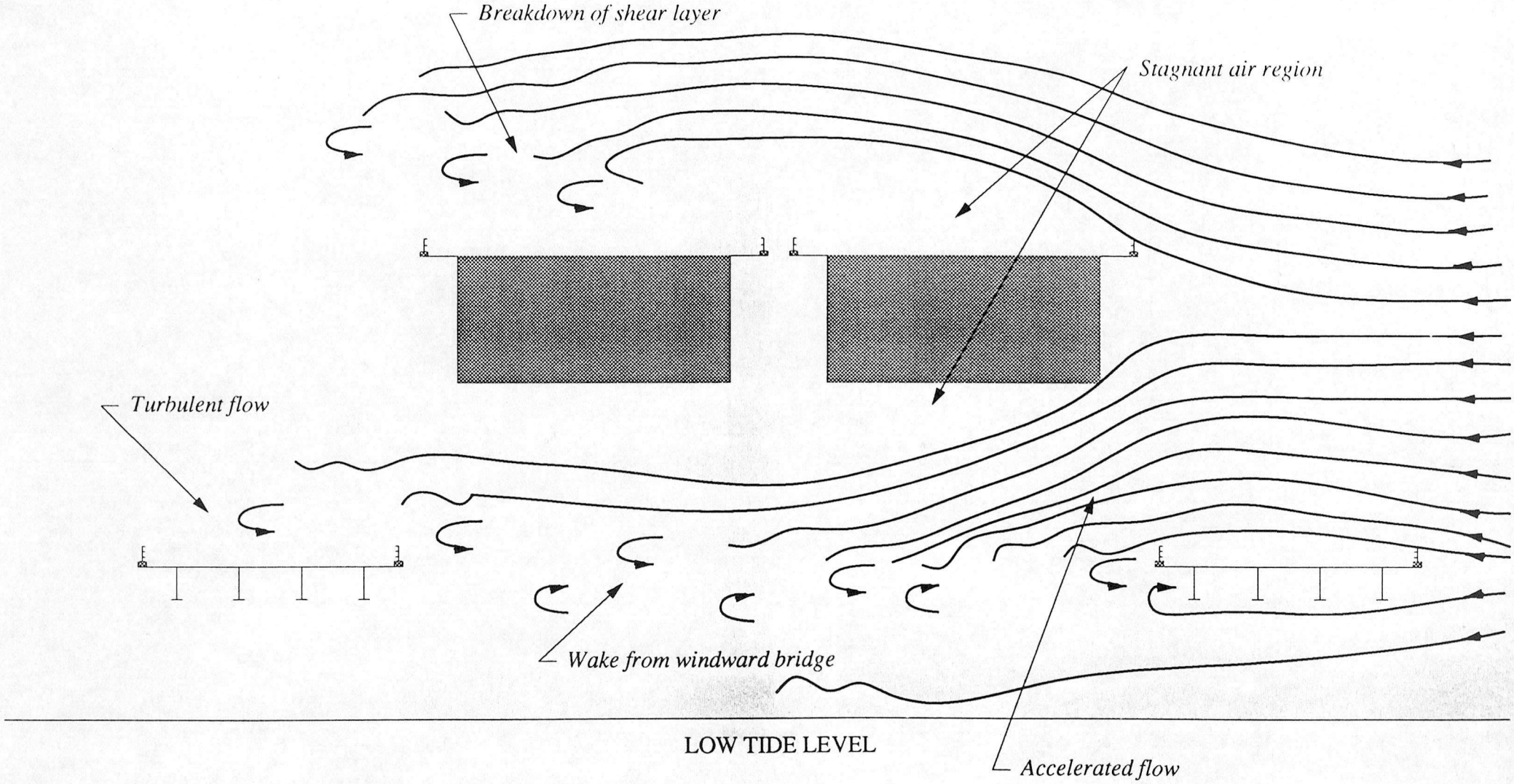

FIG. A6(d) : Flow pattern - three bridges, low tide, haunch, V = 0.88 m/s

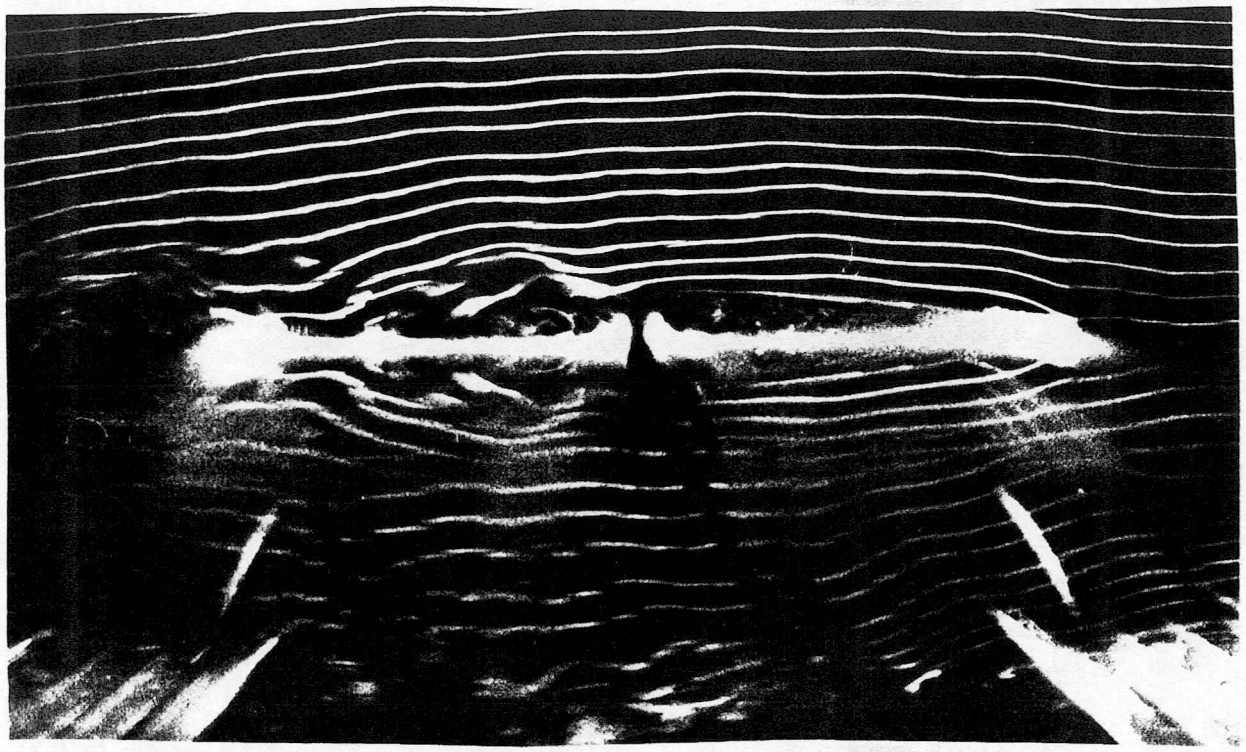

Fig. A7(a). Three bridges, low tide, reduced width, midspan, V= 0.56 m/s : flow over high level bridge.

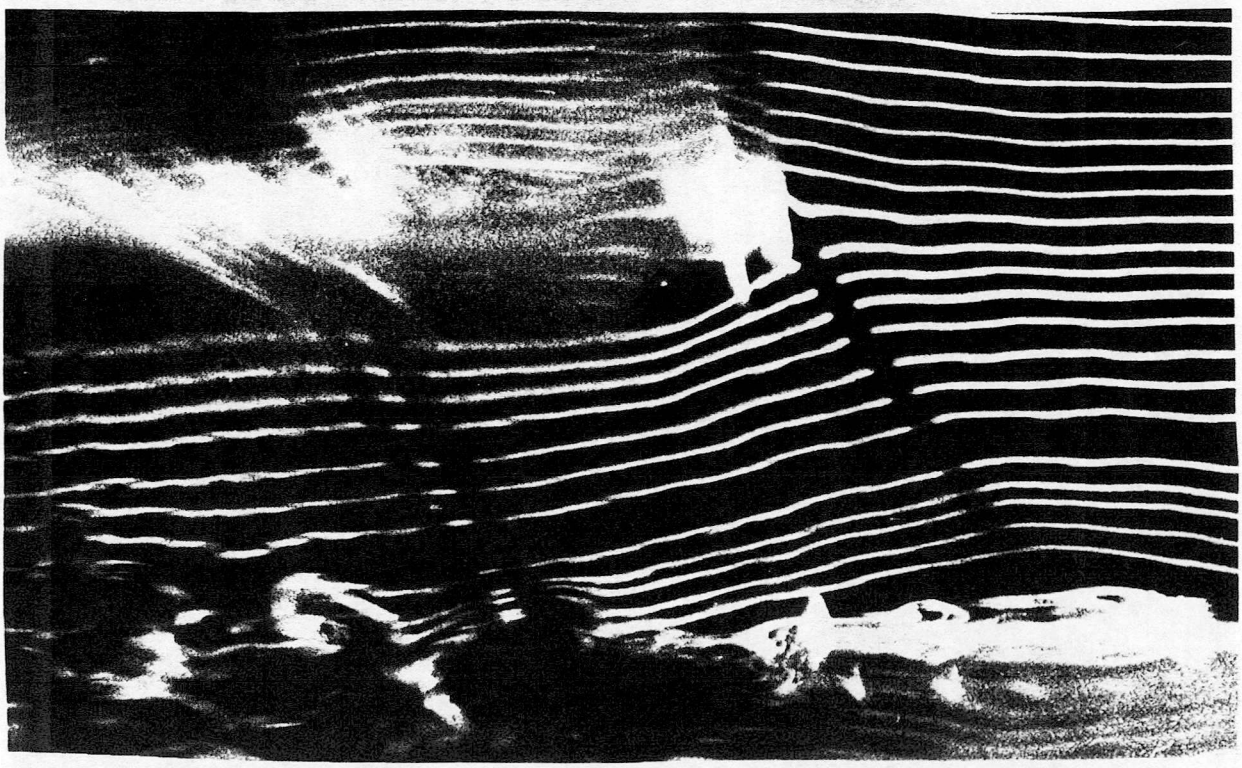

Fig. A7(b). Three bridges, low tide, reduced width, midspan, V= 0.56 m/s : flow over windward bridge.

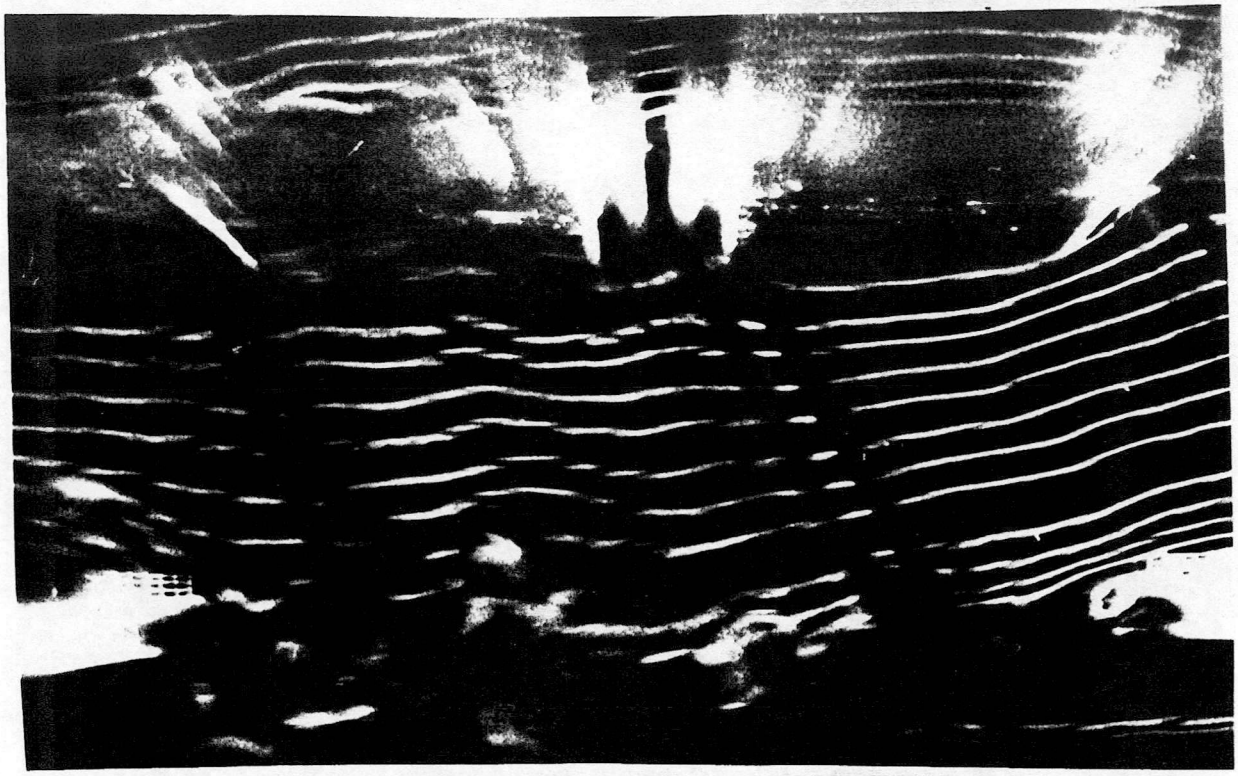

Fig. A7(c). Three bridges, low tide, reduced width, midspan, V= 0.56 m/s : flow between bridges.

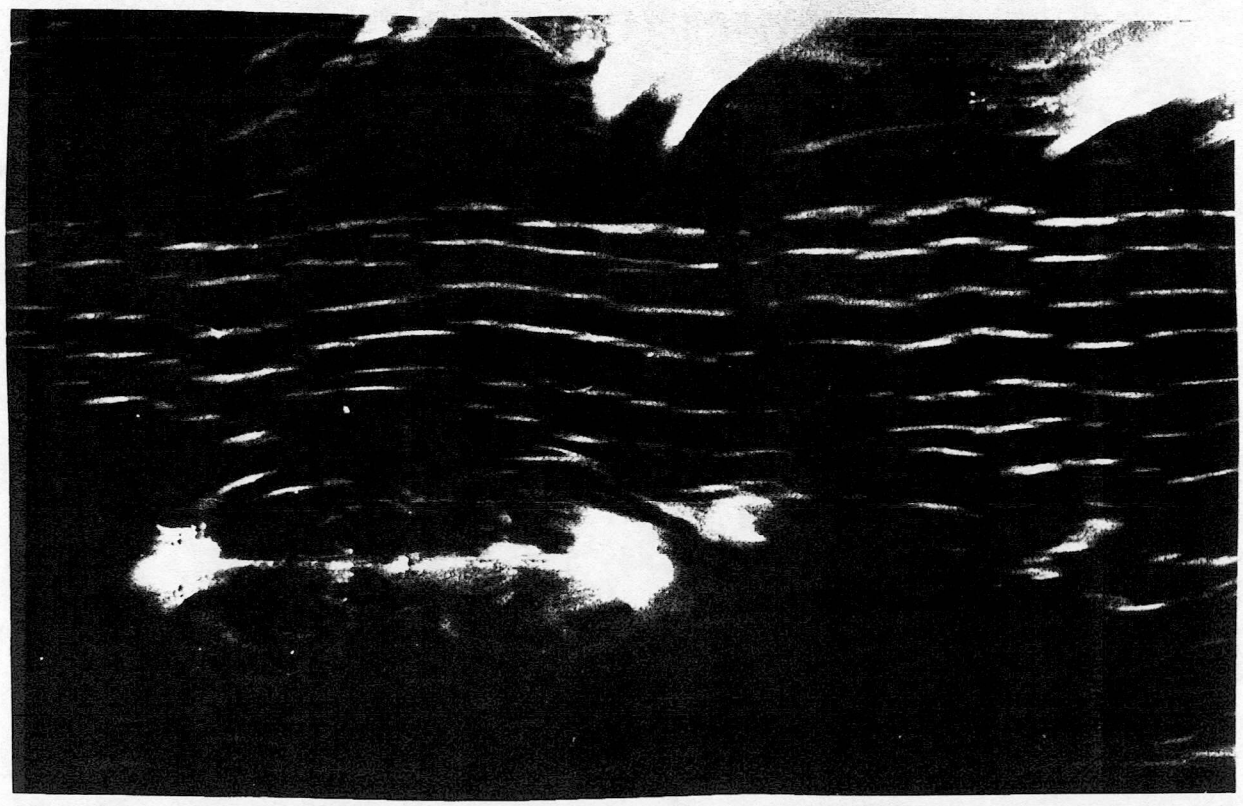

Fig. A7(d). Three bridges, low tide, reduced width, midspan, V= 0.56 m/s : flow over leeward bridge.

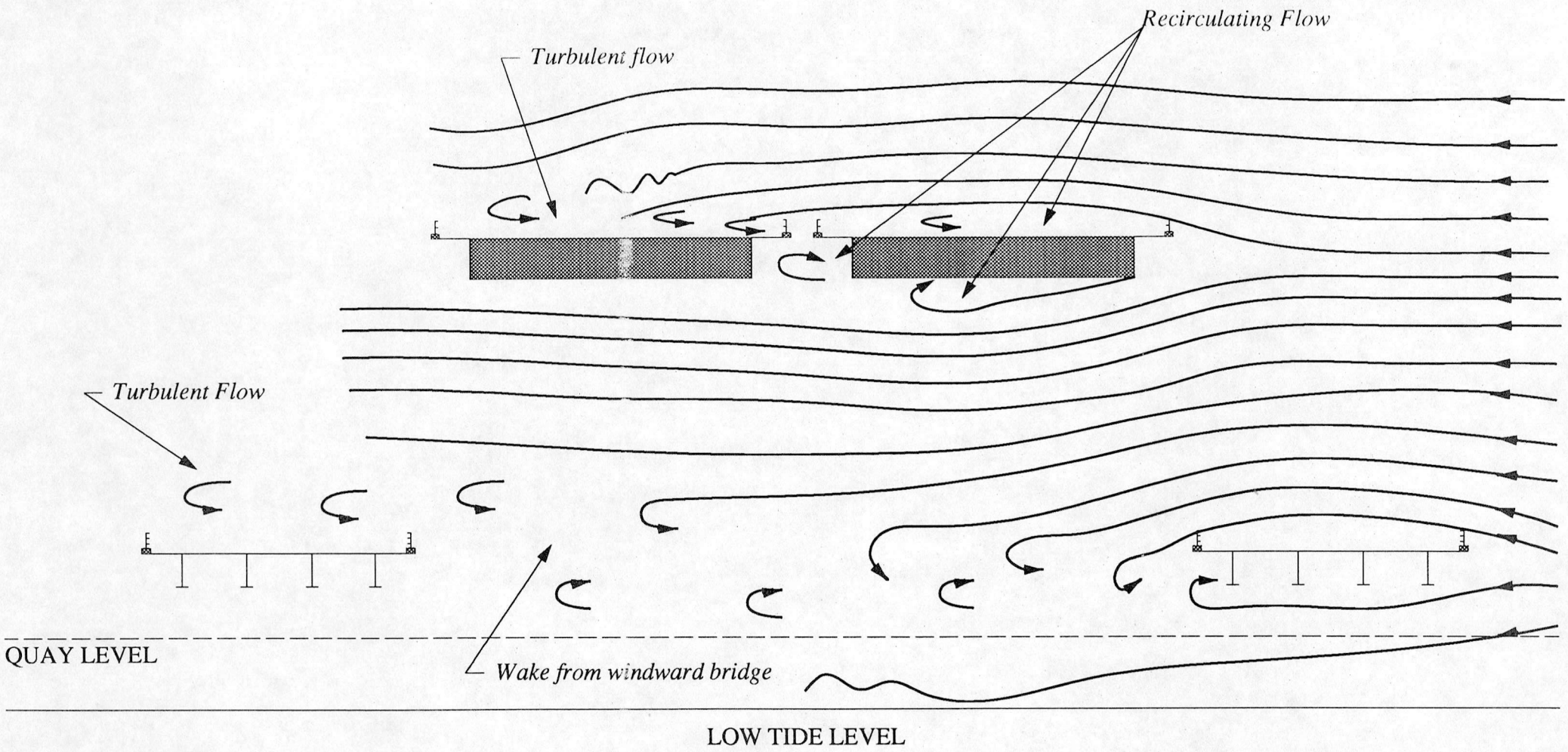

FIG. A7(e) : Flow pattern - three bridges, low tide, reduced width, midspan, V = 0.56 m/s

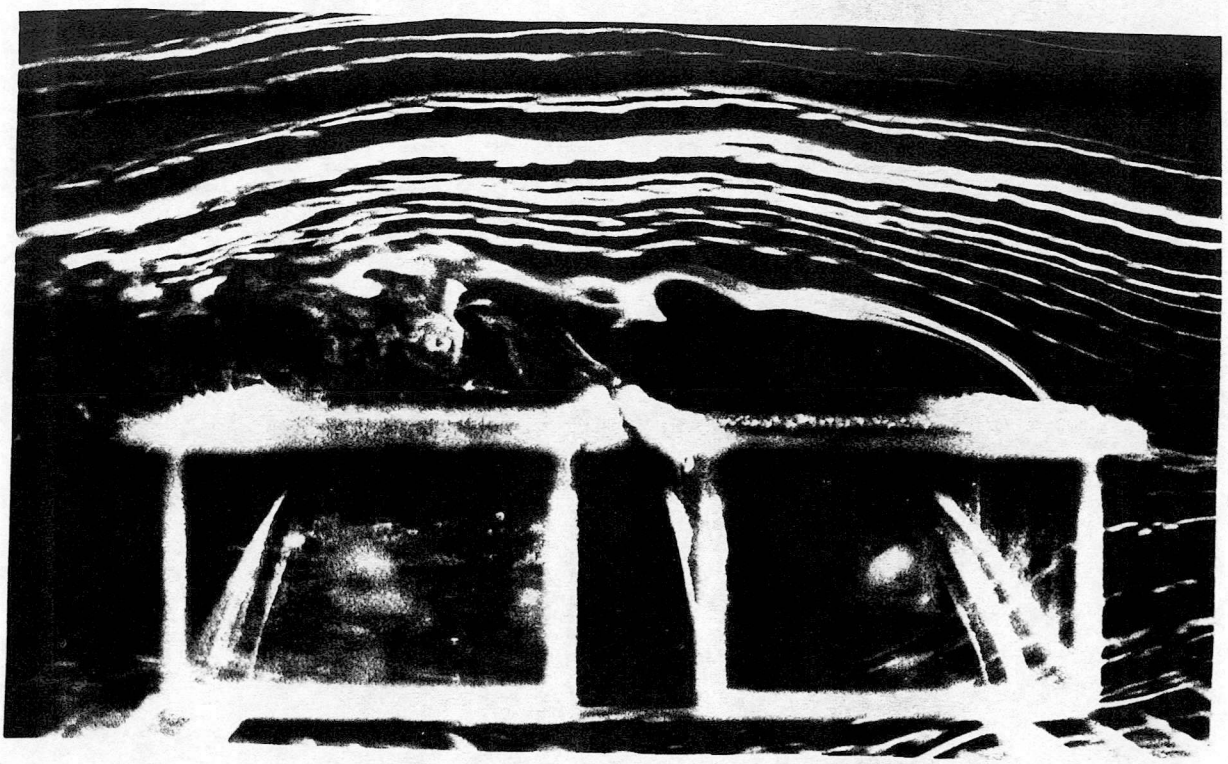

Fig. A8(a). Three bridges, low tide, reduced width, haunch, V= 0.56 m/s : flow over high level bridge.

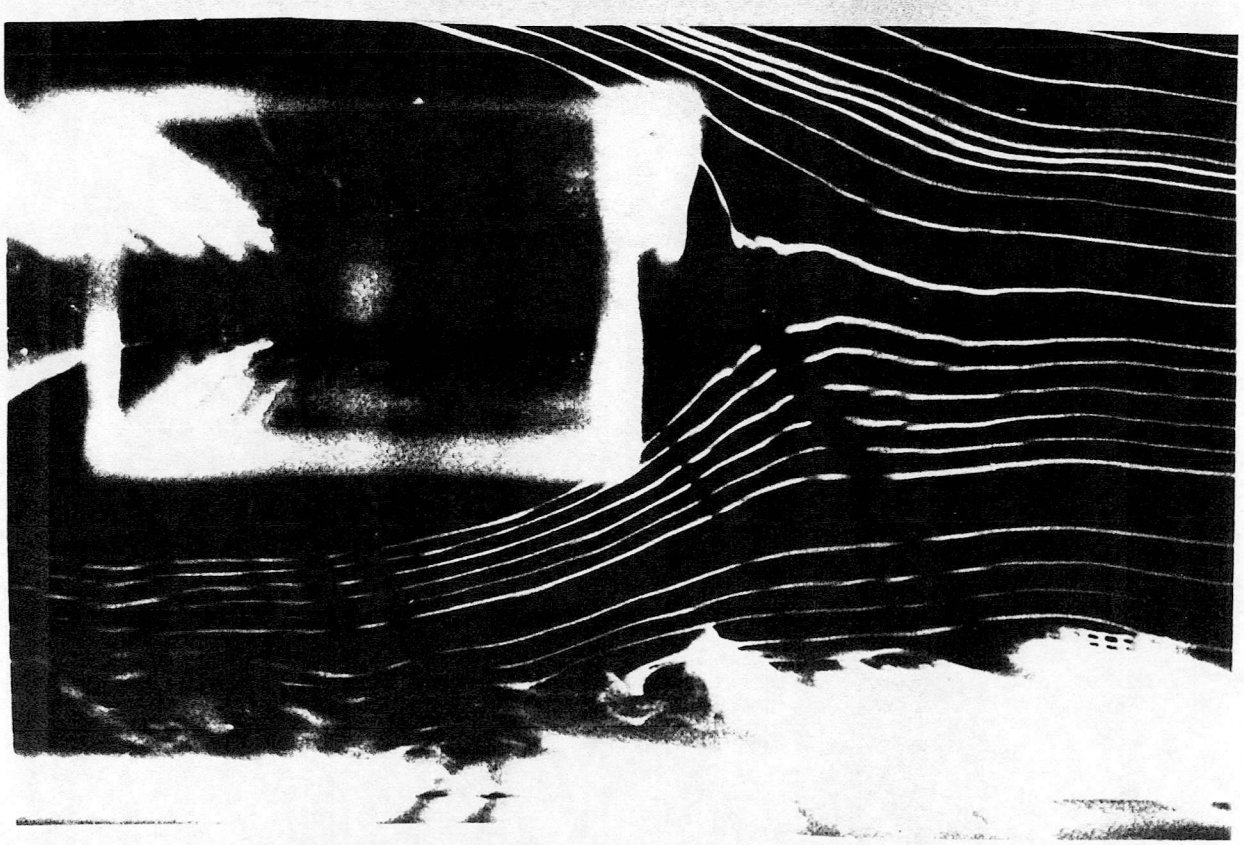

Fig. A8(b). Three bridges, low tide, reduced width, haunch, V= 0.56 m/s : flow over windward bridge.

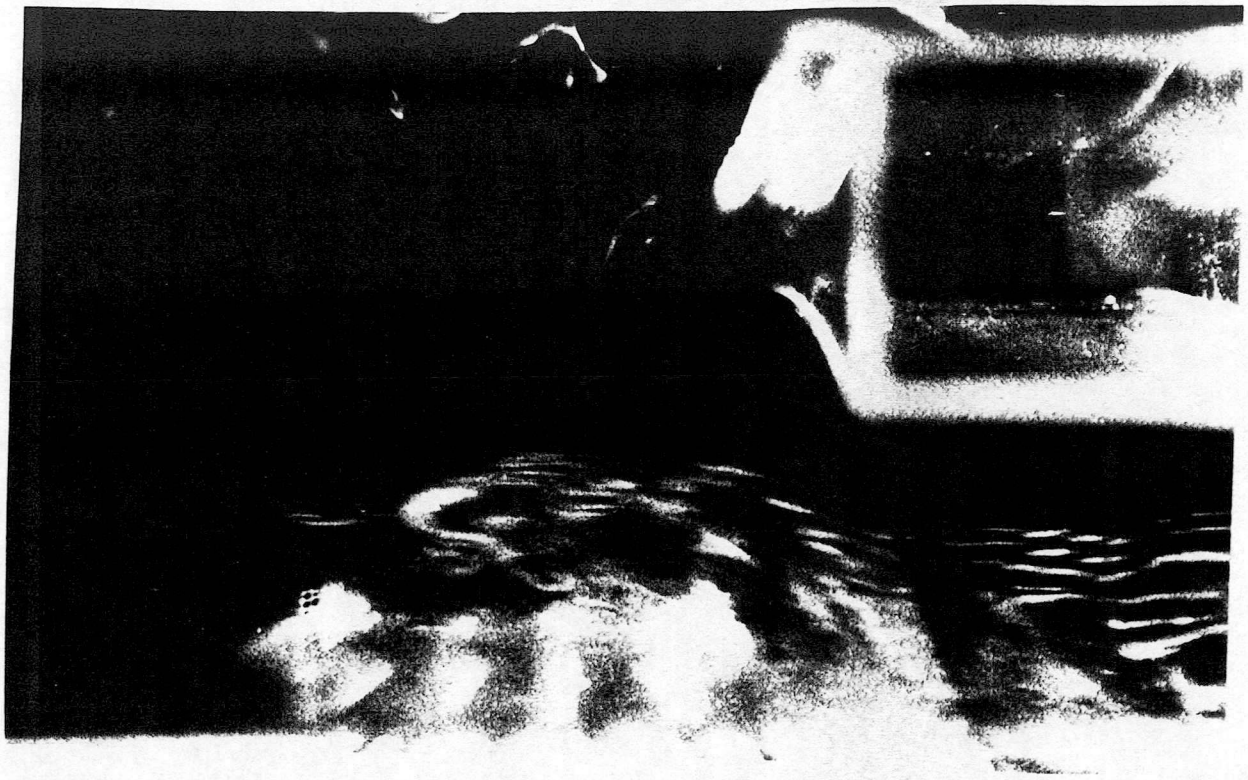

Fig. A8(c). Three bridges, low tide, reduced width, haunch, V= 0.56 m/s : flow over leeward bridge.

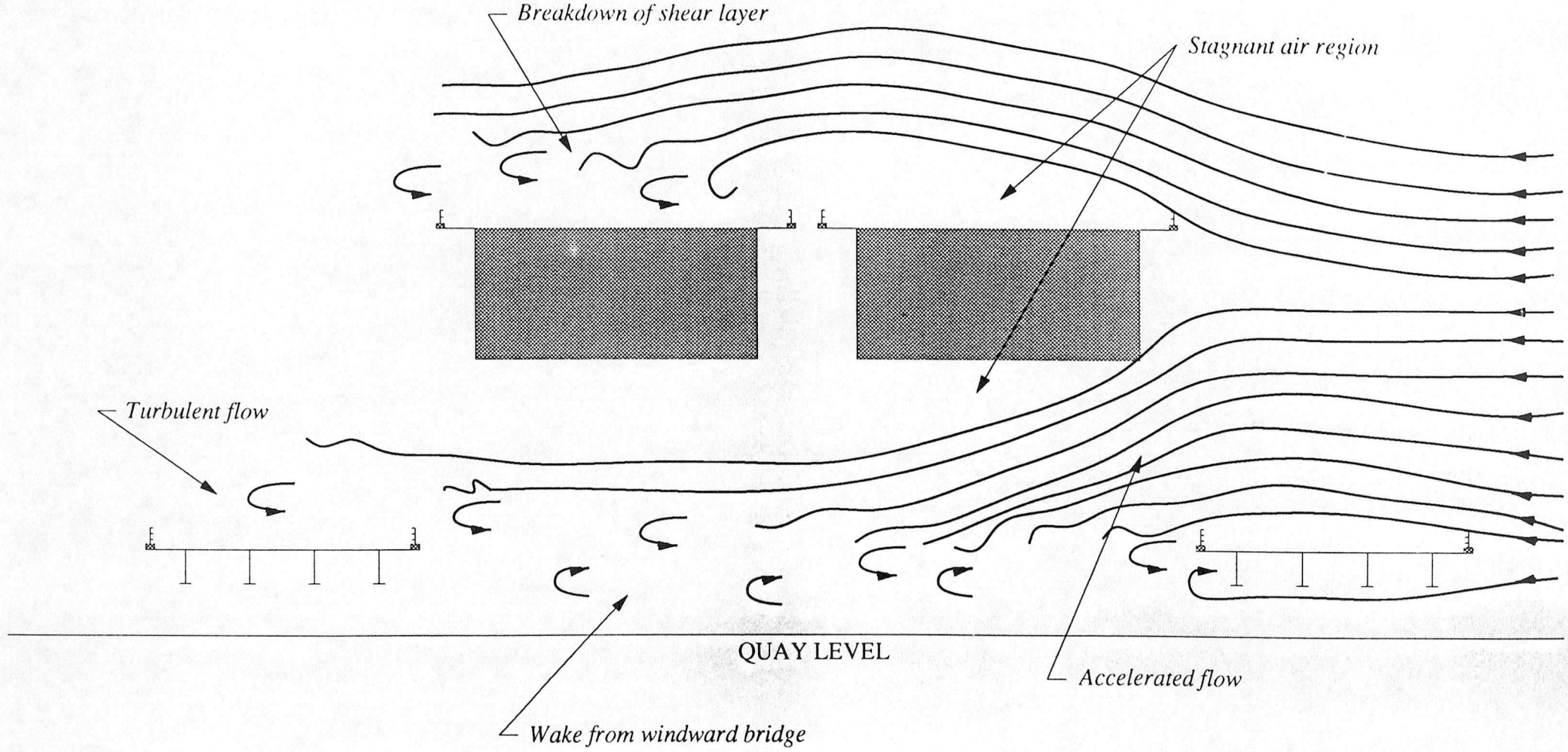

FIG. A8(d) : Flow pattern - three bridges, low tide, reduced width, haunch, V = 0.56 m/s

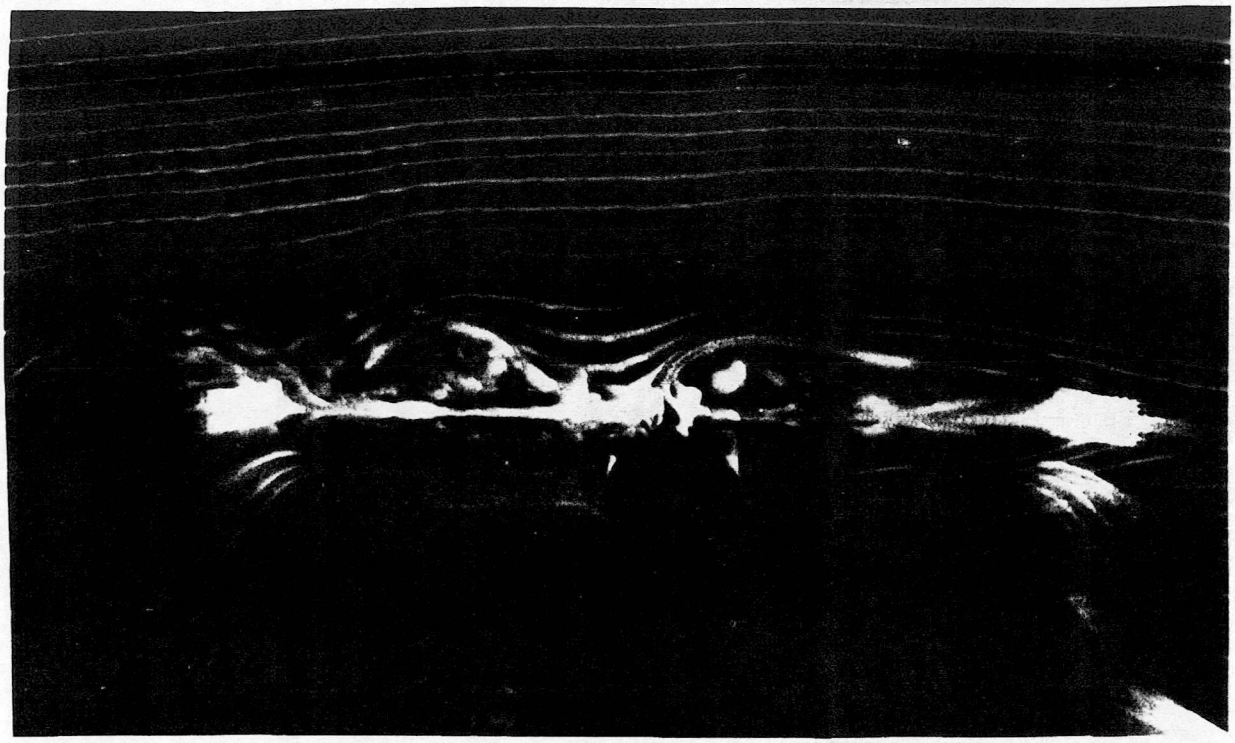

Fig. A9(a). Three bridges, low tide, traffic, midspan, V= 0.58 m/s : flow over high level bridge.

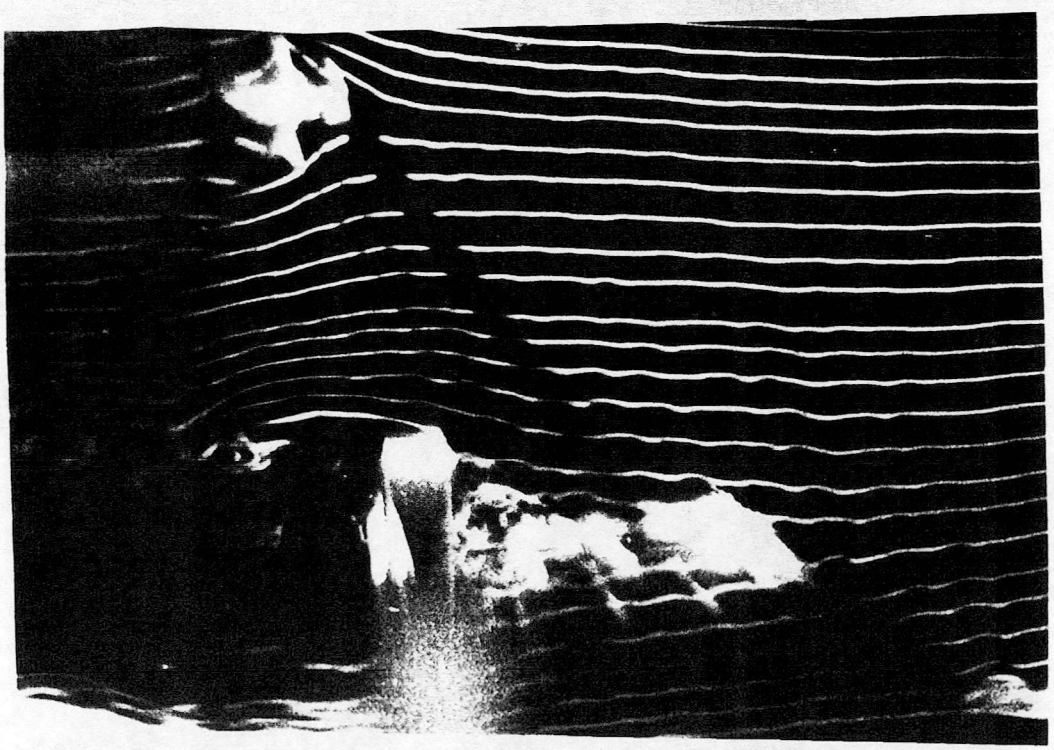

Fig. A9(b). Three bridges, low tide, traffic, midspan, V= 0.58 m/s : flow over windward bridge.

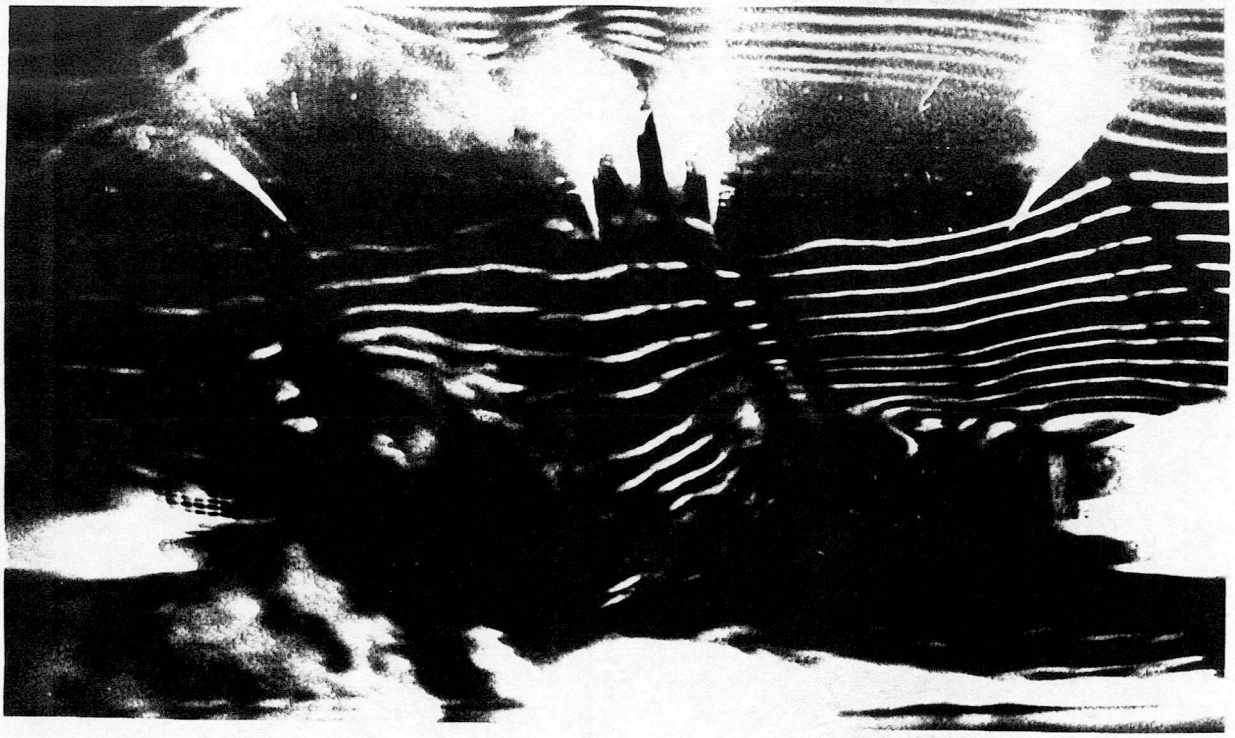

Fig. A9(c). Three bridges, low tide, traffic, midspan, V= 0.58 m/s : flow between bridges.

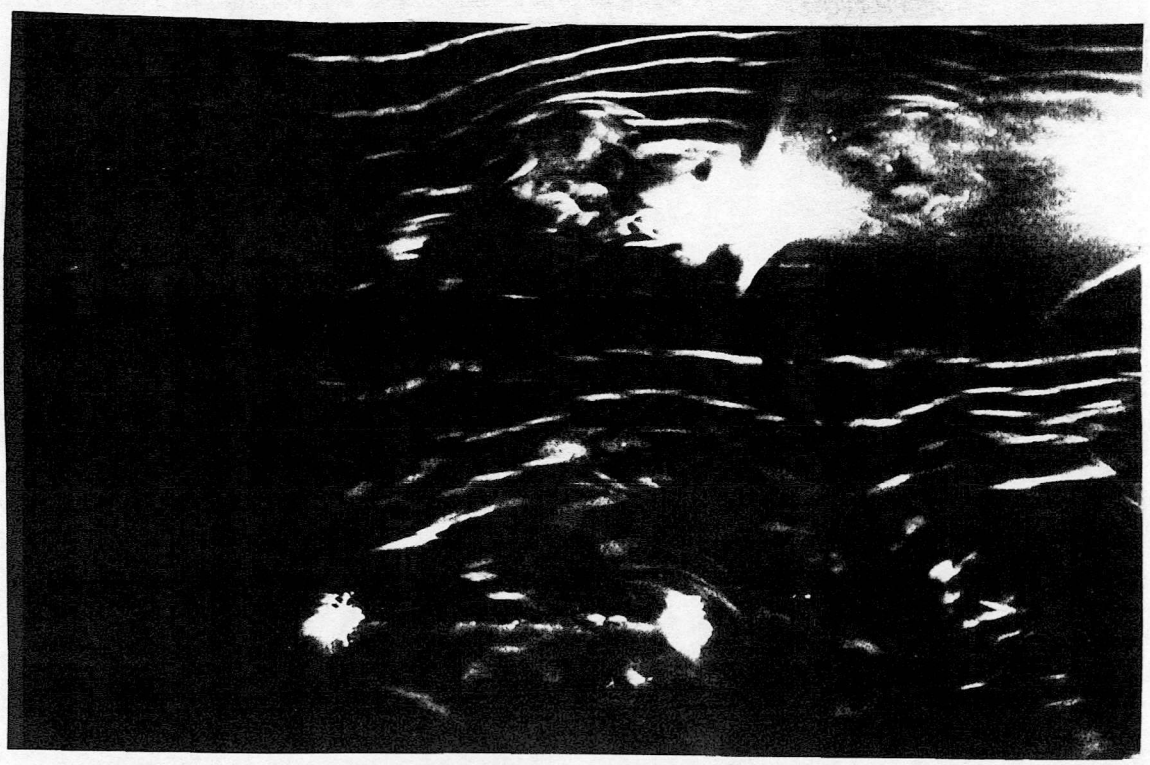

Fig. A9(d). Three bridges, low tide, traffic, midspan, V= 0.58 m/s : flow over leeward bridge.

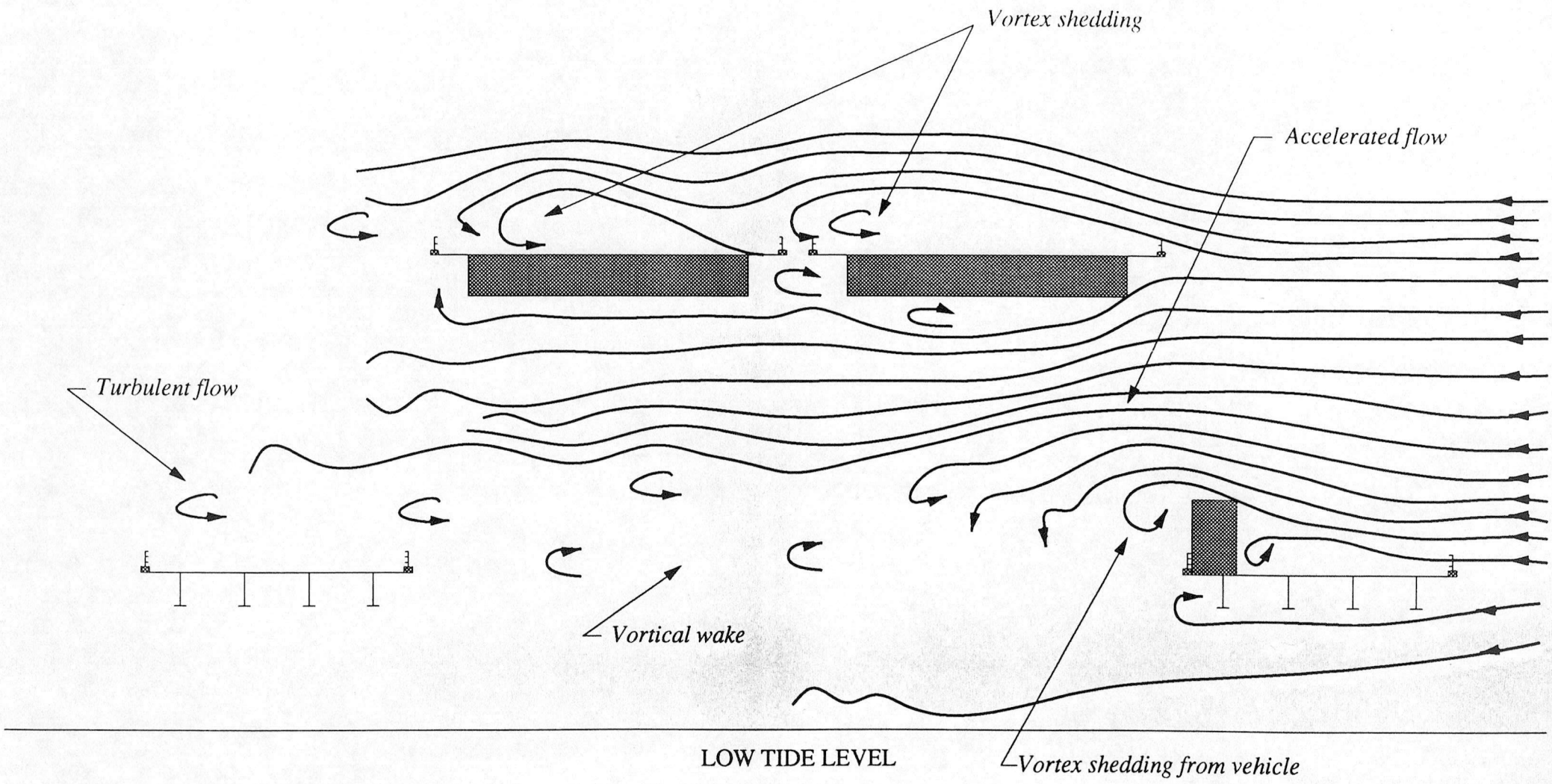

FIG. A9(e) : Flow pattern - three bridges, low tide, traffic, midspan, V = 0.58 m/s

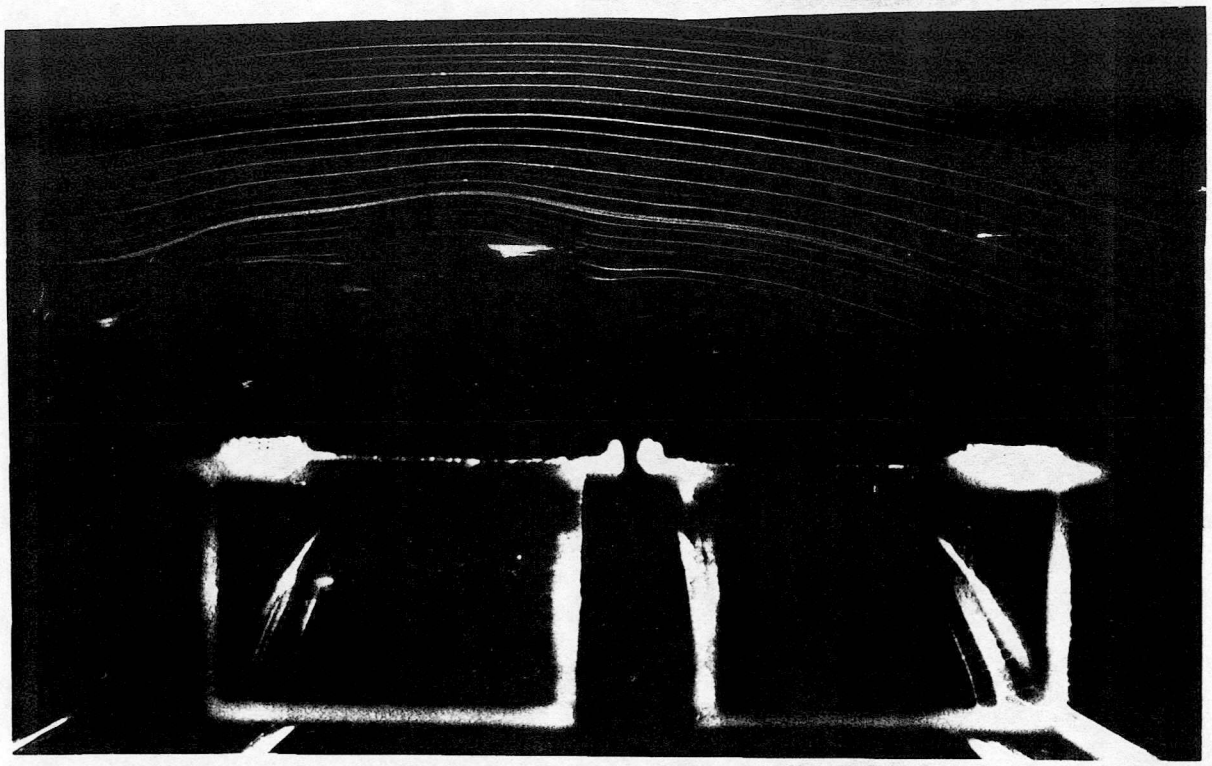

Fig. A10(a). Three bridges, low tide, traffic, haunch, V= 0.58 m/s : flow over high level bridge.

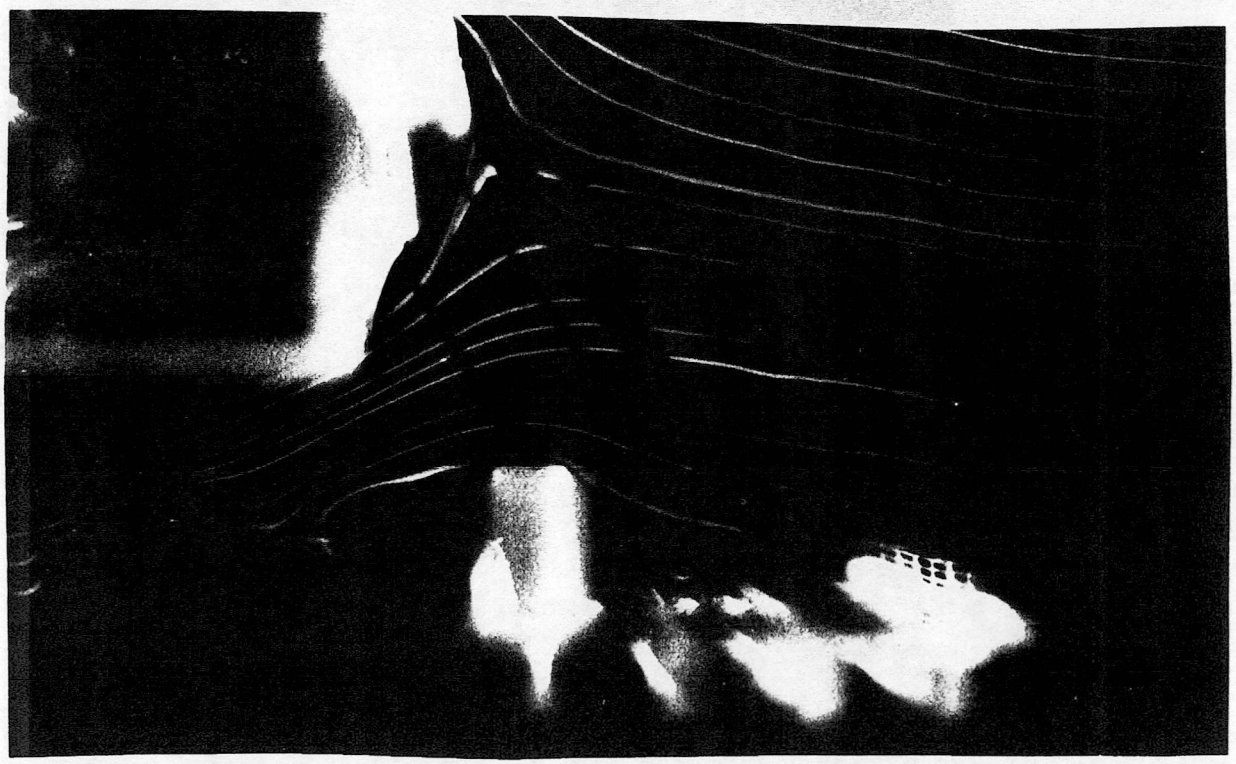

Fig. A10(b). Three bridges, low tide, traffic, haunch, V= 0.58 m/s : flow over windward bridge.

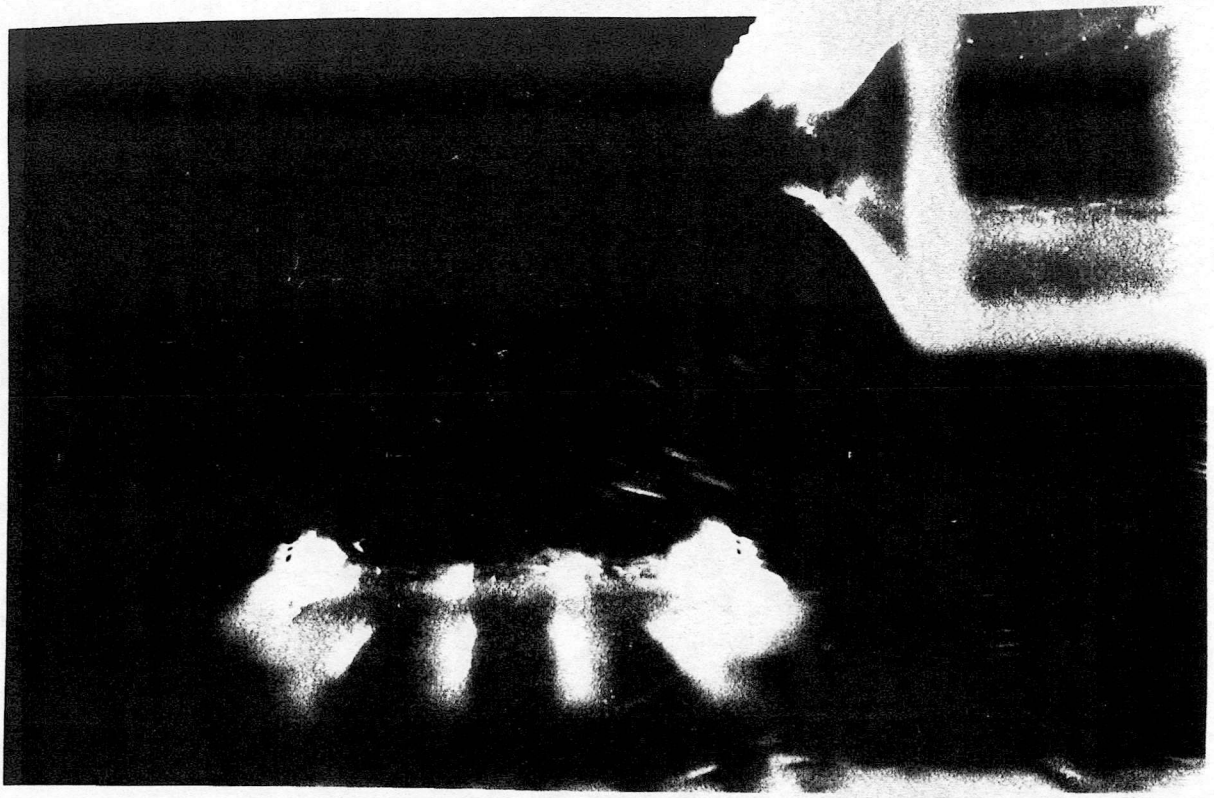

Fig. A10(c). Three bridges, low tide, traffic, haunch, V= 0.58 m/s : flow over leeward bridge.

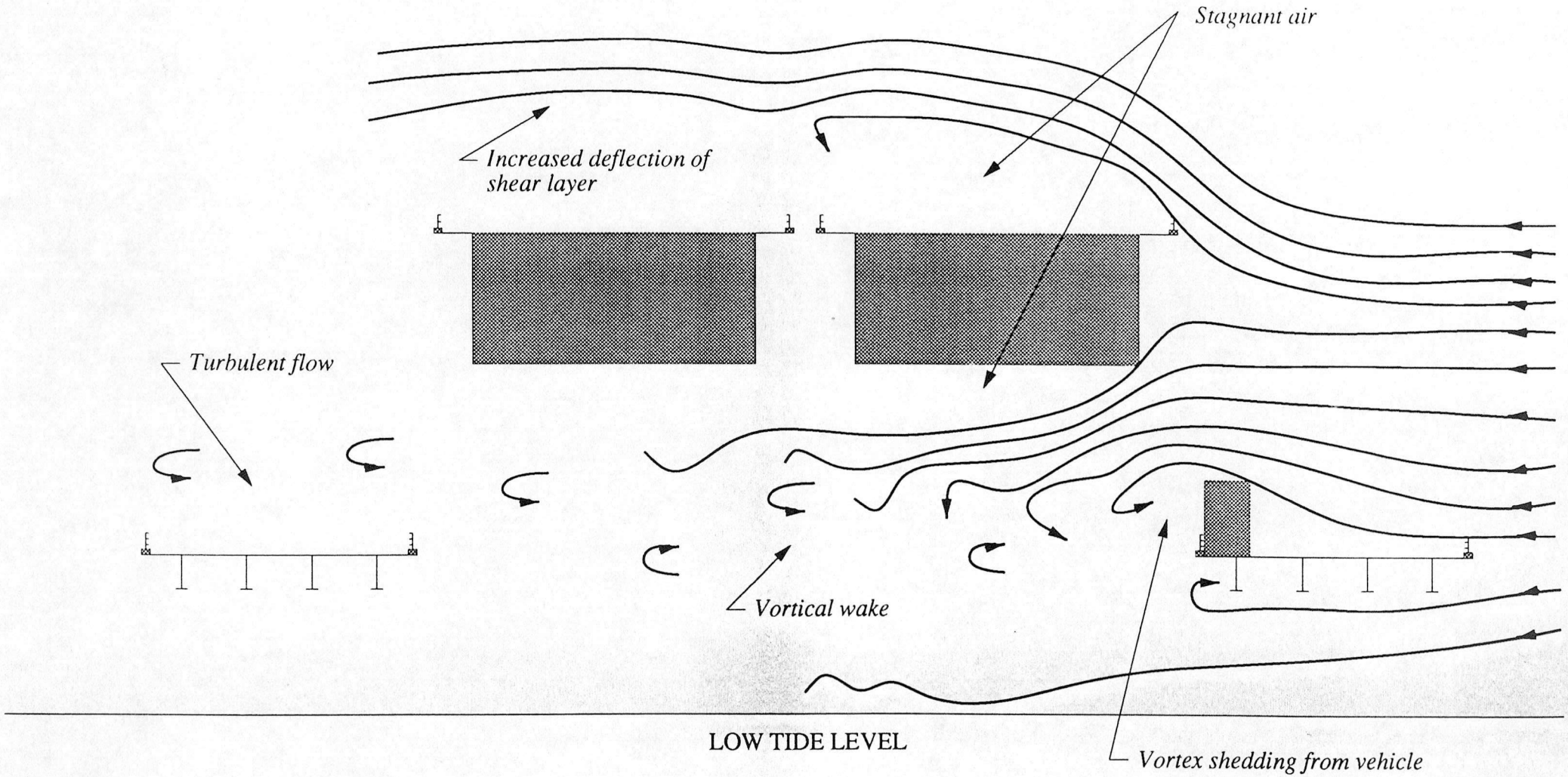

FIG. A10(d) : Flow pattern - three bridges, low tide, traffic, haunch, V = 0.58 m/s

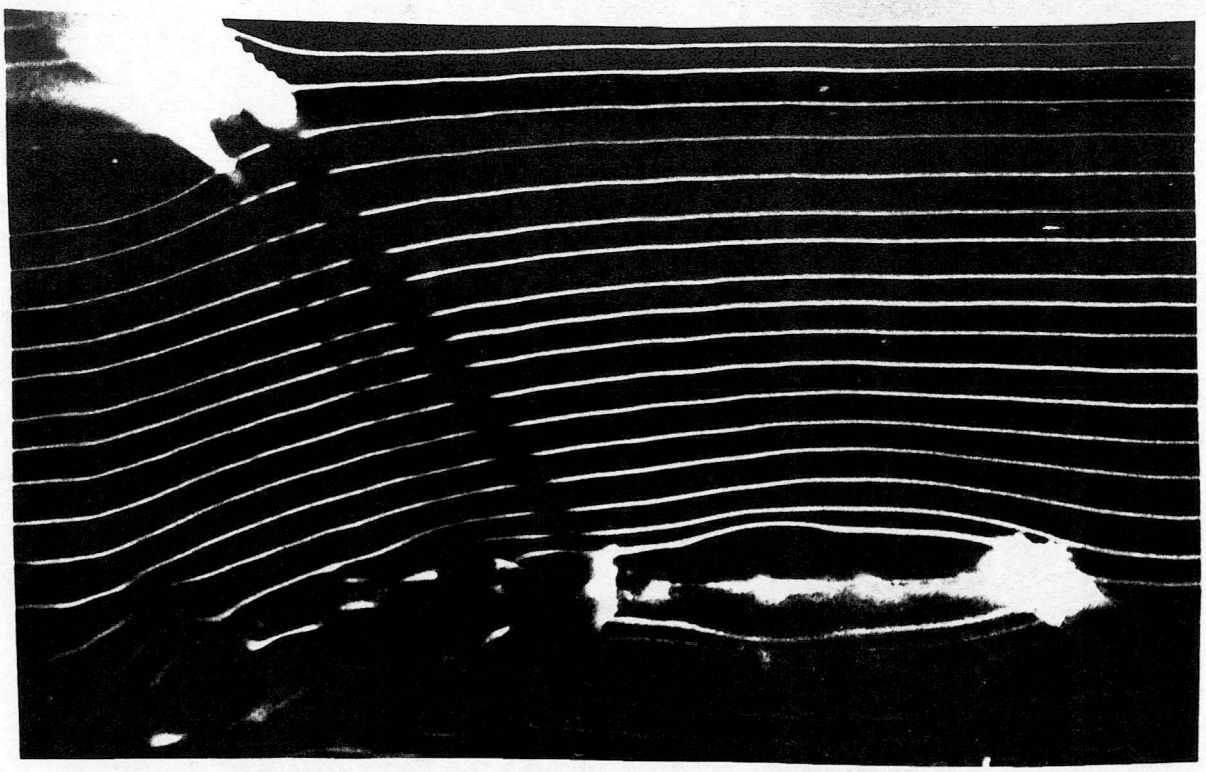

Fig. A11(a). Three bridges, low tide, 12m separation, midspan, V= 0.52 m/s : flow over windward bridge.

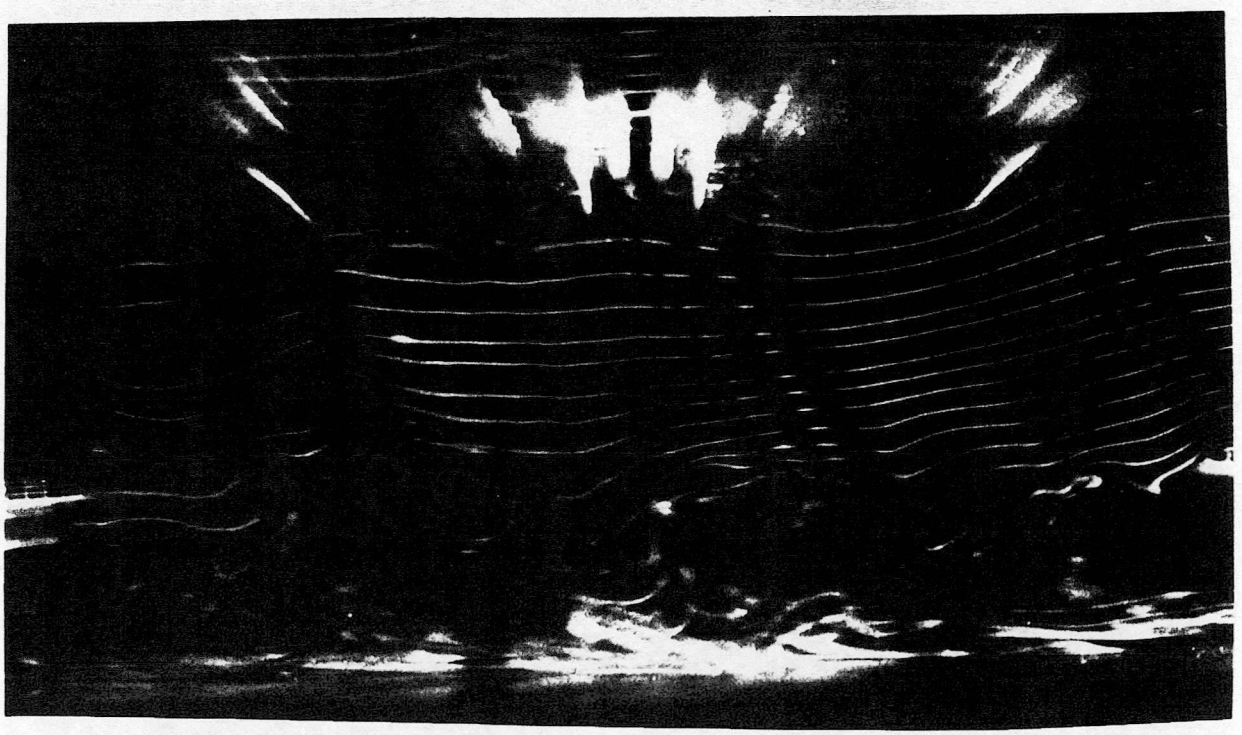

Fig. A11(b). Three bridges, low tide, 12m separation, midspan, V= 0.52 m/s : flow between bridges.

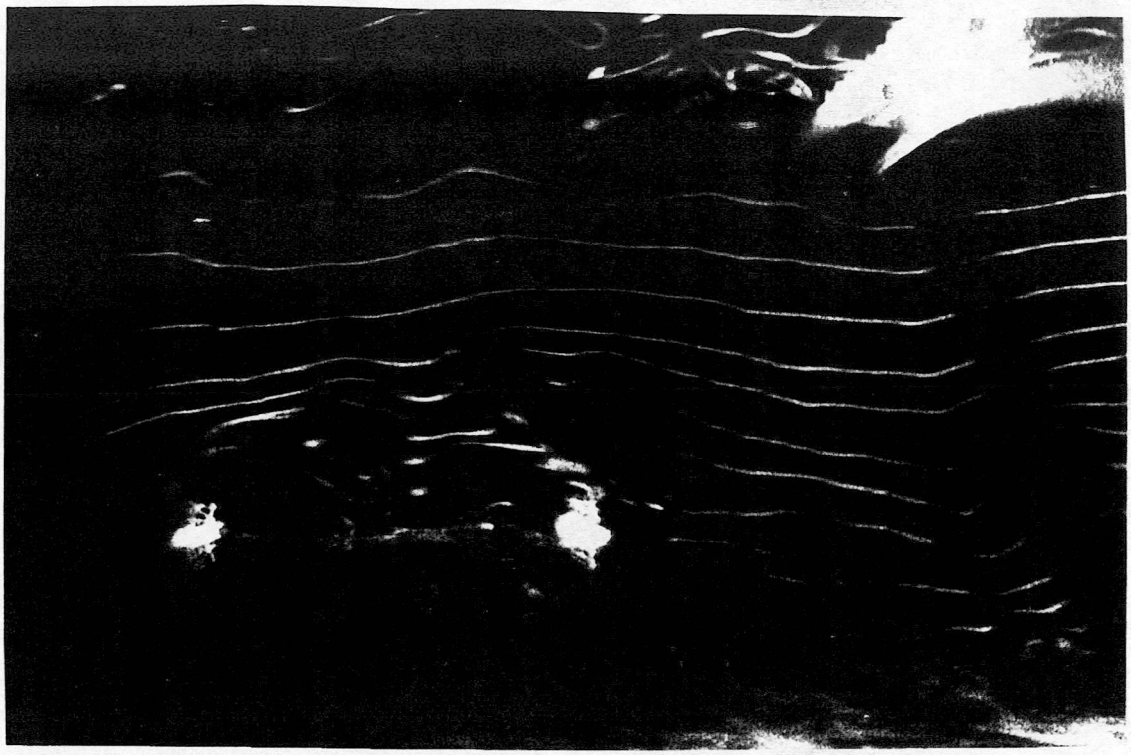

Fig. A11(c). Three bridges, low tide, 12m separation, midspan, V= 0.52 m/s : flow over leeward bridge.

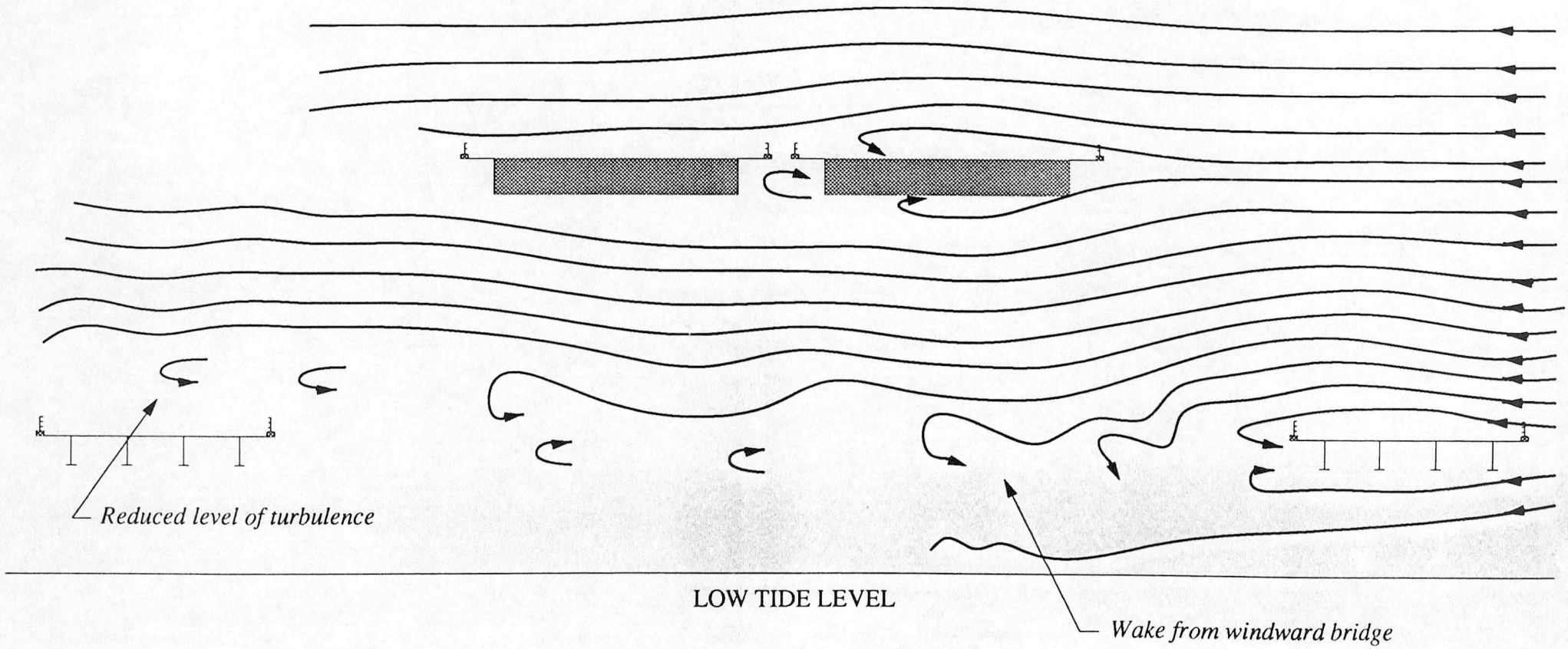

FIG. A11(d) : Flow pattern - three bridges, low tide, 12m separation, midspan, V = 0.52 m/s

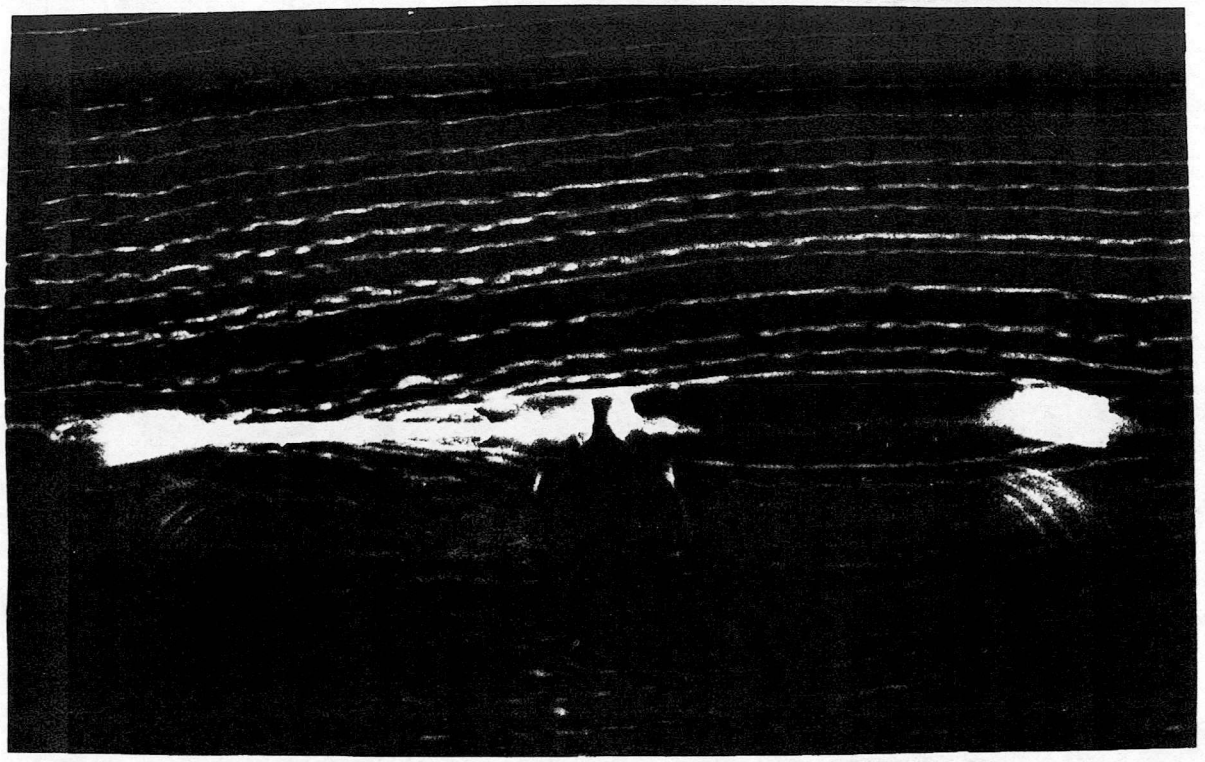

Fig. A12(a). Single bridge, low tide, parapets, midspan, V= 0.57 m/s : flow over bridge.

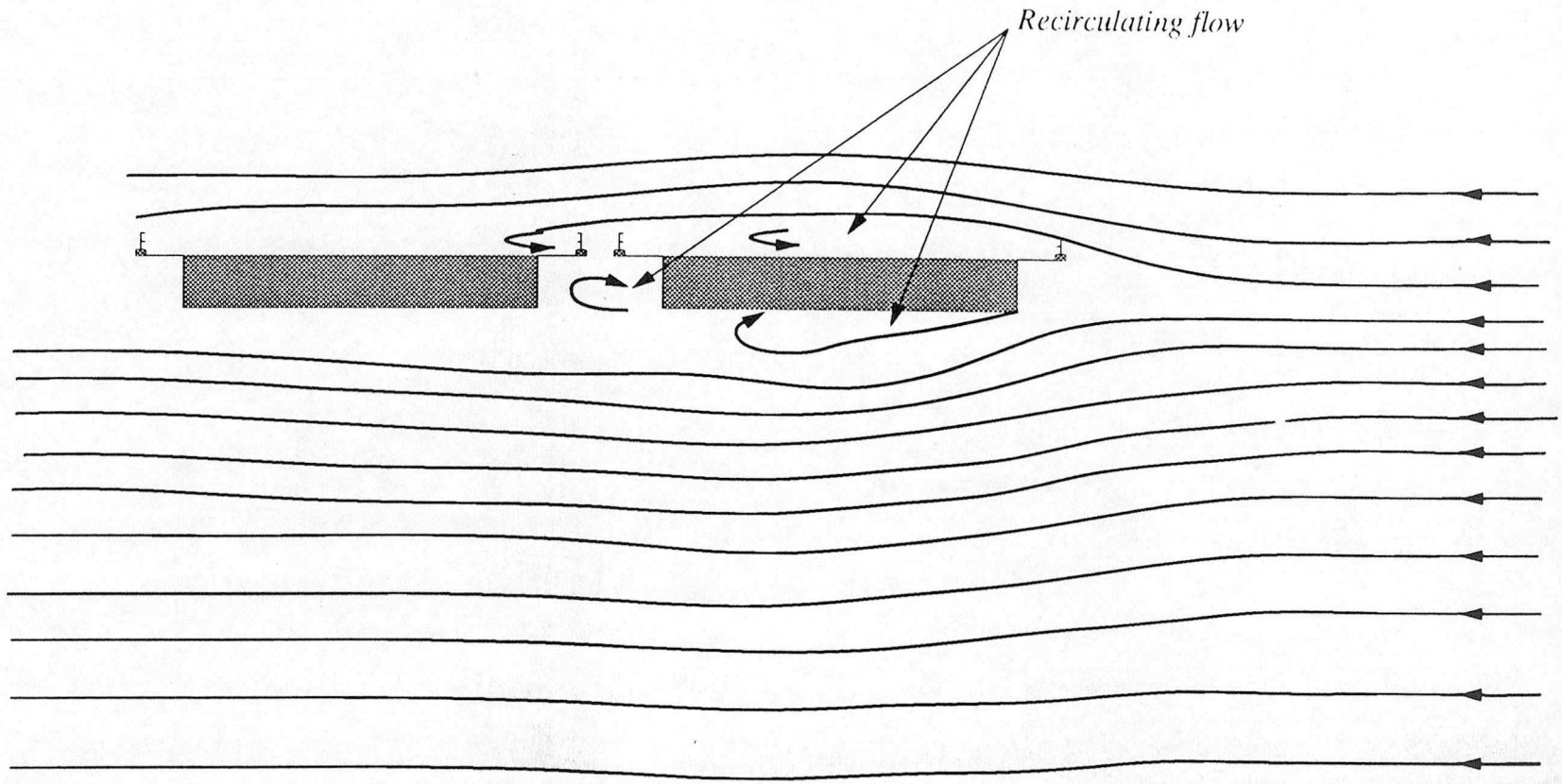

FIG. A12(b) : Flow pattern - single bridge, low tide, parapets, midspan, V = 0.57 m/s

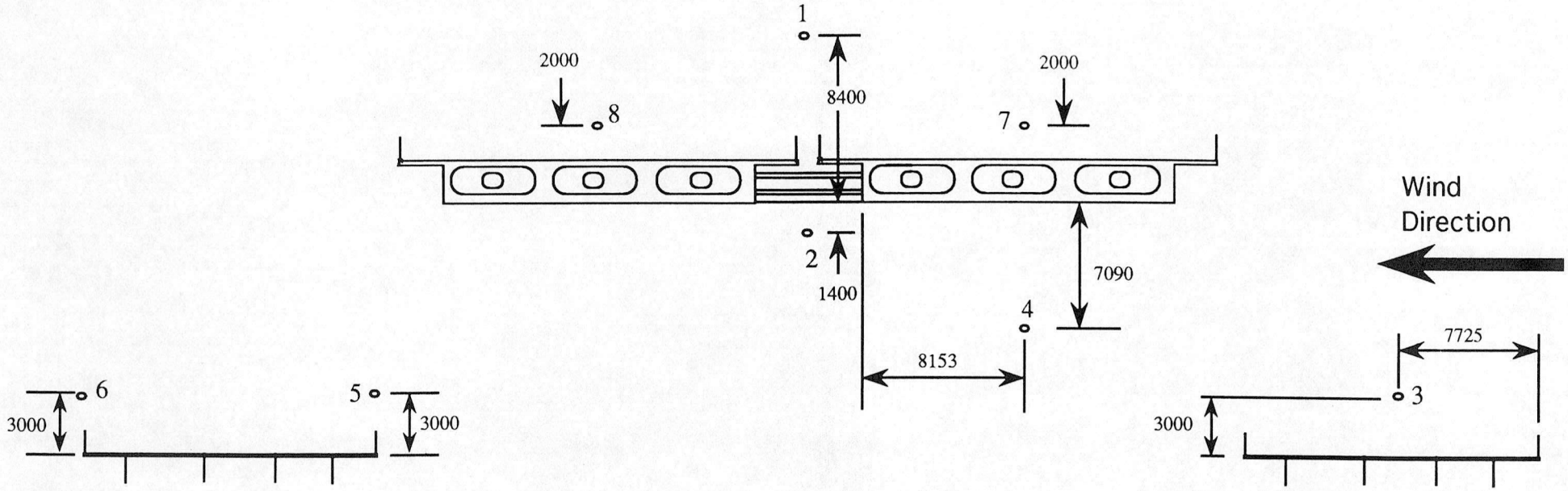

Figure B. Locations of Hot Wire Probes during Wind Tunnel Tests on Kingston Bridge (Dimensions to full scale (mm))

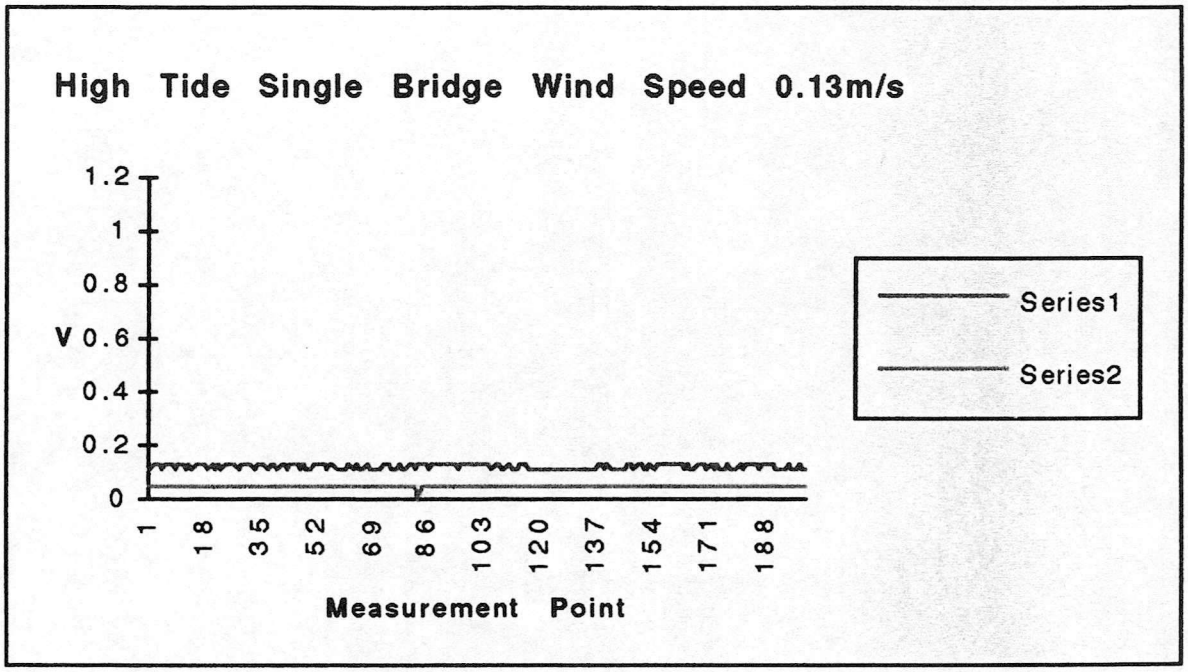
High Tide Single Bridge Wind Speed 0.13m/s
1.2
1
0.8
V 0.6
0.4
0.2
0
1
18
35
52
69
86
103
120
137
154
171
188
Measurement Point
Series1
Series2

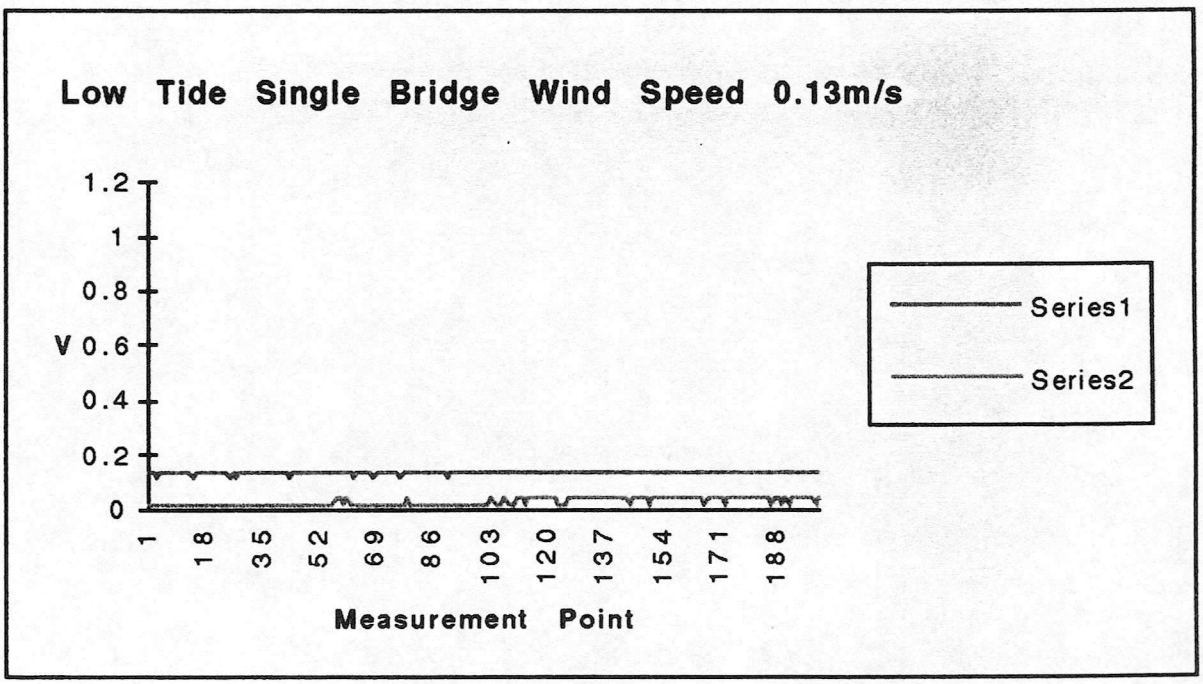
Low Tide Single Bridge Wind Speed 0.13m/s
1.2
1
0.8
V 0.6
0.4
0.2
0
1
18
35
52
69
86
103
120
137
154
171
188
Measurement Point
Series1
Series2

Figure B1

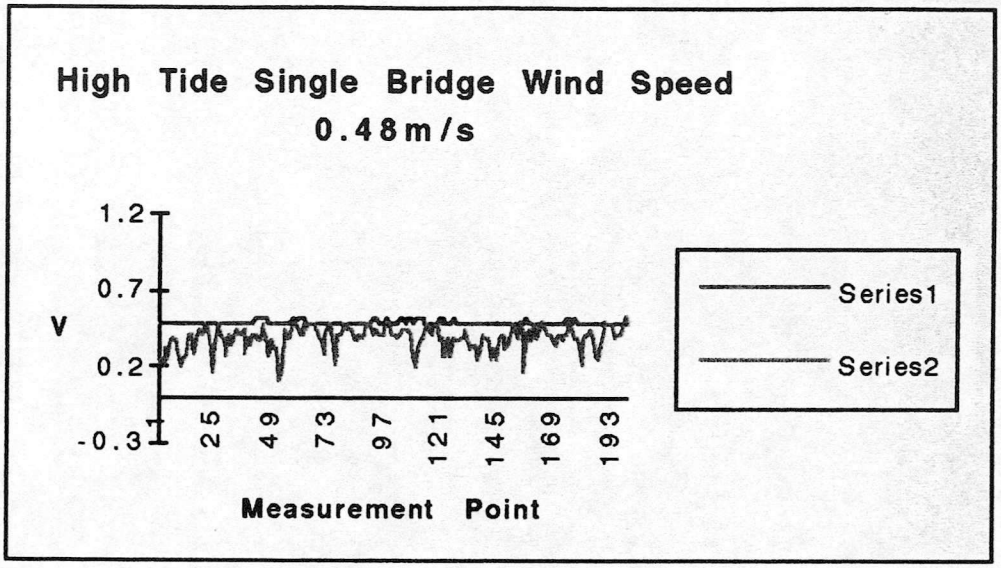
High Tide Single Bridge Wind Speed
0.48m/s
1.2
0.7
0.2
-0.3
V
1
25
49
73
97
121
145
169
193
Measurement Point
Series1
Series2

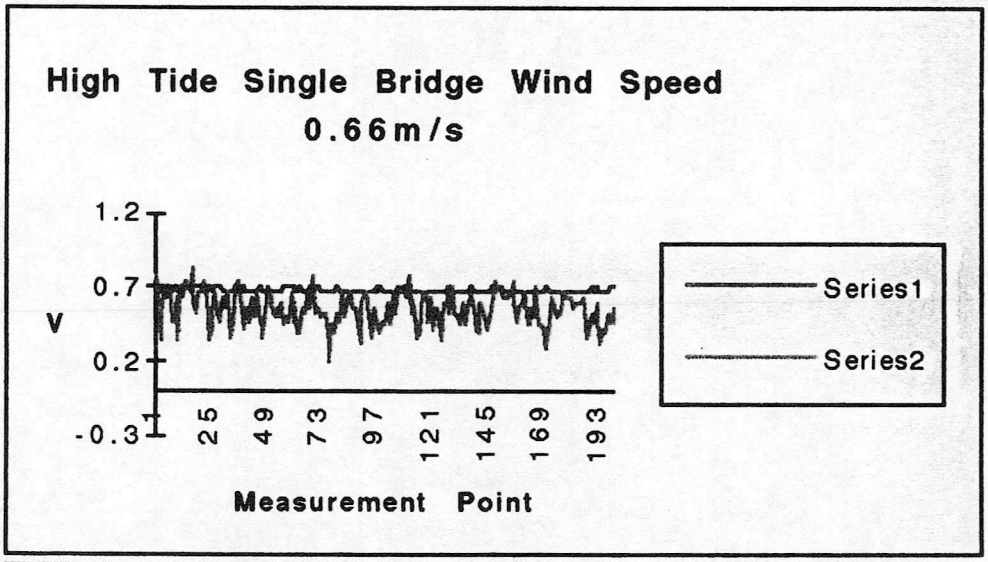
High Tide Single Bridge Wind Speed
0.66m/s
1.2
0.7
0.2
-0.3
V
1
25
49
73
97
121
145
169
193
Measurement Point
Series1
Series2

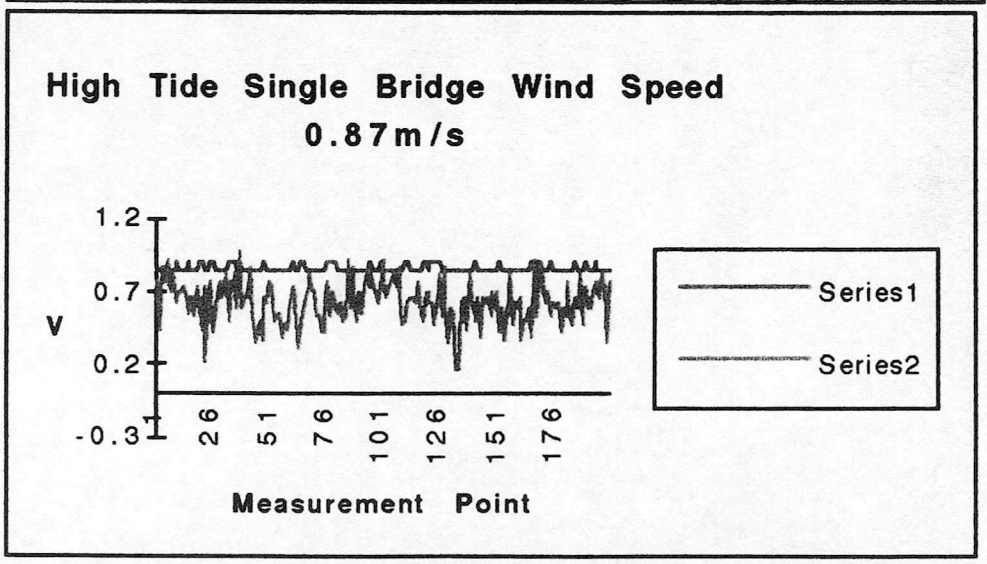
High Tide Single Bridge Wind Speed
0.87m/s
1.2
0.7
0.2
-0.3
V
1
26
51
76
101
126
151
176
Measurement Point
Series1
Series2

Figure B2

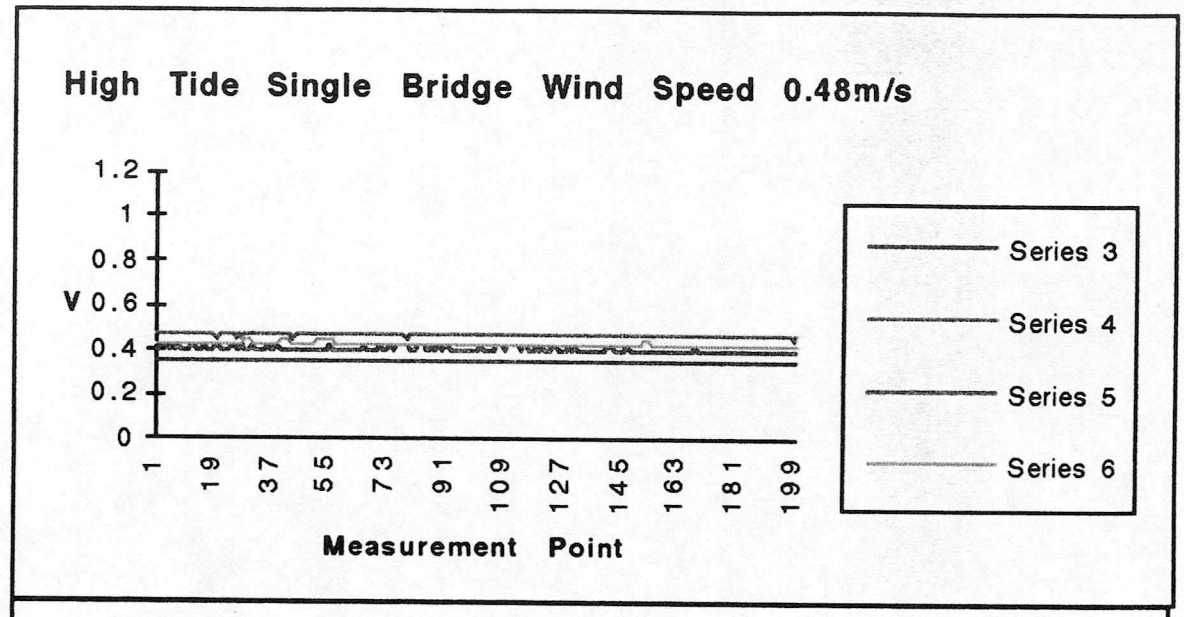
High Tide Single Bridge Wind Speed 0.48m/s
1.2
1
0.8
V 0.6
0.4
0.2
0
1
19
37
55
73
91
109
127
145
163
181
199
Measurement Point
Series 3
Series 4
Series 5
Series 6

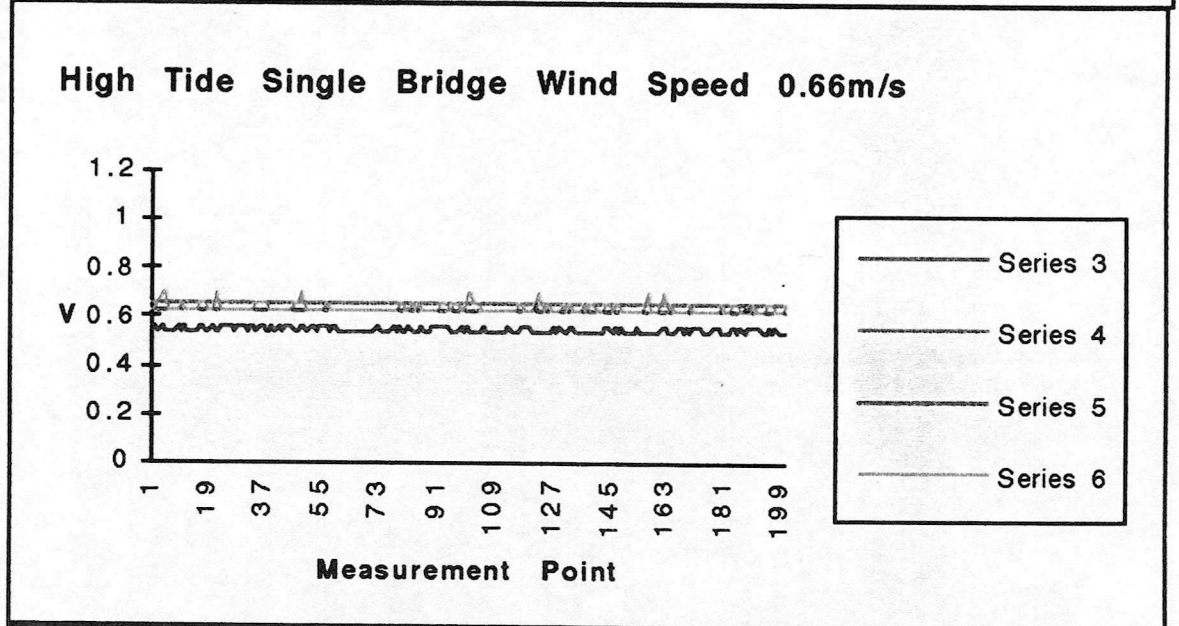
High Tide Single Bridge Wind Speed 0.66m/s
1.2
1
0.8
V 0.6
0.4
0.2
0
1
19
37
55
73
91
109
127
145
163
181
199
Measurement Point
Series 3
Series 4
Series 5
Series 6

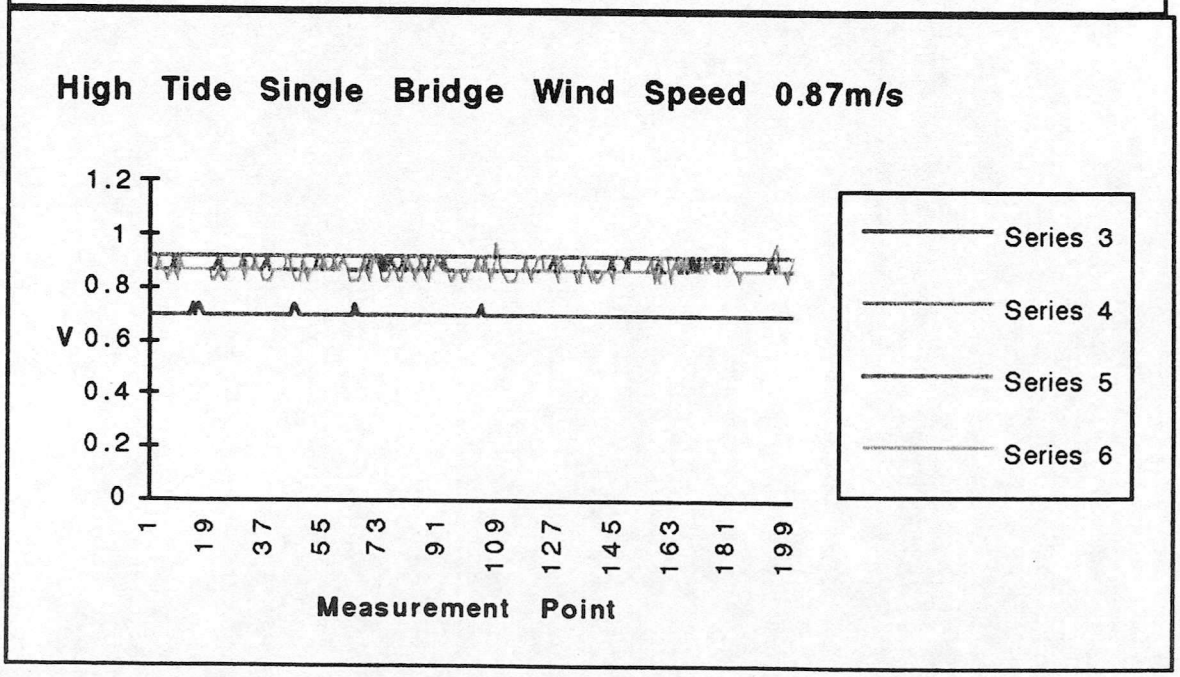
High Tide Single Bridge Wind Speed 0.87m/s
1.2
1
0.8
V 0.6
0.4
0.2
0
1
19
37
55
73
91
109
127
145
163
181
199
Measurement Point
Series 3
Series 4
Series 5
Series 6

Figure B3

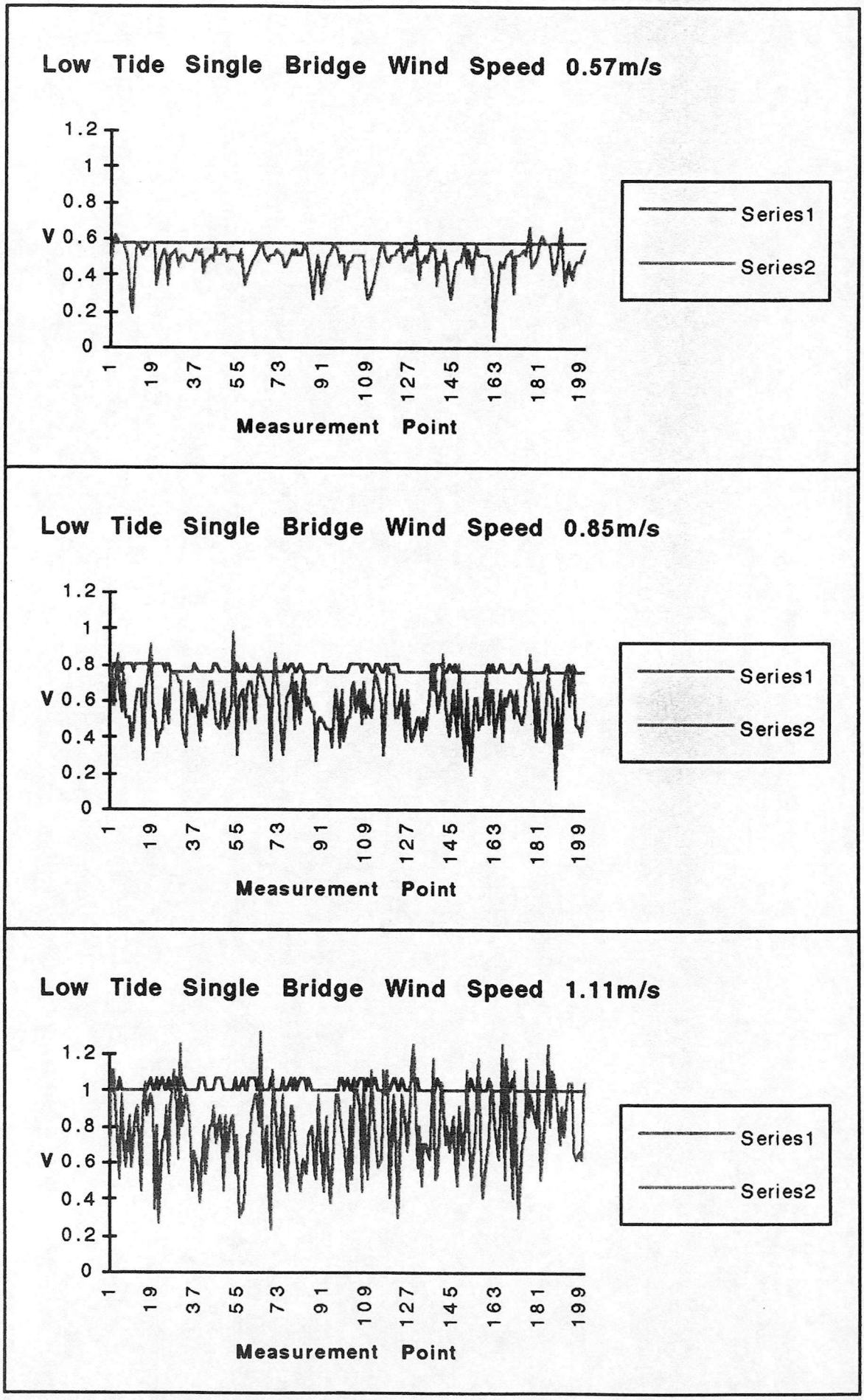
Low Tide Single Bridge Wind Speed 0.57m/s
1.2
1
0.8
V 0.6
0.4
0.2
0
1 19 37 55 73 91 109 127 145 163 181 199
Measurement Point
Series1
Series2
Low Tide Single Bridge Wind Speed 0.85m/s
1.2
1
0.8
V 0.6
0.4
0.2
0
1 19 37 55 73 91 109 127 145 163 181 199
Measurement Point
Series1
Series2
Low Tide Single Bridge Wind Speed 1.11m/s
1.2
1
0.8
V 0.6
0.4
0.2
0
1 19 37 55 73 91 109 127 145 163 181 199
Measurement Point
Series1
Series2

Figure B4

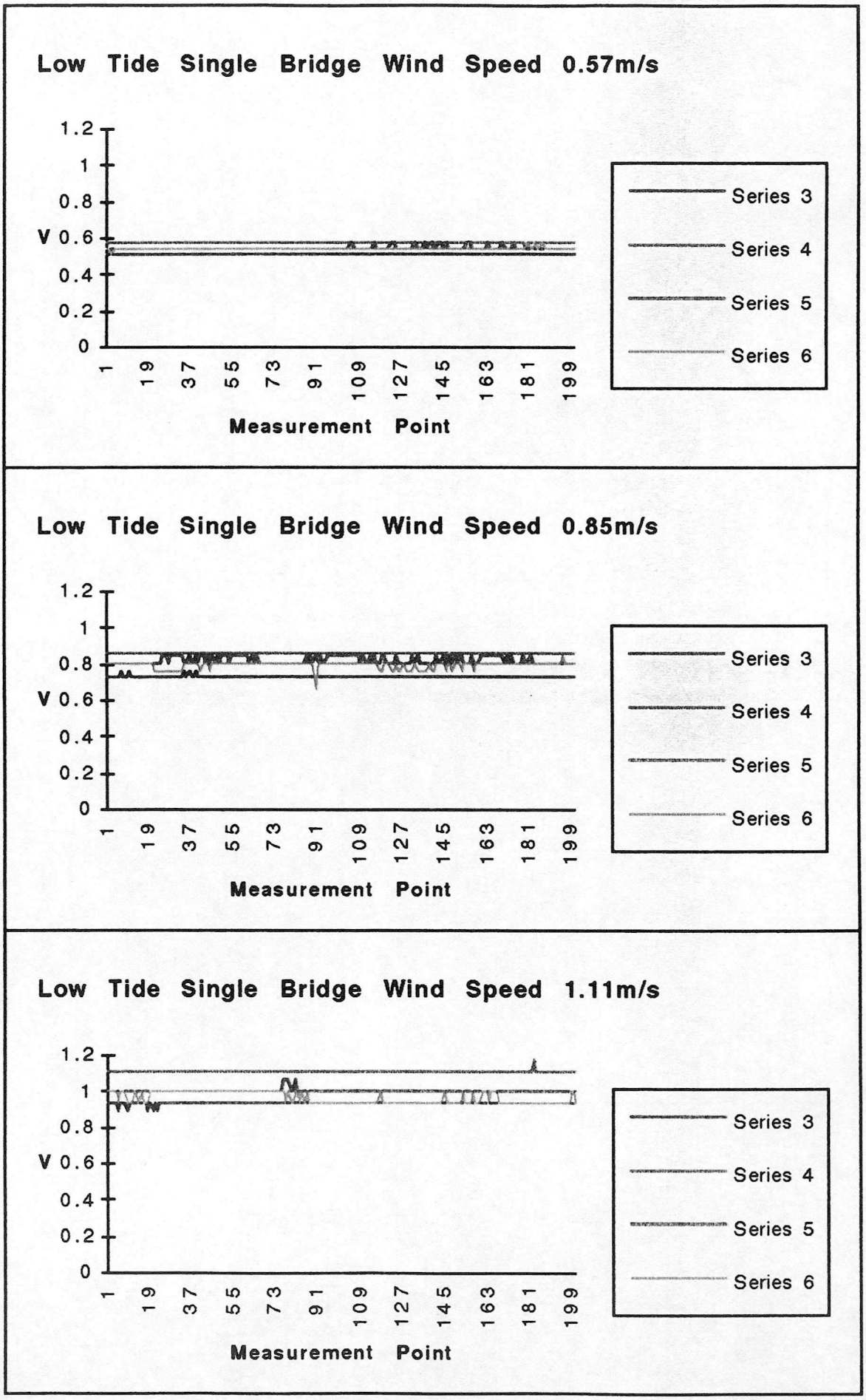
Low Tide Single Bridge Wind Speed 0.57m/s
1.2
1
0.8
V 0.6
0.4
0.2
0
1 19 37 55 73 91 109 127 145 163 181 199
Measurement Point
Series 3
Series 4
Series 5
Series 6
Low Tide Single Bridge Wind Speed 0.85m/s
1.2
1
0.8
V 0.6
0.4
0.2
0
1 19 37 55 73 91 109 127 145 163 181 199
Measurement Point
Series 3
Series 4
Series 5
Series 6
Low Tide Single Bridge Wind Speed 1.11m/s
1.2
1
0.8
V 0.6
0.4
0.2
0
1 19 37 55 73 91 109 127 145 163 181 199
Measurement Point
Series 3
Series 4
Series 5
Series 6

Figure B5

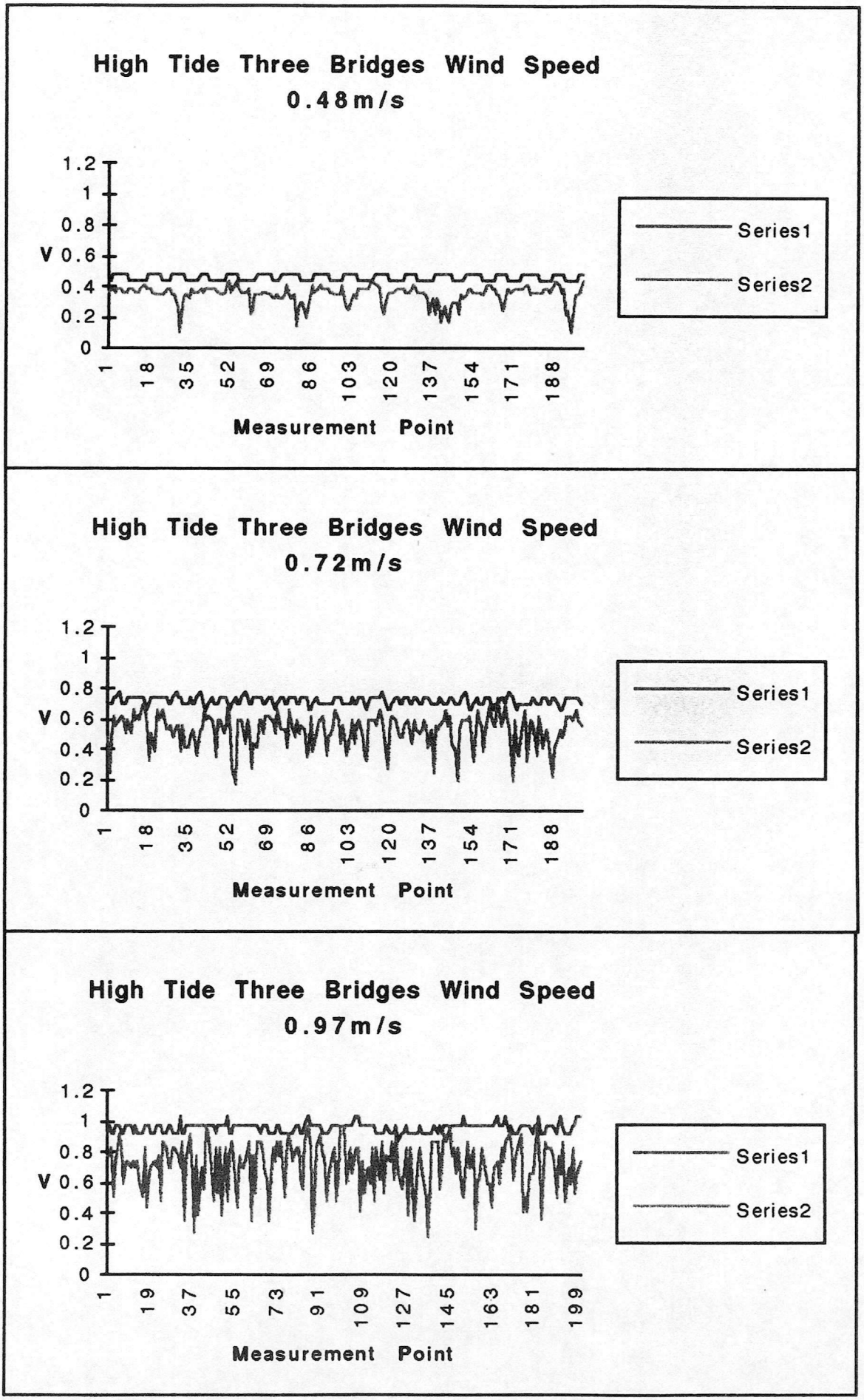
High Tide Three Bridges Wind Speed
0.48m/s
1.2
1
0.8
V 0.6
0.4
0.2
0
1
18
35
52
69
86
103
120
137
154
171
188
Measurement Point
Series1
Series2
High Tide Three Bridges Wind Speed
0.72m/s
1.2
1
0.8
V 0.6
0.4
0.2
0
1
18
35
52
69
86
103
120
137
154
171
188
Measurement Point
Series1
Series2
High Tide Three Bridges Wind Speed
0.97m/s
1.2
1
0.8
V 0.6
0.4
0.2
0
1
19
37
55
73
91
109
127
145
163
181
199
Measurement Point
Series1
Series2

Figure B6

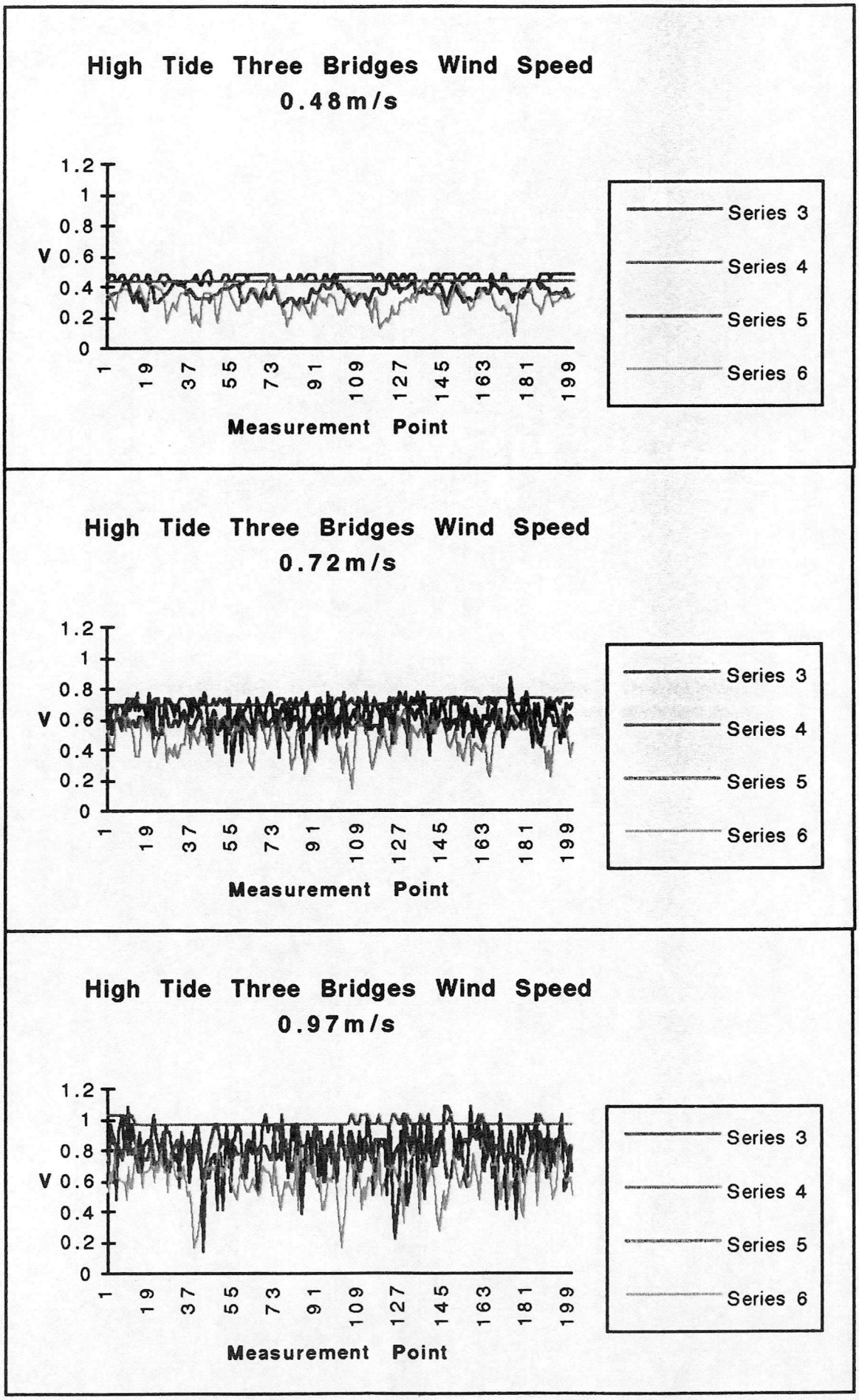
High Tide Three Bridges Wind Speed
0.48m/s
V
1.2
1
0.8
0.6
0.4
0.2
0
1
19
37
55
73
91
109
127
145
163
181
199
Measurement Point
Series 3
Series 4
Series 5
Series 6
High Tide Three Bridges Wind Speed
0.72m/s
V
Measurement Point
Series 3
Series 4
Series 5
Series 6
High Tide Three Bridges Wind Speed
0.97m/s
V
Measurement Point
Series 3
Series 4
Series 5
Series 6

Figure B7

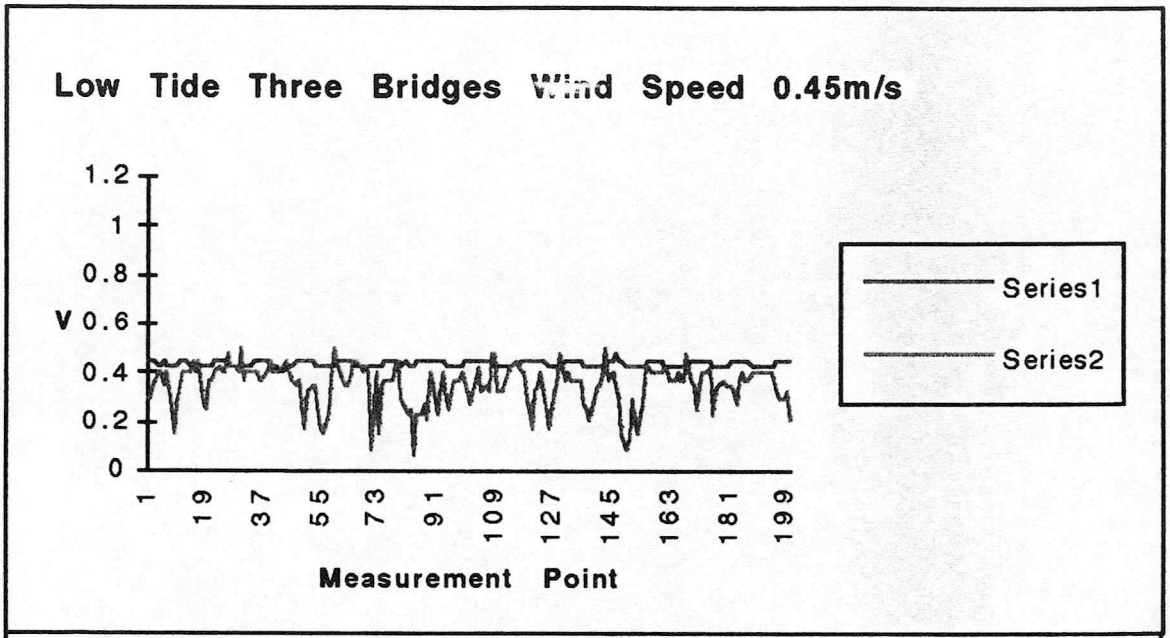
Low Tide Three Bridges Wind Speed 0.45m/s
1.2
1
0.8
V 0.6
0.4
0.2
0
1 19 37 55 73 91 109 127 145 163 181 199
Measurement Point
Series1
Series2

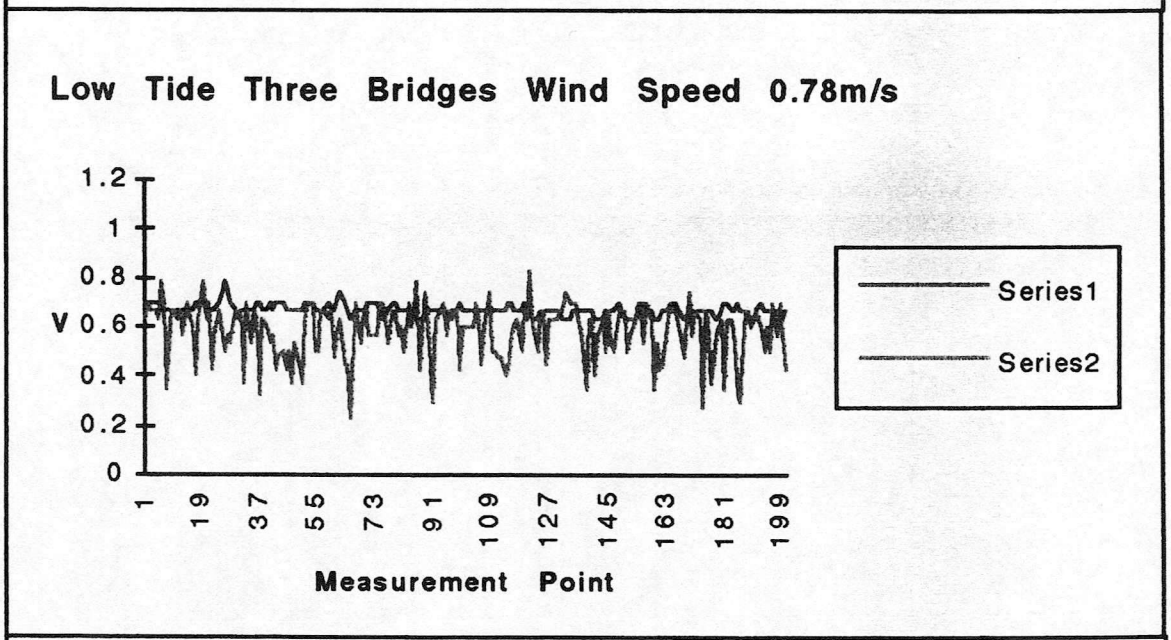
Low Tide Three Bridges Wind Speed 0.78m/s
1.2
1
0.8
V 0.6
0.4
0.2
0
1 19 37 55 73 91 109 127 145 163 181 199
Measurement Point
Series1
Series2

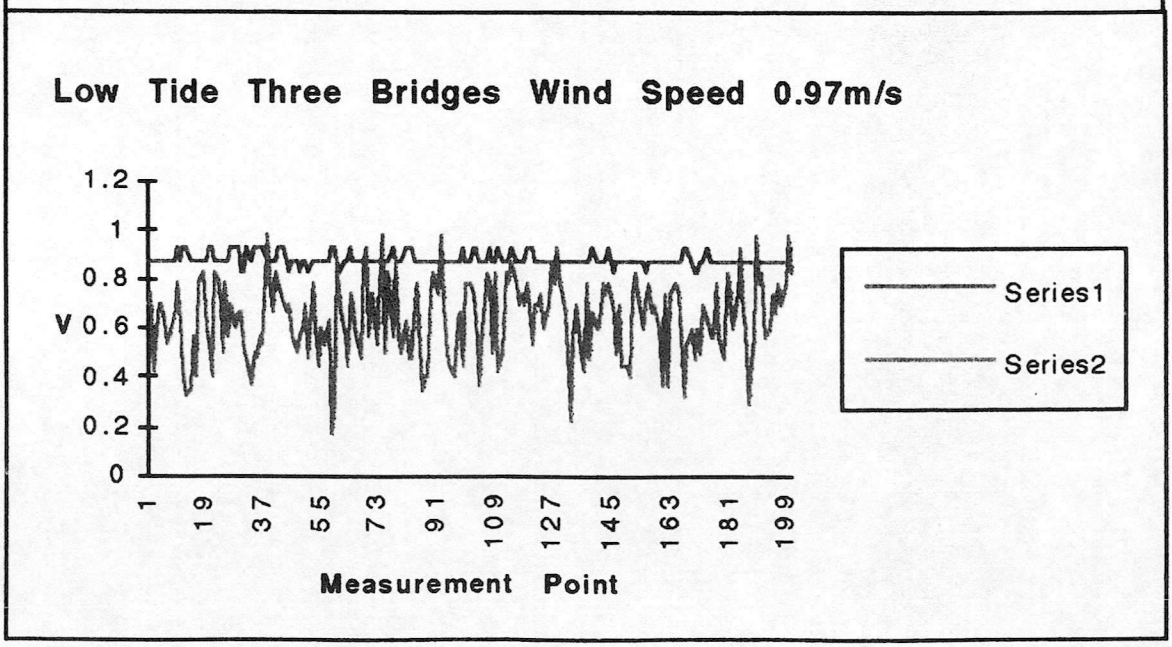
Low Tide Three Bridges Wind Speed 0.97m/s
1.2
1
0.8
V 0.6
0.4
0.2
0
1 19 37 55 73 91 109 127 145 163 181 199
Measurement Point
Series1
Series2

Figure B8

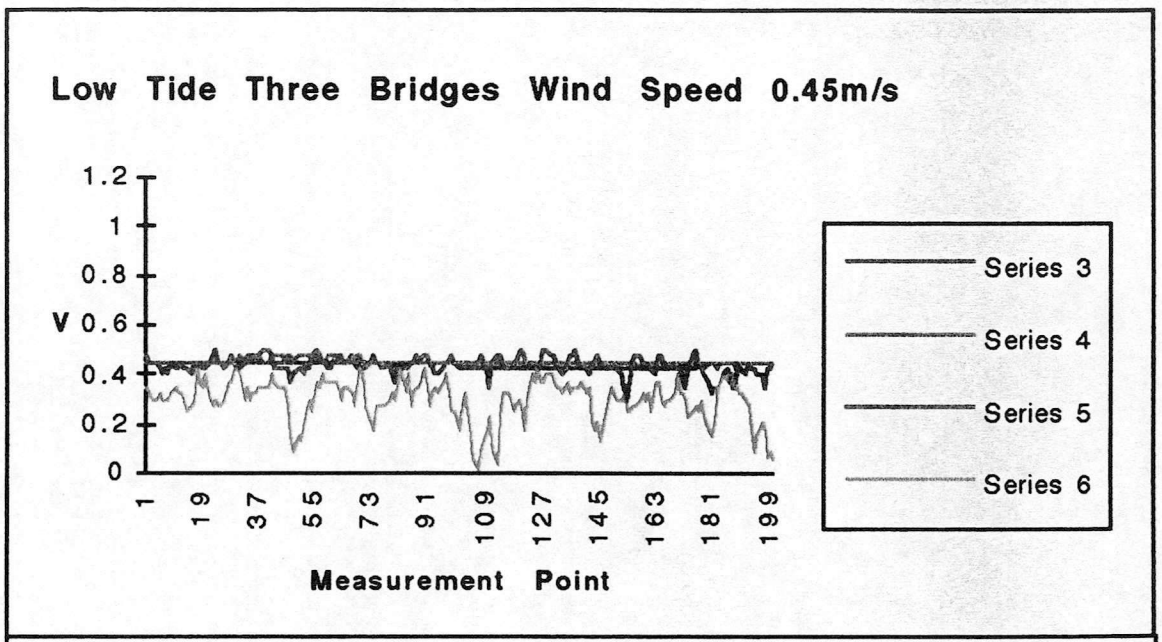
Low Tide Three Bridges Wind Speed 0.45m/s
1.2
1
0.8
V 0.6
0.4
0.2
0
1 19 37 55 73 91 109 127 145 163 181 199
Measurement Point
Series 3
Series 4
Series 5
Series 6

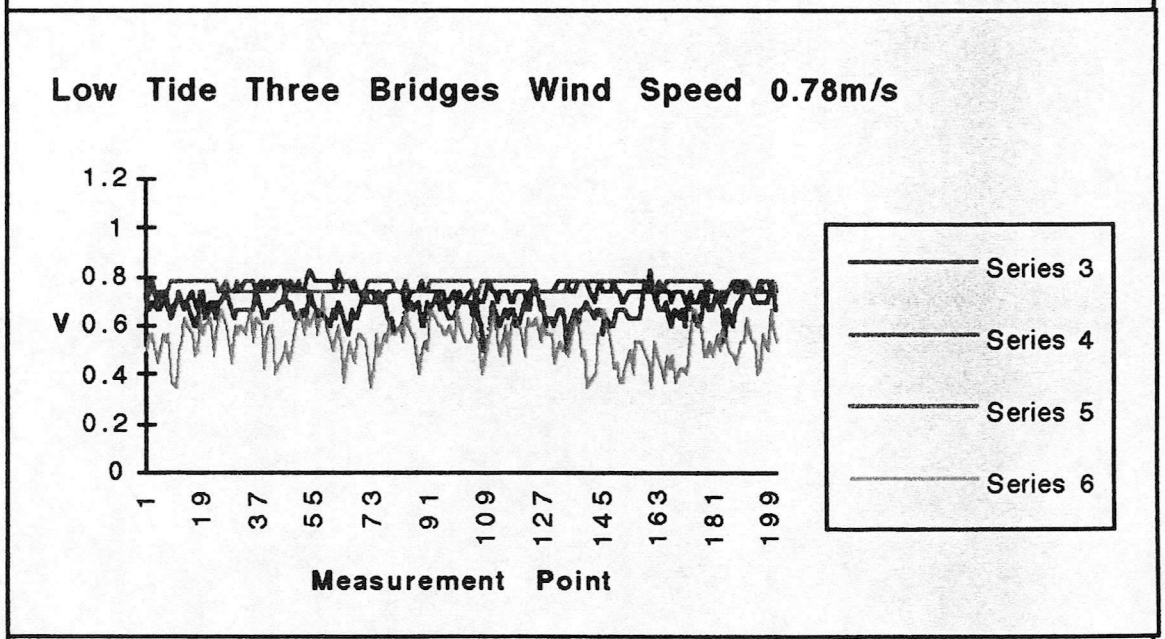
Low Tide Three Bridges Wind Speed 0.78m/s
1.2
1
0.8
V 0.6
0.4
0.2
0
1 19 37 55 73 91 109 127 145 163 181 199
Measurement Point
Series 3
Series 4
Series 5
Series 6

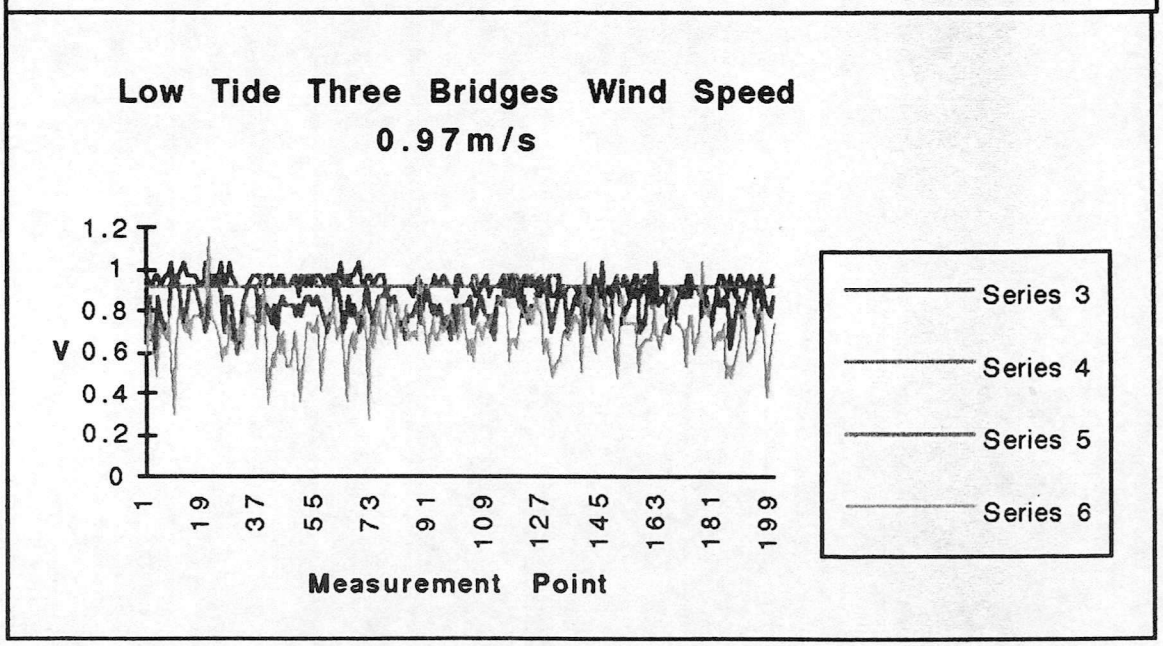
Low Tide Three Bridges Wind Speed 0.97m/s
1.2
1
0.8
V 0.6
0.4
0.2
0
1 19 37 55 73 91 109 127 145 163 181 199
Measurement Point
Series 3
Series 4
Series 5
Series 6

Figure B9

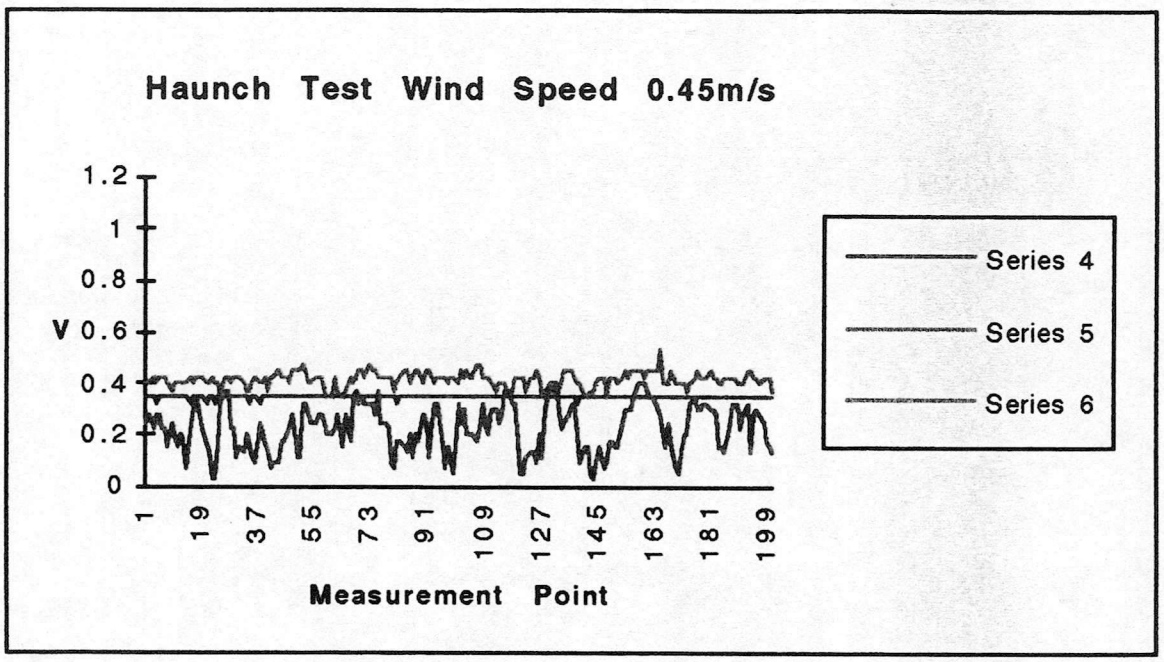
Haunch Test Wind Speed 0.45m/s
1.2
1
0.8
V 0.6
0.4
0.2
0
1
19
37
55
73
91
109
127
145
163
181
199
Measurement Point
Series 4
Series 5
Series 6

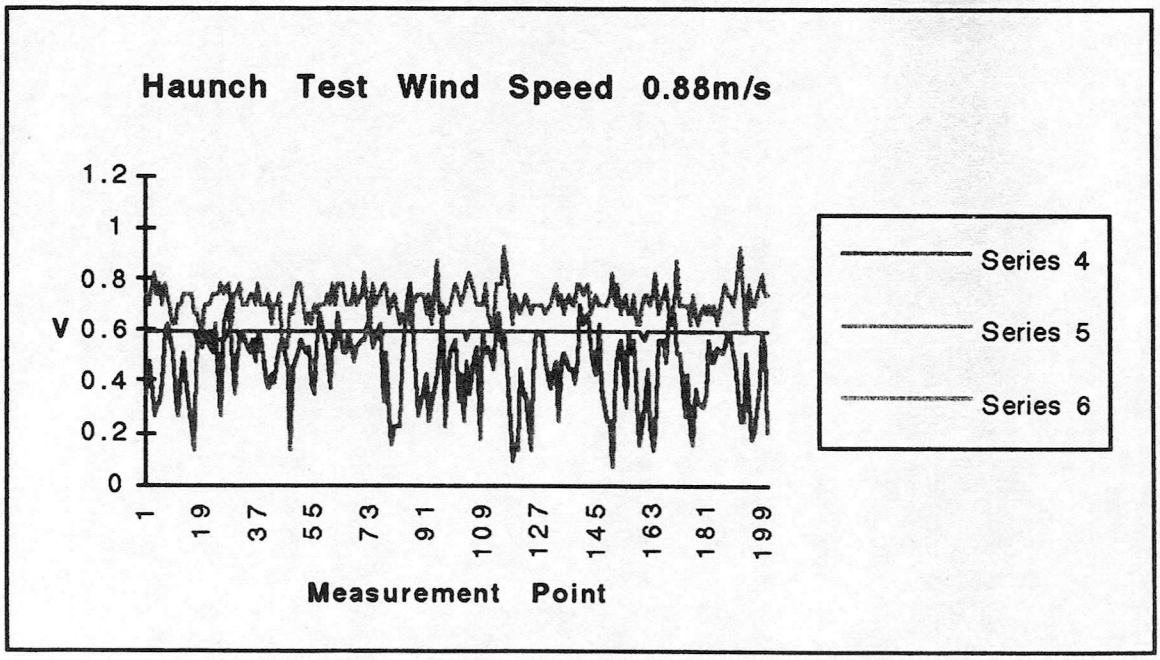
Haunch Test Wind Speed 0.88m/s
1.2
1
0.8
V 0.6
0.4
0.2
0
1
19
37
55
73
91
109
127
145
163
181
199
Measurement Point
Series 4
Series 5
Series 6

Figure B10

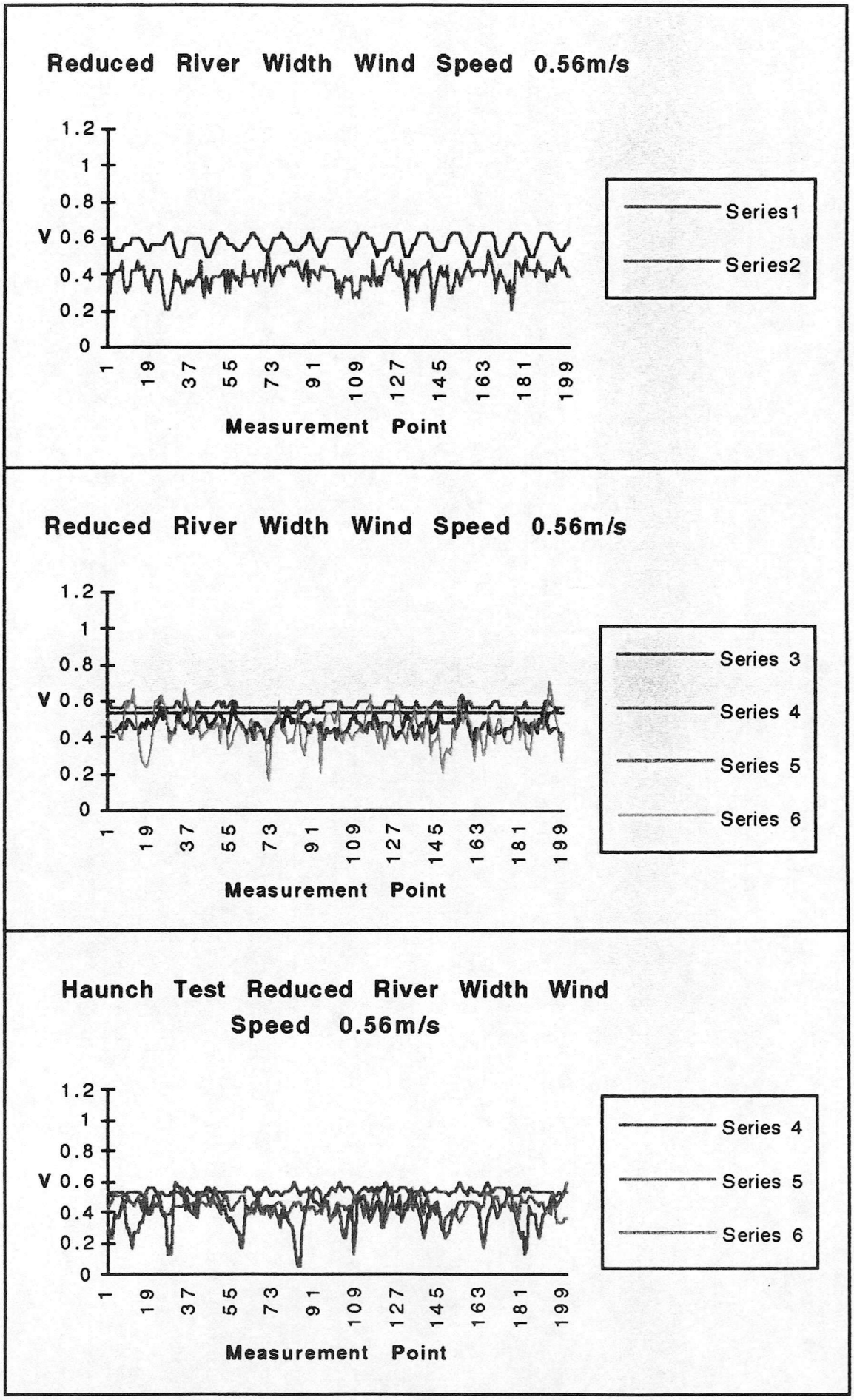
Reduced River Width Wind Speed 0.56m/s
1.2
1
0.8
V 0.6
0.4
0.2
0
1 19 37 55 73 91 109 127 145 163 181 199
Measurement Point
Series1
Series2
Reduced River Width Wind Speed 0.56m/s
1.2
1
0.8
V 0.6
0.4
0.2
0
1 19 37 55 73 91 109 127 145 163 181 199
Measurement Point
Series 3
Series 4
Series 5
Series 6
Haunch Test Reduced River Width Wind Speed 0.56m/s
1.2
1
0.8
V 0.6
0.4
0.2
0
1 19 37 55 73 91 109 127 145 163 181 199
Measurement Point
Series 4
Series 5
Series 6

Figure B11

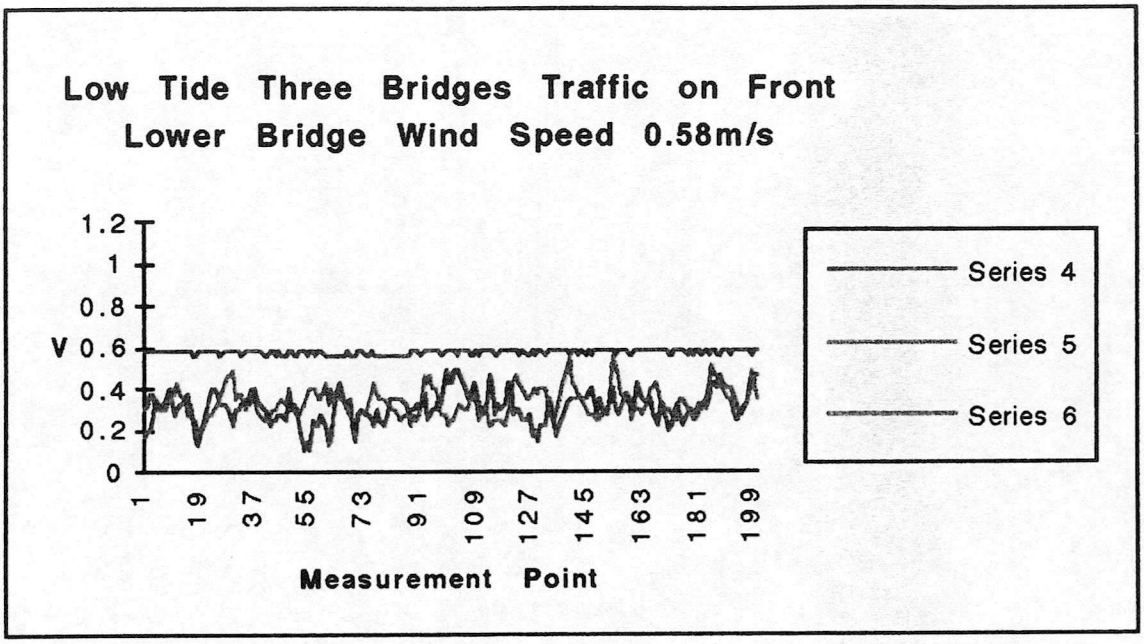
Low Tide Three Bridges Traffic on Front Lower Bridge Wind Speed 0.58m/s
1.2
1
0.8
V 0.6
0.4
0.2
0
1
19
37
55
73
91
109
127
145
163
181
199
Measurement Point
Series 4
Series 5
Series 6

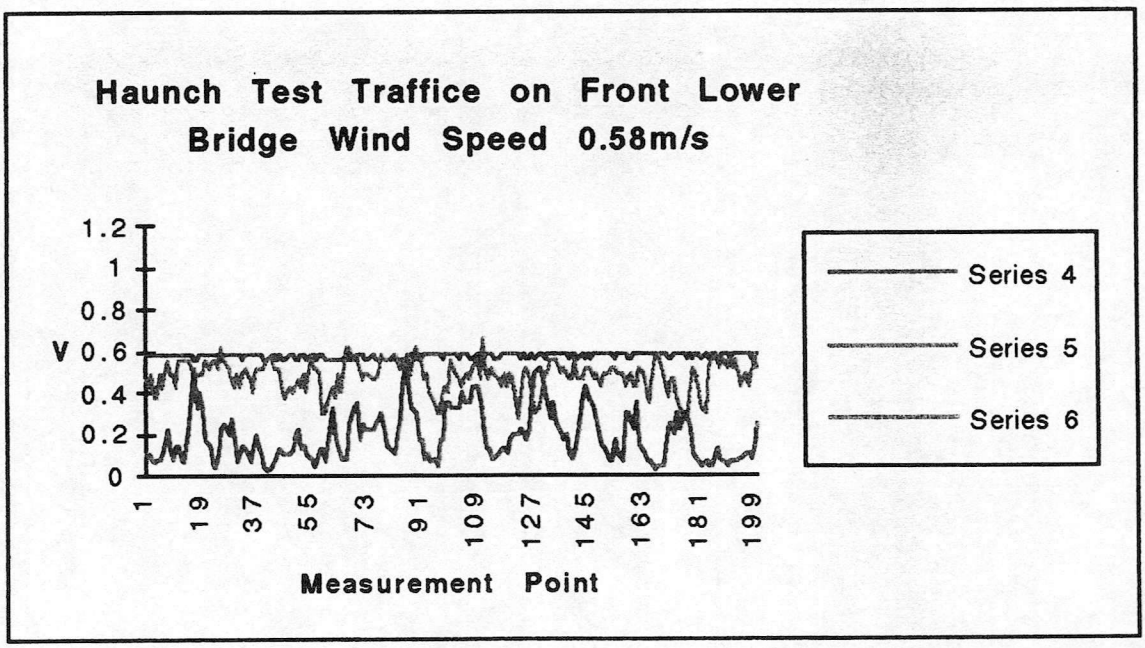
Haunch Test Traffice on Front Lower Bridge Wind Speed 0.58m/s
1.2
1
0.8
V 0.6
0.4
0.2
0
1
19
37
55
73
91
109
127
145
163
181
199
Measurement Point
Series 4
Series 5
Series 6

Figure B12

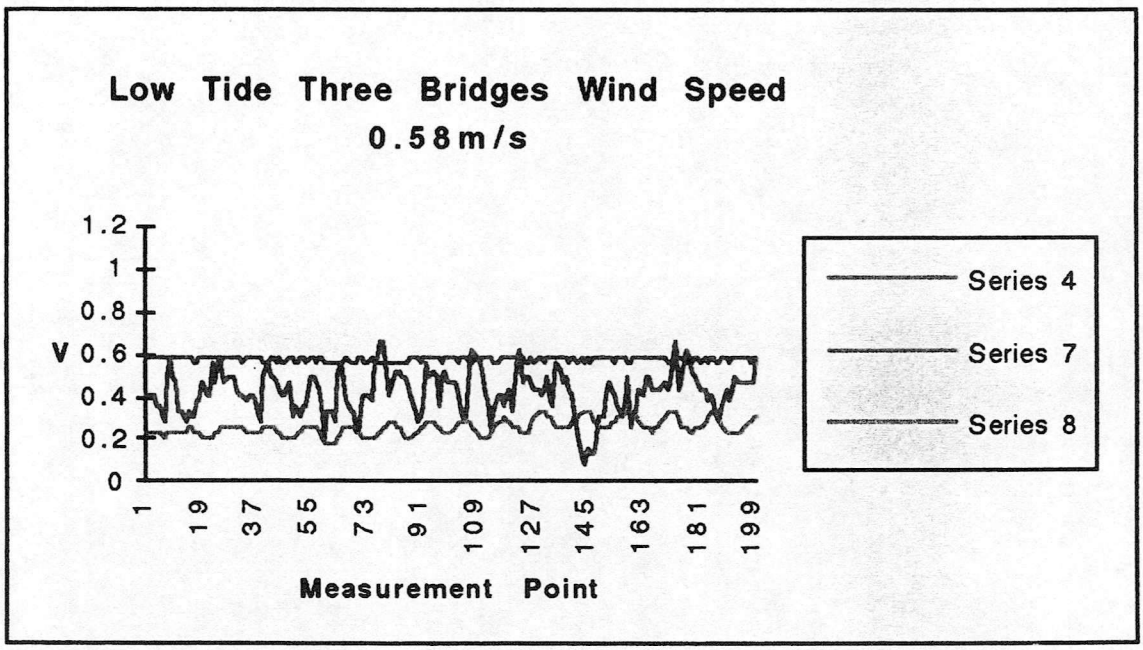
Low Tide Three Bridges Wind Speed
0.58m/s
1.2
1
0.8
V 0.6
0.4
0.2
0
1
19
37
55
73
91
109
127
145
163
181
199
Measurement Point
Series 4
Series 7
Series 8

Figure B13

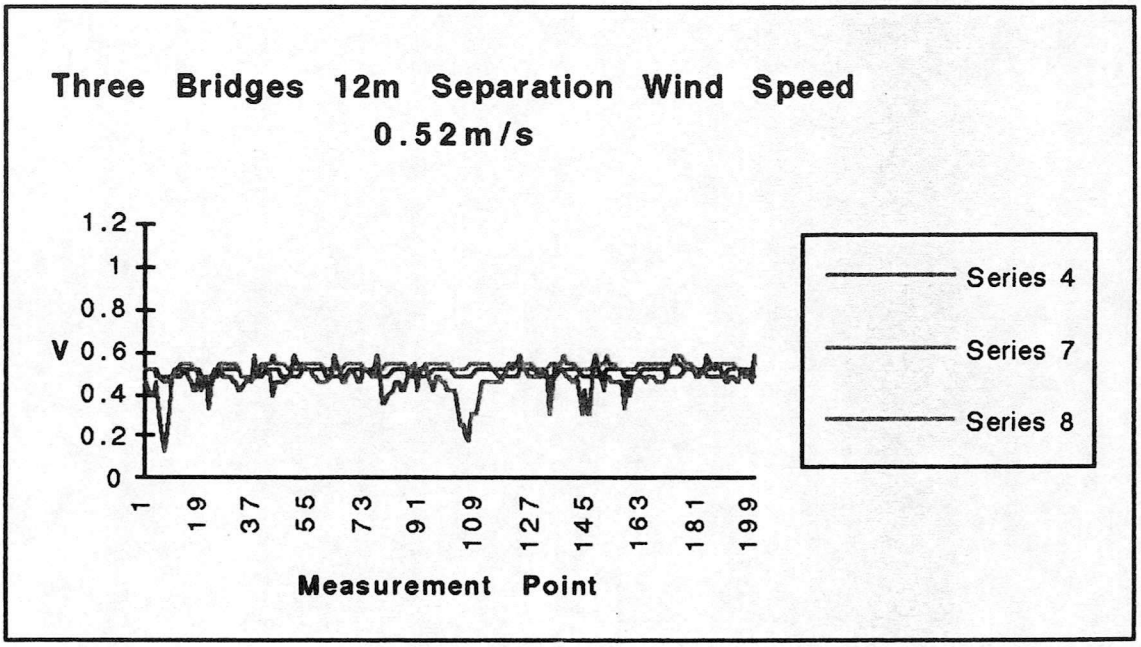
Three Bridges 12m Separation Wind Speed
0.52m/s
1.2
1
0.8
V 0.6
0.4
0.2
0
1
19
37
55
73
91
109
127
145
163
181
199
Measurement Point
Series 4
Series 7
Series 8

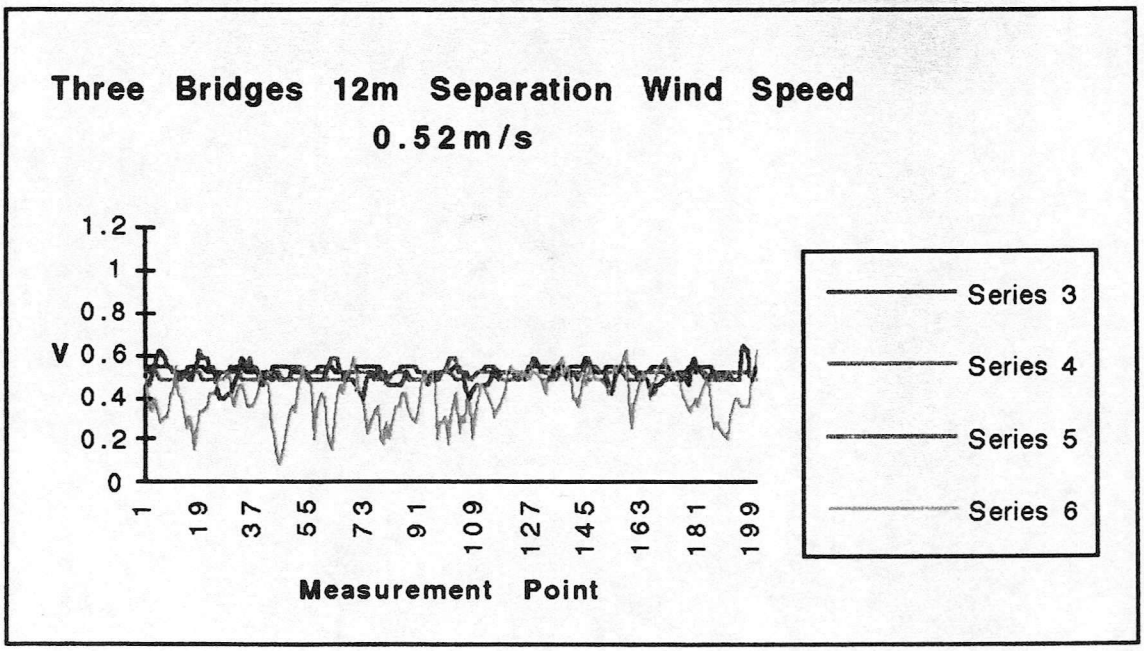
Three Bridges 12m Separation Wind Speed
0.52m/s
1.2
1
0.8
V 0.6
0.4
0.2
0
1
19
37
55
73
91
109
127
145
163
181
199
Measurement Point
Series 3
Series 4
Series 5
Series 6

Figure B14